

**SIMULATION OF FLUID FLOW MECHANISMS IN HIGH PERMEABILITY
ZONES (SUPER-K) IN A GIANT NATURALLY FRACTURED CARBONATE
RESERVOIR**

A Thesis

by

AMER H. ABU-HASSOUN

Submitted to the Office of Graduate Studies of
Texas A&M University
in partial fulfillment of the requirements for the degree of

MASTER OF SCIENCE

August 2007

Major Subject: Petroleum Engineering

**SIMULATION OF FLUID FLOW MECHANISMS IN HIGH PERMEABILITY
ZONES (SUPER-K) IN A GIANT NATURALLY FRACTURED CARBONATE
RESERVOIR**

A Thesis

by

AMER H. ABU-HASSOUN

Submitted to the Office of Graduate Studies of
Texas A&M University
in partial fulfillment of the requirements for the degree of

MASTER OF SCIENCE

Approved by:

Chair of Committee,	David Schechter
Committee Members,	Bob Wattenbarger
	Wayne Ahr
Head of Department,	Stephen A. Holditch

August 2007

Major Subject: Petroleum Engineering

ABSTRACT

Simulation of Fluid Flow Mechanisms in High Permeability
Zones (Super-K) in a Giant Naturally Fractured Carbonate
Reservoir. (August 2007)

Amer H. Abu-Hassoun, B.S., King Fahd University of
Petroleum and Minerals, Dhahran, Saudi Arabia
Chair of Advisory Committee: Dr. David Schechter

Fluid flow mechanisms in a large naturally fractured heterogeneous carbonate reservoir were investigated in this manuscript. A very thin layer with high permeability that produces the majority of production from specific wells and is deemed the *Super-K* Zone was investigated. It is known that these zones are connected to naturally occurring fractures. Fluid flow in naturally fractured reservoirs is a very difficult mechanism to understand. To accomplish this mission, the Super-K Zone and fractures were treated as two systems.

Reservoir management practices and decisions should be very carefully reviewed and executed in this dual continuum reservoir based on the results of this work. Studying this dual media flow behavior is vital for better future completion strategies and for enhanced reservoir management decisions.

The reservoir geology, Super-K identification and natural fractures literature were reviewed. To understand how fluid flows in such a dual continuum reservoir, a dual permeability simulation model has been studied. Some geological and production

data were used; however, due to unavailability of some critical values of the natural fractures, the model was assumed hypothetical. A reasonable history match was achieved and was set as a basis of the reservoir model. Several sensitivity studies were run to understand fluid flow behavior and prediction runs were executed to help make completion recommendations for future wells based on the results obtained.

Conclusions and recommended completions were highlighted at the end of this research. It was realized that the natural fractures are the main source of premature water breakthrough, and the Super-K acts as a secondary cause of water channeling to the wellbore.

DEDICATION

This effort is dedicated to my lovely wife; Entisar, for her patience, understanding, and sacrificing her time and life for me. I would like to tell her that she has been my strength, inspiration and enthusiasm to successfully complete this work. I love her and will do what it takes to compensate her for what she missed in life.

I also dedicate this work to my little angel, Sarah, may God save her soul and give me power and endurance to handle her medical condition. Having her with us, gave me all the power that a man could ever wish for.

This thesis is also dedicated to my mother, father, two sisters, and five brothers. I would like to thank them for their advice, spiritual emotions and encouragement to perform the impossible. I love you all.

ACKNOWLEDGEMENTS

I would like to express my sincere gratitude to the following members of my graduate advisory committee for their continuous support and useful advice to accomplish this research.

Thank you to the chairman of my graduate advisory committee, Dr. David Schechter, for his nonstop support, advice and patience in answering all of my questions. Working under you has been an honor.

Thank you to Dr. Bob Wattenbarger for sharing some thoughts, experience and being a member of my committee. In addition, would like to thank Dr. Wayne Ahr for serving as a member of my advisory committee and for the knowledge I gained from taking your Carbonate Geology course.

My gratitude goes to my office mate Zuher Syihab for being my CMG™ expert. Also, I would like also to thank my friend Ahmad Mohammad for his ideas and thoughts.

Thanks as well to faculty and staff of the Harold Vance Department of Petroleum Engineering at Texas A&M University for providing the facilities and accommodations to conduct my research.

Finally, I would like to thank Saudi Aramco for giving me this opportunity to acquire my M.S. Degree at such a reputable University in the Petroleum Industry.

TABLE OF CONTENTS

	Page
ABSTRACT	iii
DEDICATION	v
ACKNOWLEDGEMENTS	vi
TABLE OF CONTENTS	vii
LIST OF FIGURES.....	x
LIST OF TABLES	xv
 CHAPTER	
I INTRODUCTION	1
1.1 Reservoir Background.....	2
1.2 Geological Aspects.....	3
1.3 Objectives.....	5
II SUPER-K REVIEW	7
2.1 Pressure Transient Test Analysis	12
2.1.1 Vertical Well Intersecting a Super-K Interval.....	12
2.1.2 Slanted Horizontal Well Intersecting a Super-K Interval	13
2.2 Reservoir Simulation Studies	14
III FRACTURE REVIEW	27
3.1 Transfer and Shape Factor.....	28
3.2 Dual Permeability Modeling.....	33
IV HYPOTHETICAL HISTORY MATCHING	35
4.1 Simulation Model Construction	36
4.2 Producer P-141	38
4.3 Changes to Oil Rate.....	41
4.4 Model Limitation and Errors.....	42

CHAPTER	Page
V SENSITIVITY STUDIES	43
5.1 Fracture Length	43
5.1.1 Fractures at the Top Layers	44
5.1.2 Fractures Intersecting All Layers	44
5.1.3 Fractures in All Layers but Not the Super-K	45
5.2 Super-K Length	47
5.3 Super-K Porosity	52
5.4 Fracture Spacing Effect	54
5.4.1 Fracture Spacing: I-Direction	55
5.4.2 Fracture in the Entire Model	58
5.4.3 Fracture Spacing I = J = K	62
5.5 Super-K Permeability Variation	63
5.6 Fracture Porosity	68
5.7 Fracture Location	72
5.7.1 Position: 1	75
5.7.2 Position: 2	76
5.7.3 Position: 3	77
VI WELL COMPLETION GEOMETRY	79
VII PREDICTION	84
7.1 Case: 1	84
7.2 Case: 2	86
7.3 Case: 3	88
7.4 Case: 4	89
7.5 Case: 5	92
7.6 Case: 6	92
VIII RECOMMENDATIONS FOR BEST COMPLETION	95
8.1 Best Matching Case	95
8.2 Horizontal Completion	98
IX CONCLUSIONS AND RECOMMENDATIONS	101
9.1 Conclusions	101
9.2 Recommendations	102
NOMENCLATURE	104

	Page
REFERENCES	105
APPENDIX A MODEL PROPERTIES	109
APPENDIX B ADDITIONAL FIGURES FOR DATA USED IN SIMULATION RUNS	111
VITA	114

LIST OF FIGURES

FIGURE	Page
1.1 Ghawar Field Location.....	2
1.2 Reservoir Geological Overview	3
1.3 Reservoir Zones.....	4
2.1 Example of Super-K Layer Contributing to 70 % of Total Flow.....	9
2.2 Another Example of a Super-K Zone.....	10
2.3 Production Profile of Adjacent Well	11
2.4 Pressure Derivative	13
2.5 Adjacent Slanted Well Shows Production from Super-K	14
2.6 X-Shape Relative Permeability Curve for Super-K and Fractures	15
2.7 Sharp Water Cut Increase Caused by Super-K	16
2.8 Water-Cut and Cumulative Oil History Match	19
2.9 Fracture Grids Embedded in Fine Grids	22
2.10 Geological Zones of the Reservoir.....	22
2.11 Horizontal and Vertical Flow in the Super-K	23
2.12 Fast Water Movement in Zone-3A Due to Fractures.....	24
2.13 Water Production History Match	25
2.14 Advancement of the Flood Front through the Super-K.....	25
3.1 Warren and Root Fracture Model.....	29
3.2 Kazemi and Gilman Fracture Model	30

FIGURE	Page
3.3 Interconnected Vertical Fracture Planes	34
4.1 CMG™ Builder Used for Simulation Runs	36
4.2 Four Regions in the Model: Matrix (Blue), Boundary Sector (Pink), Super-K Sector (Red) and Fractures Sector (Green)	37
4.3 Well P-141 Production Logging Profile Showing Super-K Zone.....	40
4.4 Good History Match Until 1998.....	41
4.5 Improved History Match After Year 1998.....	42
5.1 Run Results of Fractures at the Top Layers	44
5.2 Fractures Intersecting All Layers Run	45
5.3 Fractures Not Intersecting the Super-K Layer	46
5.4 Comparison Plot to the Three Runs	47
5.5 Run Results of the 300 ft Super-K Length.....	48
5.6 Run Results of the 10200 ft Super-K Length.....	48
5.7 Run Results of the 10200 ft Super-K Length, No Fractures	49
5.8 Comparison Plot of Cumulative Production for the Model, No Fractures...	50
5.9 Water Slowly Approaches P-141 in Layer-5 by End of Simulation Run	51
5.10 Fractures Presence Cause Quick Water Channeling	52
5.11 45 % Super-K Porosity Results	53
5.12 75 % Super-K Porosity Results	54
5.13 1 ft Fracture Spacing Run Results.....	55
5.14 1000 ft Fracture Spacing Run Results.....	56

FIGURE	Page
5.15 Different Fracture Spacing Comparison to Produced Water.....	57
5.16 Water Invasion After 1999 from Top of Fifth Layer	58
5.17 Fractures in Entire Model: 1 ft Fracture Spacing	59
5.18 Fractures in Entire Model: 500 ft Fracture Spacing	59
5.19 Water Breakthrough by the End of 1997	60
5.20 Oil Swept from Most of Layer-5.....	61
5.21 High Oil Potential in Layer-4 by End of Simulation Run.....	61
5.22 Comparison of Water Production of Fractures in the Entire Model	62
5.23 Comparison Plot for Equal and Different Fracture Spacing	63
5.24 Simulation Results of 10 Darcies Super-K Permeability	64
5.25 Simulation Results of 70 Darcies Super-K Permeability	64
5.26 Comparison Plot to Super-K Layer Intersecting Fractures	65
5.27 Simulation Results of 10 Darcies Super-K Permeability Model with No Fractures.....	66
5.28 Simulation Results of 70 Darcies Super-K Permeability Model with No Fractures	67
5.29 Comparison Plot to Different Super-K Permeability with No Fractures.....	68
5.30 Simulation Results for 0.1 % Fracture Porosity	69
5.31 Simulation Results for 15 % Fracture Porosity	70
5.32 22-D Diagram Shows Water Cut Increase at the Center by End of 1991	71
5.33 Comparison Results of Different Fracture Porosity	72
5.34 Three Different Locations of Fractures in the Model.....	73

FIGURE	Page
5.35 Results of Running Fractures at Three Locations	73
5.36 3-D Diagram Shows Water Movement	74
5.37 Water Movement in Fifth Layer.....	75
5.38 First Fractures Position (Green), Super-K Layer in Red.....	75
5.39 Results of First Fracture Position Run	76
5.40 Second Fracture Position (Green), Super-K Layer in Red.....	76
5.41 Results of Second Fracture Position Run.....	77
5.42 Third Fracture Position (Green), Super-K Layer in Red.....	77
5.43 Results of Third Fracture Position Run.....	78
6.1 Horizontal Producer Placed in Third Layer	79
6.2 Simulation Results for a Horizontal-Hole Intersecting Super-K and Fractures	80
6.3 Simulation Results for a Horizontal-Hole Intersecting Super-K, No Fractures	81
6.4 Simulation Results for a Horizontal-Hole above Super-K with Fractures Presence in the Model	82
6.5 Simulation Results for a Horizontal-Hole above Super-K; No Fractures	83
7.1 Case 1: Prediction Run.....	85
7.2 Water Encroachment near P-141 by End of Simulation Run.....	86
7.3 Case 2: Prediction Run.....	87
7.4 Good Oil Potential in Layers 1 and 2.....	88
7.5 Case 3: Prediction Run.....	89

FIGURE	Page
7.6 Case 4: Prediction Run.....	90
7.7 Water Encroachment by the End of Simulation Run	91
7.8 3-D View of Water Flooding Up to Layer-3.....	91
7.9 Case 5: Prediction Run.....	92
7.10 Case 6: Prediction Run.....	93
7.11 Water Encroachment below the Horizontal Hole.....	94
7.12 Water Encroachment in Layer-2	94
8.1 Layer-5 Watered Out by End of Year 2013	97
8.2 Water Invaded Producer P-141 in Layer-4 by End of Year 2019	97
8.3 Comparison Plot of Production from Horizontal Wellbore	99
8.4 Water Cut Increases in Case Fractures Present	100

LIST OF TABLES

TABLE	Page
3.1 Shape Factor Values Based on Different Authors	32
A.1 Reservoir and Fluid Properties	109
A.2 Matrix Properties	109
A.3 Fracture Sector Properties	110
A.4 Super-K Sector Properties	110

CHAPTER I

INTRODUCTION

One of the most heterogeneous oil carbonate reservoirs in the world is located in the Middle East (see **Fig. 1.1**). Understanding fluid flow mechanisms in extremely high permeable thin intervals referred to as a **Super-K** zone with natural fractures present and perhaps in communication with Super-K zones is a very difficult task. The Super-K zone dominates production rates from thin zones. Reservoir management practices and decisions should be very carefully reviewed and executed in this dual continuum reservoir. There is a reservoir management strategy argument of whether the existence of those super permeable zones will be beneficial in terms of productivity and recovery or the zones will have a negative influence when water breaks through causing the well to produce at high water cut eventually reducing oil production.

Studying the abnormal flow in the two systems of the Super-K and fractures is important for future placement of oil producers and water injectors, for better completion practices to decrease the probability of wells being completed in undesired locations and for avoiding early water breakthrough and or water coning. Super-K layers are of secondary reservoir management problems. Some wells were abundant and found out to be attributed to Super-K. Super-K layers can act as thief zones as to sometimes prevent zonal isolation by cement squeezing. The advantage of the Super-K zones is that they can contribute to primary recovery efficiency in dry areas which can provide high conductive conduits from high storage facies units.

This thesis follows the style of the *Society of Petroleum Engineering Journal*.

So, Super-K is desirable in areas effectively still under primary production that have not yet experienced the outcome of water flooding.¹ In the next sections of this chapter, a brief reservoir background will be given, then some geological aspects of the reservoir will be described and finally the objectives of this thesis will be discussed.



Fig. 1.1 - Ghawar Field Location

1.1 Reservoir Background

The field is considered to be the largest oil field in the world with dimensions of 230 km in length and 25 km in width. The reservoir of interest is very heterogeneous and located in a highly porous and permeable carbonate of the Arab-D formation. The reservoir has been under secondary recovery process of peripheral water flooding for 40

years. Several wells in the area have experienced early water-breakthrough where water has moved quickly to the middle of the field. The dolomitic section in the center of the reservoir that has high horizontal permeability was believed to be the source of the sharp and uneven flood front movement. The availability of borehole image logs and production profile logs have added much to the understanding of Super-K presence in the field.

1.2 Geological Aspects

The Arab-D reservoir belongs to the Arab formation, Upper Jurassic, sealed by the massive overlying Hith anhydrite formation, dated Tithonian and provides a final Jurassic regional stratigraphic datum. It also comprises of high energy shallow marine carbonate sequence capped by evaporates, and oolitic grainstones that form the upper part of the reservoir. Based on seismic, simulation modeling and data observations, the reservoir can be broken into the following geological components (see **Fig. 1.2**): Faults and fracture clusters; background fractures, highly permeable matrix layers (Super-K) and background matrix.²

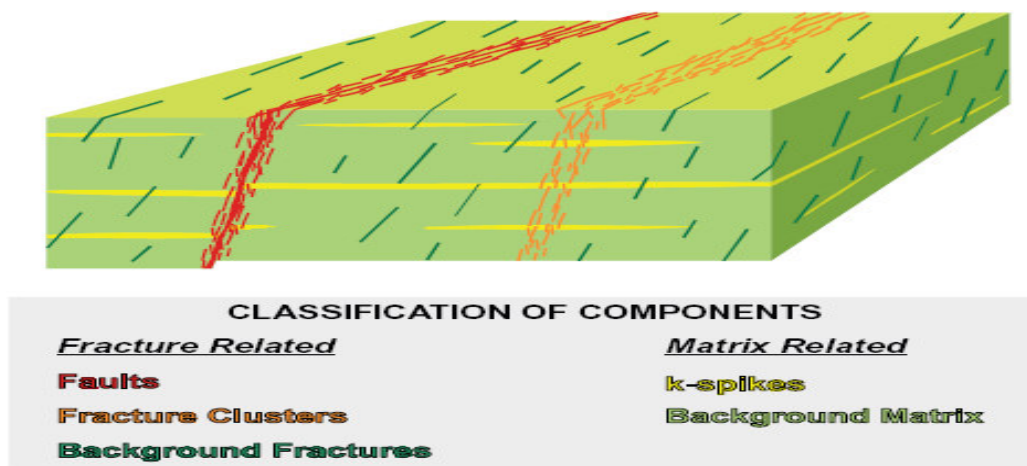


Fig. 1.2 - Reservoir Geological Overview

Typically, the background fractures do not greatly enhance horizontal permeability but can significantly increase vertical permeability. The Super-K or k-spikes fluid transfer depends on both the permeability of the surrounding matrix and on the density of background fractures. The k-spikes and faults/fracture clusters represent high permeability values, however correspond to a small fraction of the total pore volume and both are allocated to the fracture component of the dual porosity/dual permeability description.^{3,4} The reservoir is divided into 4 main geological zones. At the top, Zone-1 which is non-porous with low permeability values, below it is Zone-2A that is usually associated with vuggy skeletal oolitic limestone, scattered vugs and local Super-K zones. In the middle, Zone-2B exists where dolomite occurrences are abundant. Below Zone-2B are Zone-3A and Zone-3B which has the poorest rock quality. Illustration of the reservoir zones is presented in **Fig. 1.3**.

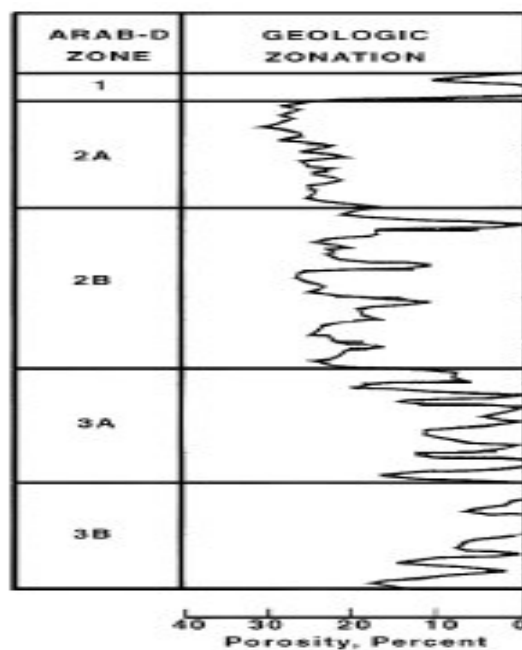


Fig. 1.3 - Reservoir Zones

Super permeabilities are found in all the zones; at the top associated with skeletal oolitic limestone, exists in the middle with leached “*Cladocoropsis*” dolomite or at the bottom associated with “*Stromatoporoid*”. The Super-K zones are well known for the cause of early water breakthrough. The super-K associated with the leached *Cladocoropsis* dolomite and *Stromatoporoid* are primarily the main cause of premature water breakthrough.⁵

1.3 Objectives

The objective of this thesis is to build a simulation model that will help understand the fluid flow behavior of high permeability layer associated with naturally fractured carbonate reservoir. Also, it is essential to give an overview of the work done to characterize and understand the abnormal fluid flow behavior of extremely permeable intervals called the “Super-K” embedded in some areas in a large carbonate reservoir located in the Middle East. The phenomenon of the Super-K is linked with abnormal high production rates from very thin zones. To help understand the production mechanism of those high permeability layers, which will impact making future decisions for drilling completions, a dual permeability simulation model must be built. Commercial software called CMG™ (Computer Modeling Group) will be used to accomplish the objectives.

The simulation model will be discussed in detail and sensitivity studies (mechanistic- cause and effect) will be conducted to study the interaction between different Super-K length and permeability with the rest of the reservoir parameters; matrix and fractures. These sensitivity studies include varying some parameters like: Super-K length, Super-K permeability, Super-K porosity, fractures length, fracture

spacing, fracture porosity and fracture locations. All results will be discussed in details and recommended completion strategies will be concluded based on the results obtained.

CHAPTER II

SUPER-K REVIEW

In a well intersecting a Super-K zone, the wellbore flow is dominated by high flow rates from few feet interval with permeability that can range up to tens of darcies. Those high rate zones are thin and bounded above and below by impermeable layers. Those thin permeable layers are believed to be hydraulically connected to high conductivity beds or channels under condition of high interface transmissibility. The high transmissibility could be originated from fractures, faults, or eroded surfaces which have breached the bounding impermeable layers. If those thin layers were not connected to a prolific beds or channels, the rate could have been much lower and depletion is faster.¹

The Super-K zone can be either a stratiform (high permeability layer) or fracture/fault related. There are three main facies that control the Super-K occurrence. The first is skeletal oolitic lithofacies occurring in the upper part of the reservoir; Zone-2A which was deposited on high energy shoals that resulted in coarse grained ooid beds. The second is leached *Cladocoropsis* dolomite. The heterogeneous and poorly sorted limestone facies is frequently dolomitized. The *Cladocoropsis* voids are often interconnected and are normally oriented parallel to the bedding, thus creating highly-permeable horizontal channels. The *Cladocoropsis* subsequently leached out leaving pencil-sized vugs yielding horizontal permeability in darcies. The third character is *Stromatoporoid* – red algae/coral lithofacies, which is found at the base of Zone-2B.

There are many available tools to identify the Super-K zone for better characterization and understanding of the Super-K behavior. Some of the Super-K layers detection methods include complete loss of circulation, core analysis, sonic and

formation density logs and flowmeters. Lost circulation during drilling can reflect the presence of Super-K. Several wells had complete loss of circulation found out later to have a Super-K phenomenon. Coring operations provide a physical evidence of Super-K zones. Visual inspection of field cores can show several layers of porosity anomalies and vuggy intervals. Lab tests of the cores show high horizontal permeabilities of the Super-K ranging in darcies. Sonic log is important and is affected by primary porosity. A wide reading variation indicates vugs, channels or fractures. Since the Super-K layers exist in dolomite sequence, the identification of dolomite through neutron/formation density log is important. Flowmeter logging is an excellent tool to identify the Super-K layers by checking for crossflow between layers in every stop. If the pressure of the high permeability layers is the same as the rest of the zones and if the temperature sensors do not show any anomaly, it means that the Super-K layers are in communication with the rest of the reservoir either through fractures or good matrix flow. If there is a crossflow or vertical communication between layers, wells with Super-K zones should be restricted for better sweep efficiency since it will dominate the flow and to delay early water breakthrough especially if the Super-K is connected to fractures.^{6,7,8}

As an example, a single well with a fault related Super-K zone can provide 15 Mstb/d of flow from a 3 ft interval; about 75% of the total well rate.³ Production logs can show clearly the Super-K layer by providing a high percentage of total fluid influx. **Figs. 2.1 and 2.2** present examples of Super-K zones that contributed to more than 70 % of total well production which is coming only from 5' interval. A normal production profile of an adjacent well is shown in **Fig. 2.3**. Based on some lab studies done earlier in Super-K zones, the basic permeability of a stratiform Super-K permeability varies from 600 mD

to 5000 mD. The Super-K permeability has a positive impact on oil production because it enhances well productivity.⁹

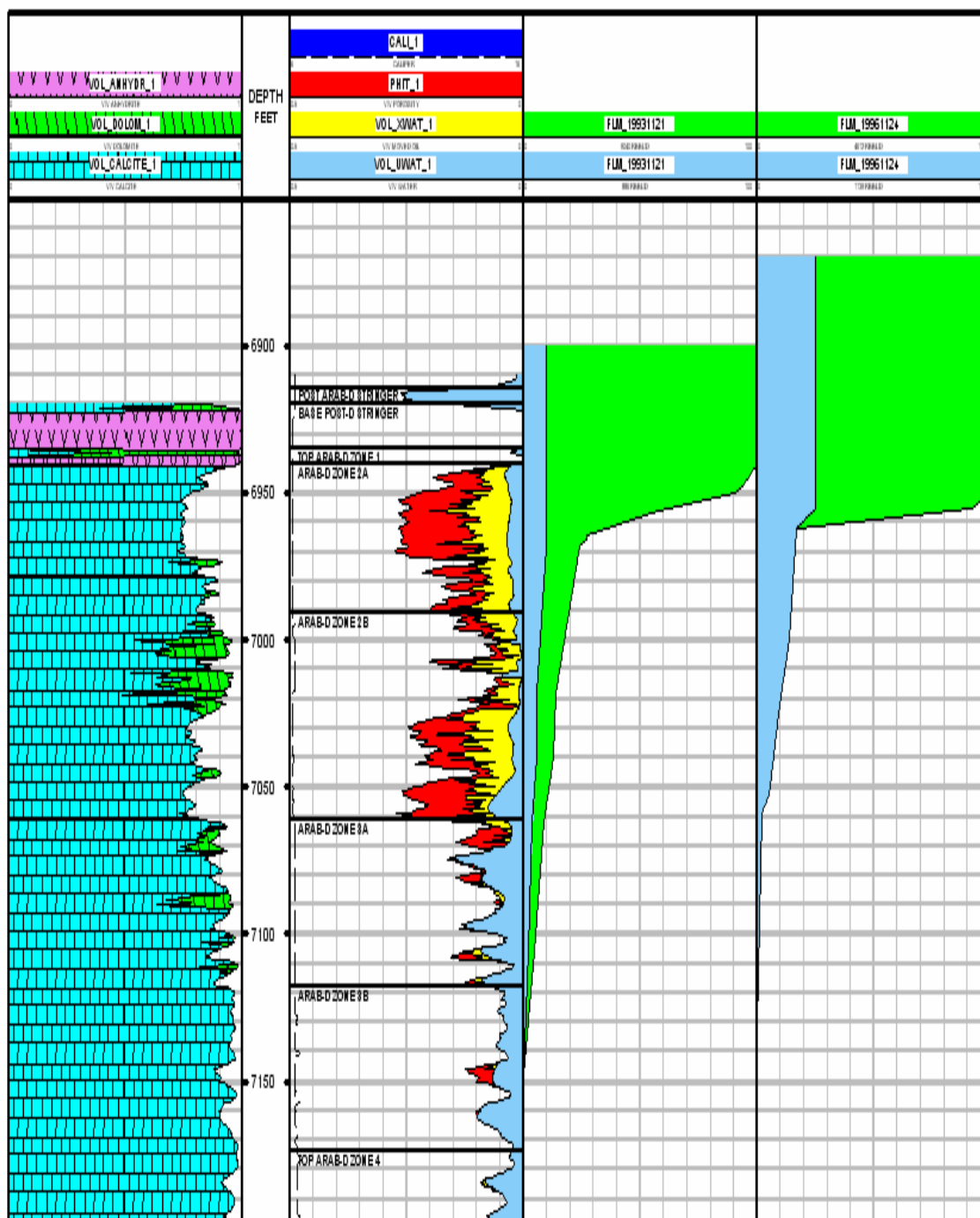


Fig. 2.1 - Example of Super-K Layer Contributing to 70 % of Total Flow

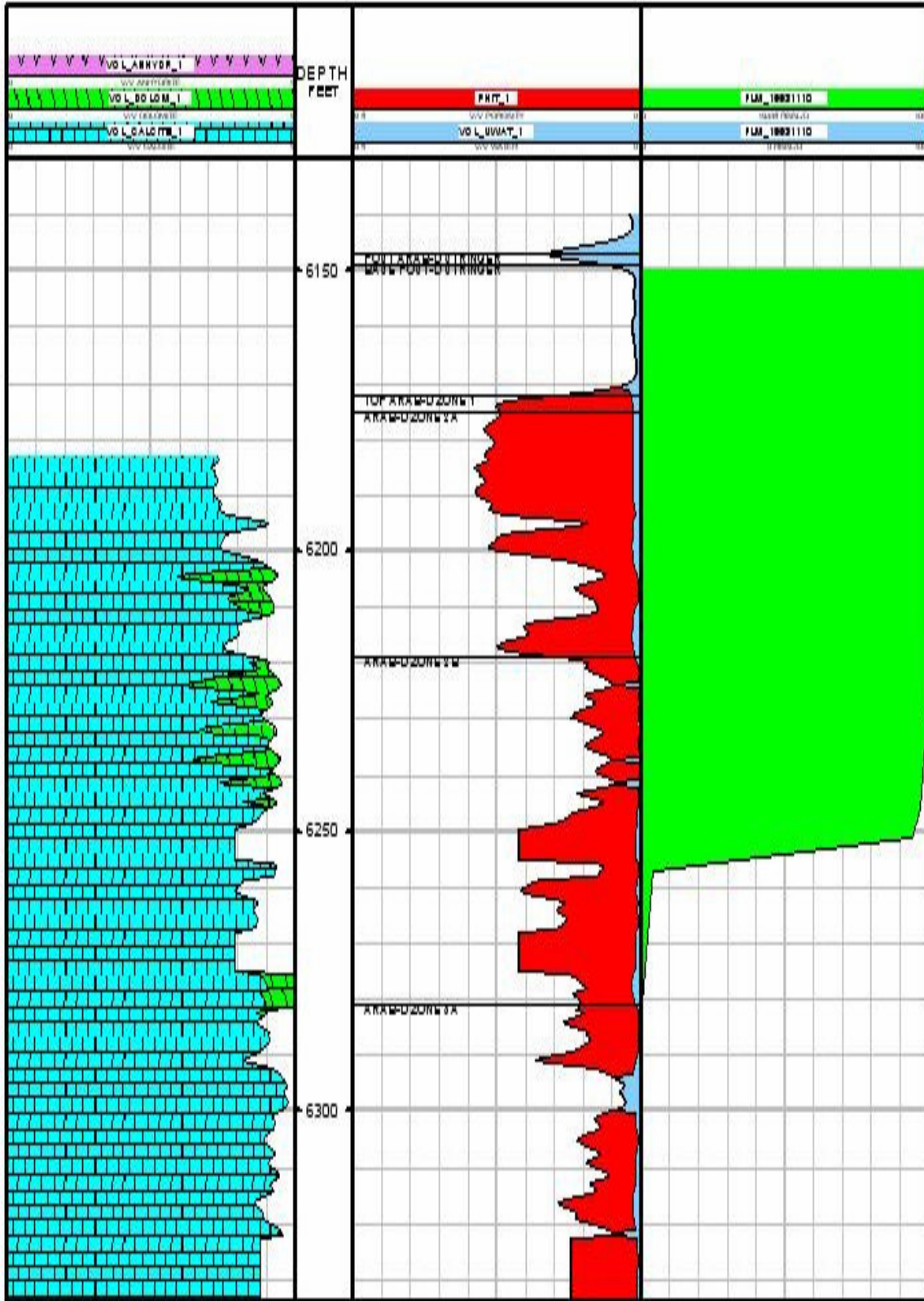


Fig. 2.2 - Another Example of a Super-K Zone

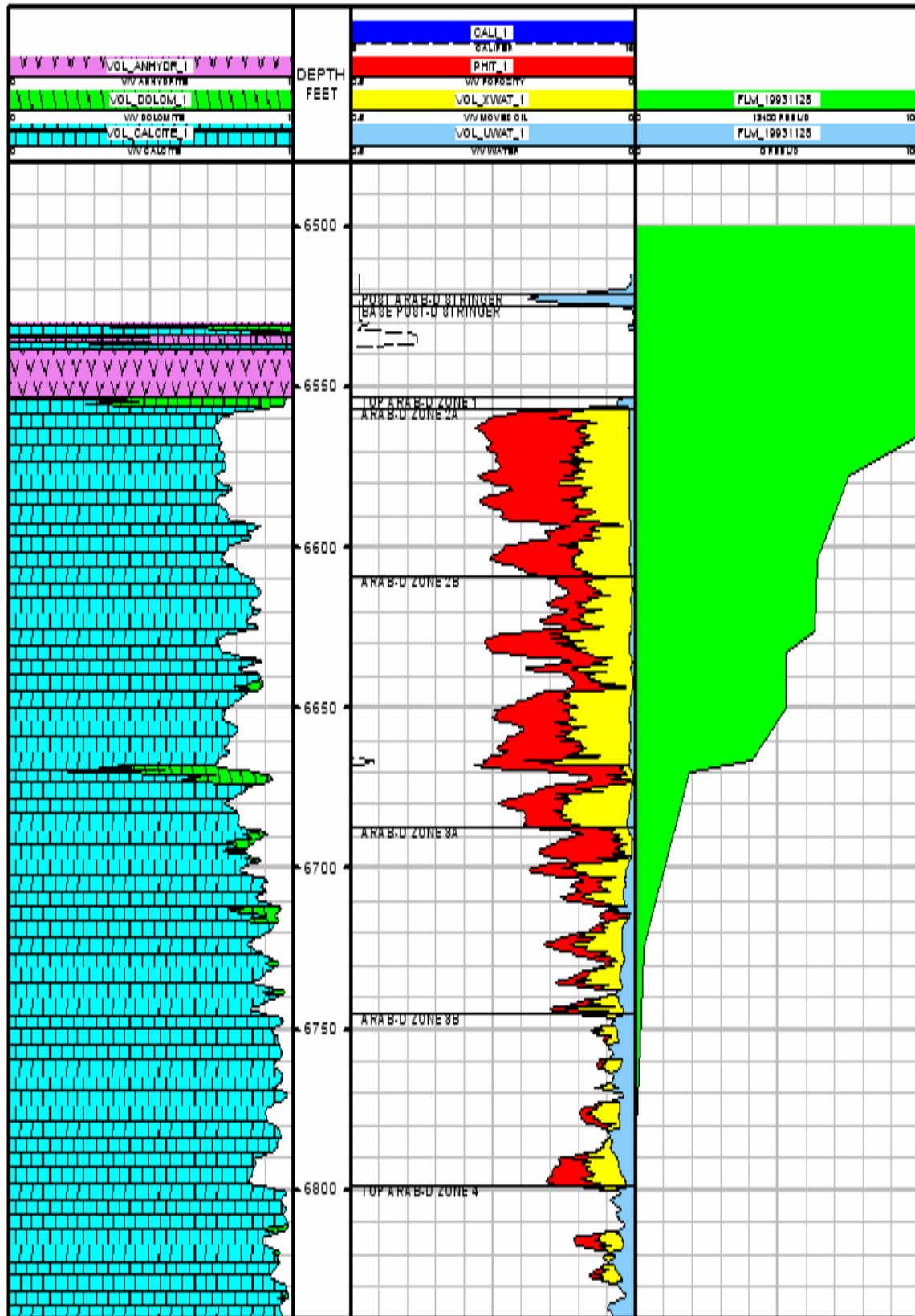


Fig. 2.3 - Production Profile of Adjacent Well

2.1 Pressure Transient Test Analysis

Analysis of pressure test data in the Arab-D reservoir is a challenge with presence of the Super-K intervals with multi-phase flow and wellbore phase redistribution effects. The Super-K intervals can be identified by: 1) Loss of circulation during drilling, 2) Cores, 3) Openhole logs, and 4) Flowmeter surveys. Two pressure transient cases will be presented for a vertical well intersecting a Super-K interval, and another case for a slanted horizontal well intersecting a Super-K interval.

2.1.1 Vertical Well Intersecting a Super-K Interval

A well was drilled and completed as a vertical open-hole with complete loss of circulation at 6,370 ft. The production log analysis showed that around 80% of the flow is coming from about 20 ft interval at the top of Zone-2A. The derivative plot of the pressure build up test is shown in **Fig. 2.4** showing a drawdown of 21 psi at a dry oil flow rate of 15,100 bbls/d. The pressure derivative shows a radial flow followed by more likely to be a bi-linear flow representing a dual porosity transient pressure behavior for fractured reservoir. Analysis of the pressure build up indicates a Super-K layer flow capacity of 1,500,000 mD*ft which results in a Super-K permeability of ~ 77 darcies from a 20 ft interval.

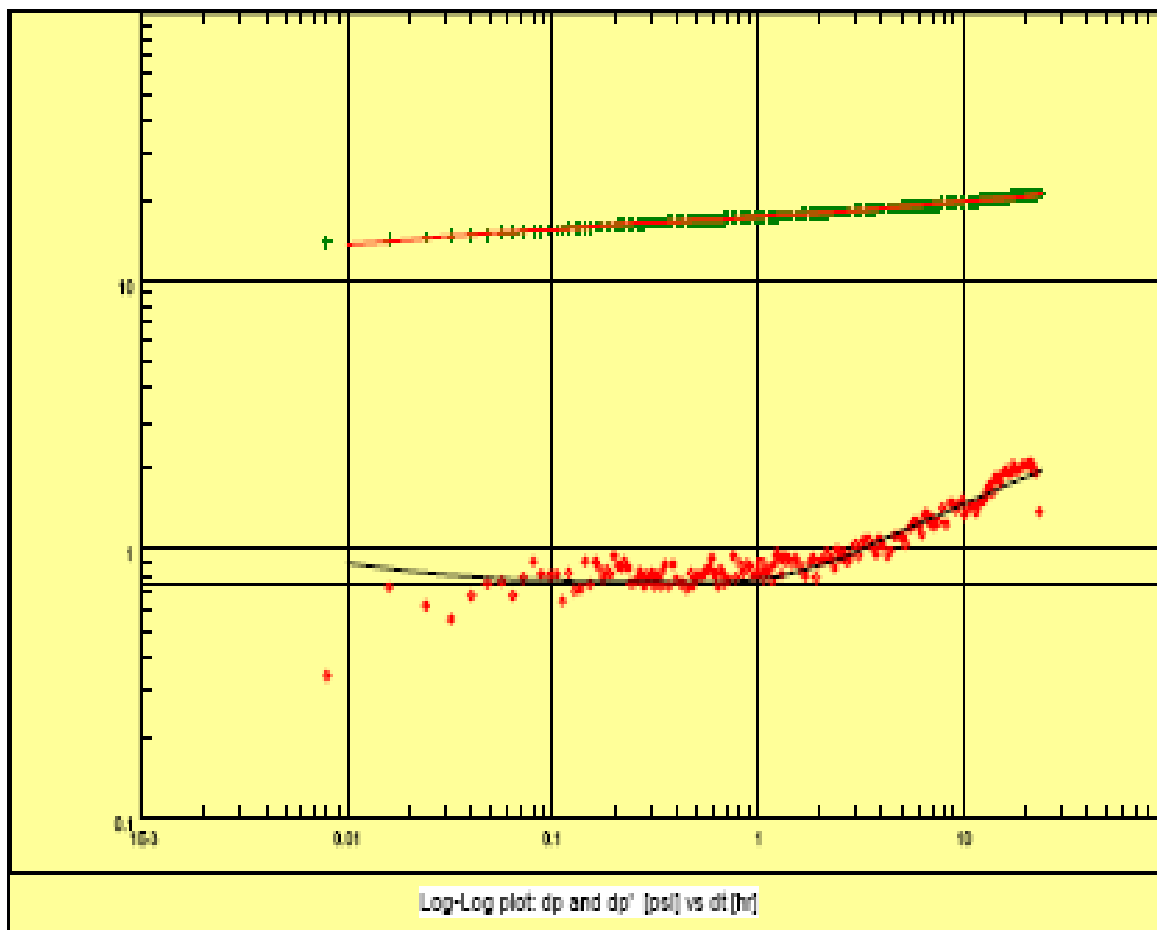


Fig. 2.4 - Pressure Derivative

2.1.2 Slanted Horizontal Well Intersecting a Super-K Interval

The well for this case was completed as a 1,600 ft open-hole slanted producer through the entire Arab-D. A production log from adjacent well indicated that the majority of the flow occurs in a Super-K layer (see **Fig. 2.5**). The flow rates were 5,000 bbls/d and 945 bbls/d at a 128 psi drawdown. The wellbore phase redistribution effect was a major parameter affecting the pressure transient response. The stabilization at the end of the test indicates early radial flow that is consistent with the flow in the Super-K layer.¹⁰

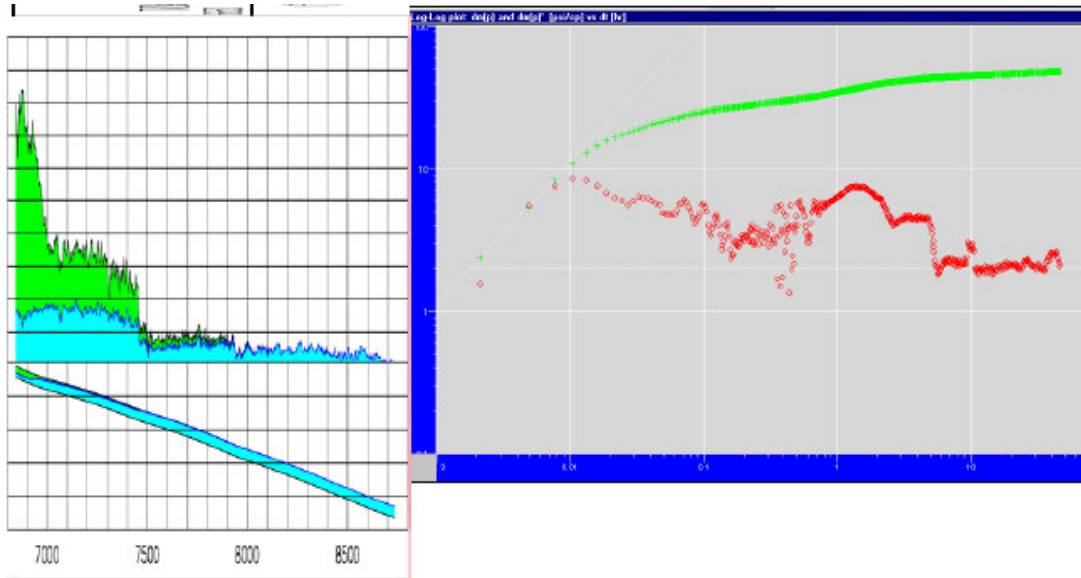


Fig. 2.5 - Adjacent Slanted Well Shows Production from Super-K

2.2 Reservoir Simulation Studies

Several reservoir simulation studies were conducted to build models that could capture the fluid flow behavior of Super-K zones. Some studies will be presented in this section. Special relative permeability curves were used to model the fluid flow in the Super-K layers. The Super-K relative permeability curve is of X-shape when plotted versus water saturation as in **Fig. 2.6**. Good well bottom-hole pressure and water cut match for wells in the simulation model were achieved only by including the Super-K behavior in the model. Most of the Super-K occurrence was in the range of 10 to 50 darcies which was enough to bringing pre-mature early water breakthrough to the wellbore. Wells that are influenced by Super-K effect, exhibit a sharp increase in water cut once the wells start producing water as seen in **Fig. 2.7**.⁸

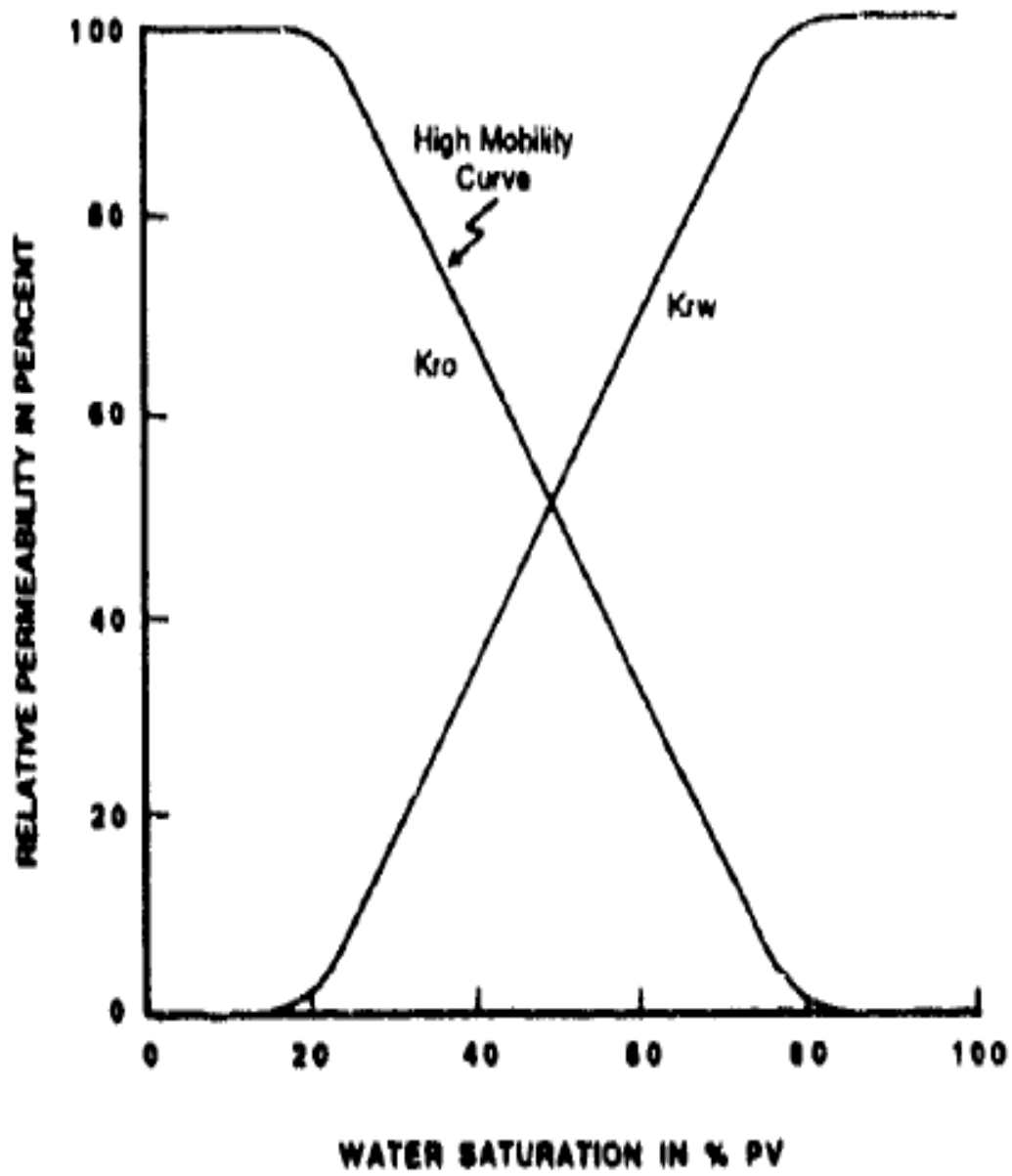


Fig. 2.6 - X-Shape Relative Permeability Curve for Super-K and Fractures

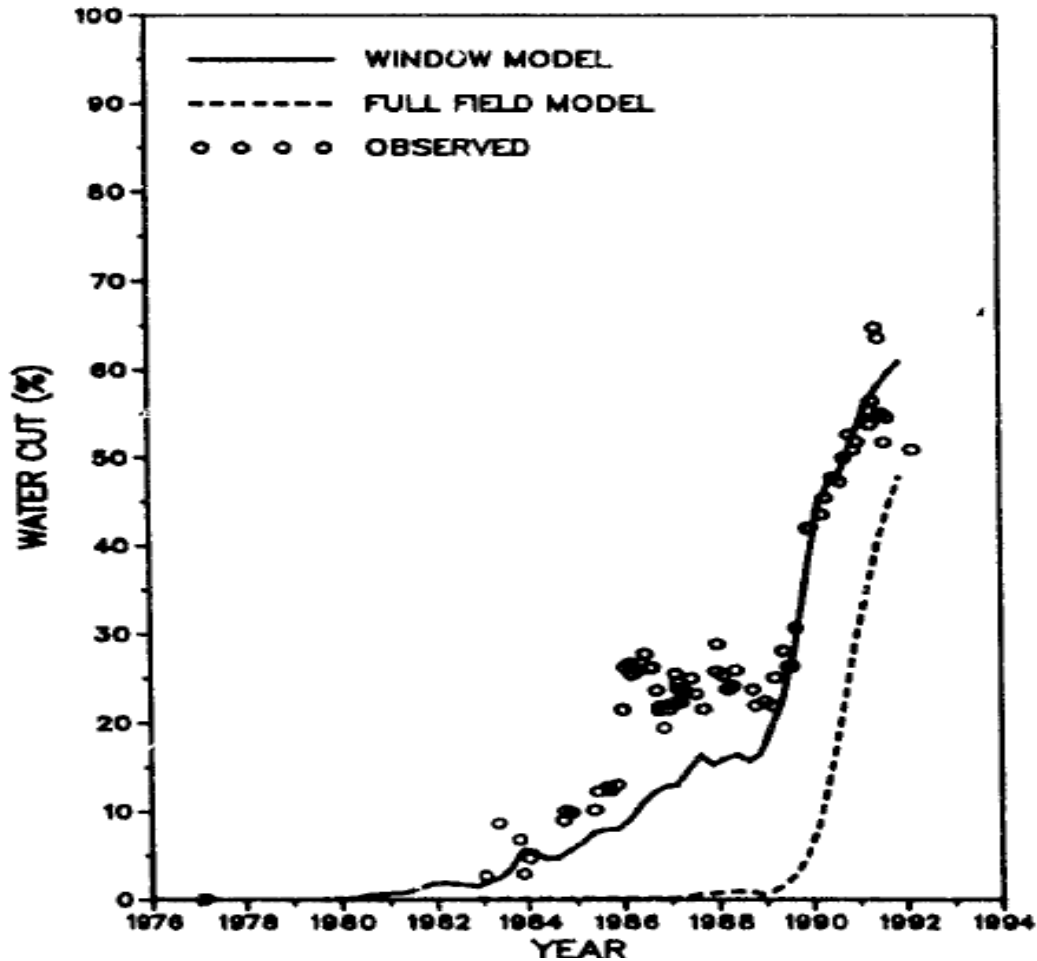


Fig. 2.7 - Sharp Water Cut Increase Caused by Super-K

A study conducted on the same reservoir done by Cosentino et al¹¹ discusses modeling a sector area of the field using a dual porosity, dual permeability model to represent the heterogeneity of the reservoir which is identified as matrix properties, stratiform Super-K intervals and fracture distribution. The main objective of the model is to capture the irregular water advancement and early water breakthrough observed in some areas after the beginning of the peripheral injection. The reservoir has two flow systems: one with high storage capacity and low conductivity which is the matrix and the other one has low storage capacity and high conductivity as in Super-K layers and

fractures. The dual media approach (dual porosity/dual permeability) was used because it explicitly accounts for the different hydraulic properties of each heterogeneous system. Also, the model accounted for different displacement mechanisms of dual-media reservoir (expansion, capillarity, gravity, and viscosity). The sector was up-scaled to the dimension of 88 x 40 x 13 with 250 x 250 cells width in the X-Y directions with 13 heterogeneous layers.

The effective permeability of the Super-K zone at the simulation grid has been determined in terms of transmissibility as in the following equations.

$$\Phi_{SK(i, j, k)} = NG_{SK(i, j, k)} * \Phi_{SK} \dots\dots\dots 2.1$$

Where NG_{SK} is net/gross ration (i.e., the ration of the Super-K thickness to the total cell thickness) and Φ_{SK} is the absolute Super-K porosity. The horizontal transmissibility between two adjacent cells in the presence of Super-K layers is computed according to the following equations:

$$\text{IF } \Phi_{SK(i, j, k)} \neq 0 \text{ AND } \Phi_{SK(i + 1, j, k)} \neq 0$$

$$\text{TRAN}_{X(i, j) \rightarrow (i + 1, j)} = K_{SK} * e_{SK} \dots\dots\dots 2.2$$

$$\text{IF } \Phi_{SK(i, j, k)} \neq 0 \text{ AND } \Phi_{SK(i, j + 1 + k)} \neq 0$$

$$\text{TRAN}_{Y(i, j) \rightarrow (i, j + 1)} = K_{SK} * e_{SK} \dots\dots\dots 2.3$$

Where K_{SK} is the absolute stratiform permeability and e_{SK} is the stratiform Super-K thickness. A phenomenological model was run with one injector and two producers to test how fast water breaks through. The observations were as follows:

- 2 darcies Super-K has a significant impact on water cut but little on water breakthrough.

- Super-K accelerates water breakthrough only when permeability is higher than 2 darcies.
- Super-K interconnecting fractures could delay water breakthrough as a consequence of the gravity segregation and storage capacity of the Super-K zone.
- The results showed that early water breakthrough is related mainly to fractures and Super-K layers come as a minor reason.

The simulation model covers 220 km² with 39 producers and 18 injectors. The Super-K layer was assigned 35% porosity and permeability of 2 darcies. A constant fracture conductivity of 40 D*m has been applied to all fractures in the model. Also, a single saturation with Kr curves was used for matrix cells and X-shape Kr was used for the fractures. The results of the simulation confirmed that fractures system is the controlling factor in the water-displacement process. **Fig. 2.8** represents excellent history matching to the water cut trend and cumulative oil achieved from the model. The results showed that water breakthrough occurs faster in the fractures than in the matrix and Super-K zones. Final remark was that the water movement is controlled by the complex network of the stratiform Super-K and tectonic fractures.⁴

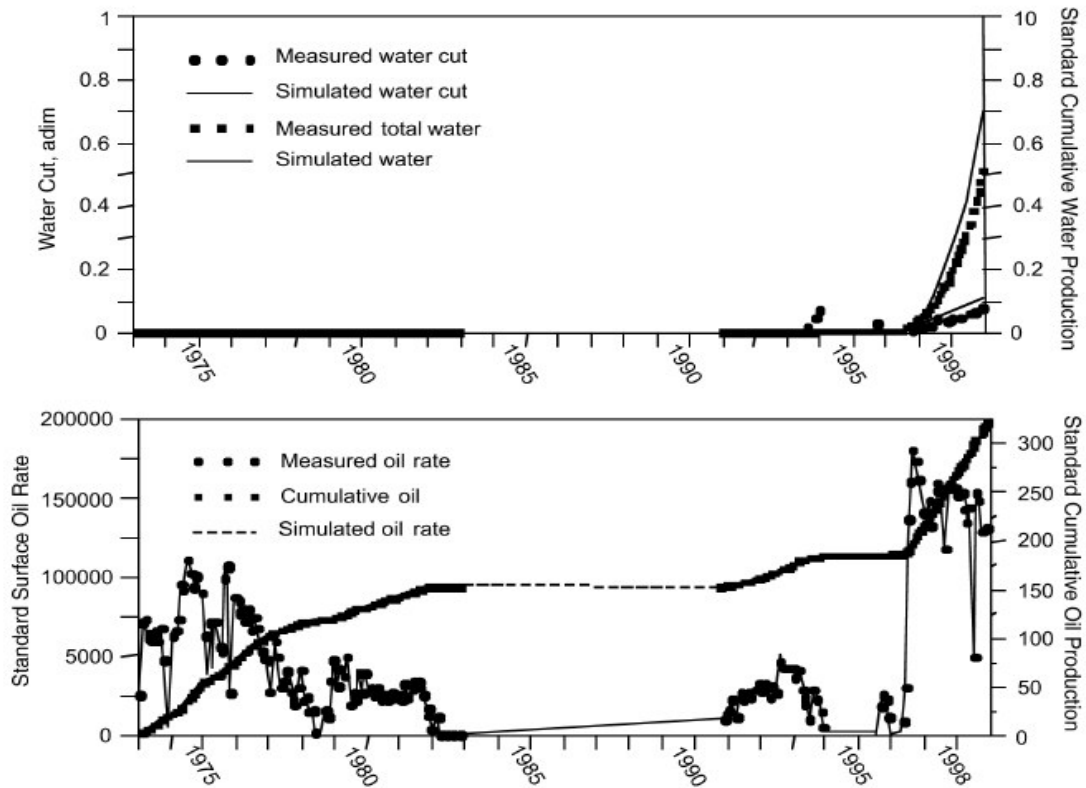


Fig. 2.8 - Water-Cut and Cumulative Oil History Match

Phelps and Strauss and Phelps *et al.*^{3,2} described a reservoir simulation model that investigates the effect of faults, fractures and super-k layers on reservoir performance. To simulate the vertical fractures, multiple of Local Grid Refinement regions (LGR) were used extending from the injectors to the Crestal area. The model also incorporated the Super-K phenomena to understand its impact on fluid flow dynamics. Before building a model, permeability and porosity values were given to each interval within a zone. A dual porosity model which was introduced by Warren and Root was used. The model consists of matrix properties and fracture properties. Fluid transfer between components is controlled by the pressure difference between components, fluid viscosity, matrix permeability, and a geometric factor known as shape factor. The shape factor is an

important parameter in understanding the transfer function or fluid mechanism between the matrix and fractures and vice versa. The shape factor will be highlighted in Chapter IV. The shape factor introduced by Kazemi is given by

$$\sigma = 4 * \left(\frac{1}{L_x^2} + \frac{1}{L_y^2} + \frac{1}{L_z^2} \right) \dots\dots\dots 2.4$$

To account for the Super-K layers, the shape factor was modified as

$$\sigma = 4 * \left(\frac{1}{L_x^2} + \frac{1}{L_y^2} + \frac{K_z}{K_y} * \rho_{sp}^2 \right) \dots\dots\dots 2.5$$

Where ρ_{sp} is the density of the Super-K layer on a vertical scan line (number of spikes per unit length). The model used is 118 x 74 x 17, with a 250-m grid width and 78 different vertical fractures simulated in the LGR.

Water production from the top of the reservoir (bottom of Zone-3) has been attributed to channeling through vertical faults and fractures according to field performance analysis. The model showed that no history match was achieved with out incorporating faults and fractures into the system. Those fractures were spaced every 500 meters in the simulation model. Water cut history matching was achieved based on adjustments made to the boundary condition, permeability values especially in the high permeable Super-K layers, and PVT data. Study of the outcrop showed that the top of Zone-4 was highly fractured and based on this information, the horizontal permeability of layers 12 and 13 were multiplied by a factor of 50. The optimum case that showed best water cut history match scenario was using a 35 multiplier in layers 12 and 13. Fracture spacing and super permeable layers played important factor in history matching the water cut. The stratified water encroachment was achieved after implementing all factors (vertical fracture spacing and Super-K layers).

Dogru *et al.*¹¹ studied a portion of the giant Ghawar field for the purpose of analyzing the Super-K phenomenon. Pressure in Ghawar field is maintained by peripheral water injection. The field contains faults, fractures and Super-K zones. The authors used POWERS simulator to simulate the Super-K behavior. GOSP-11 section of the Uthmaniyah was chosen as a candidate for the simulation study. GOSP-11 has stratiform dolomitic Super-K zones with extreme permeabilities and shown premature breakthrough and irregular flood front movement.

A small five-layer model (113 x 74 x 5) was created to test the model assumptions before building a large simulation model. A fracture grid was imbedded on the regular fine grids as shown in **Fig. 2.9**. Initial modeling showed reasonable results compared to overall historical reservoir performance. After simulating the small model, a multimillion-cell model was constructed using the same concept where the fine grid contains 100 x 100 meter cells. The fractures were superimposed using a 1-km spacing and 20 meters fracture width. The reservoir consists of 134 layers which were up-scaled to 67 layers. **Fig. 2.10** shows the geological zones of the reservoir. The model has 256 cells in the X-direction, 148 cells in the Y-direction and 67 layers summing a total of 2.54 million cells. Premature water breakthrough is most probably related to the combination of both the Super-K and faults. To simulate such a case, a super fast flow in the horizontal and vertical planes must be incorporated. The Super-K flow takes place in the horizontal and vertical planes as shown in **Fig. 2.11**.

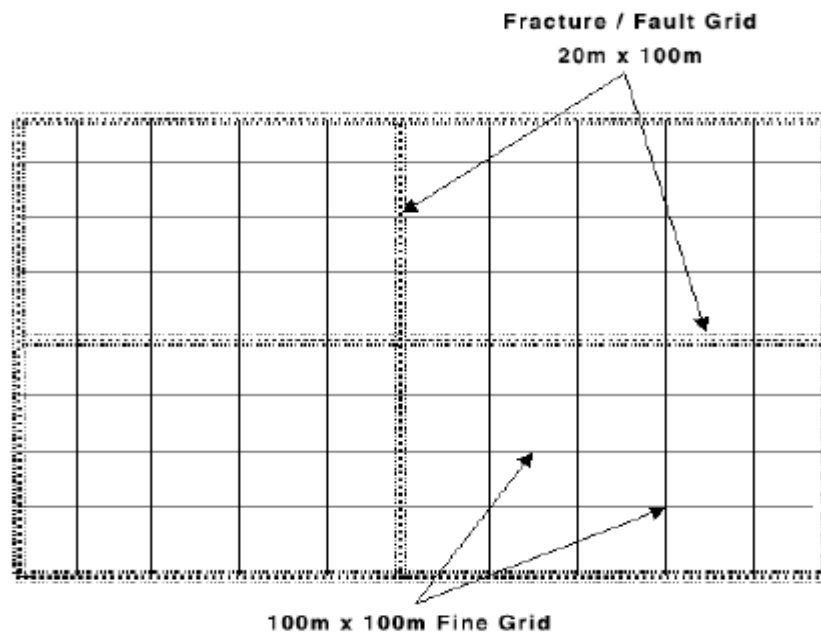


Fig. 2.9 - Fracture Grids Embedded in Fine Grids

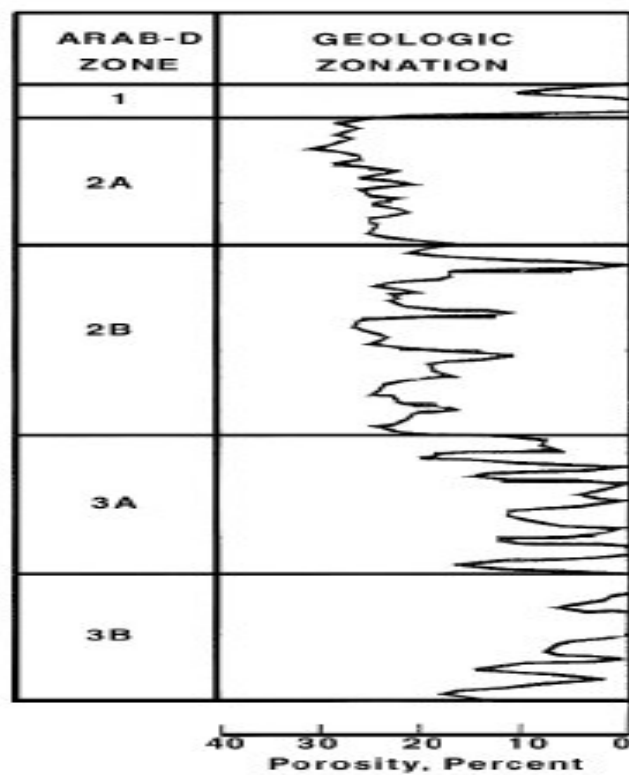


Fig 2.10 - Geological Zones of the Reservoir

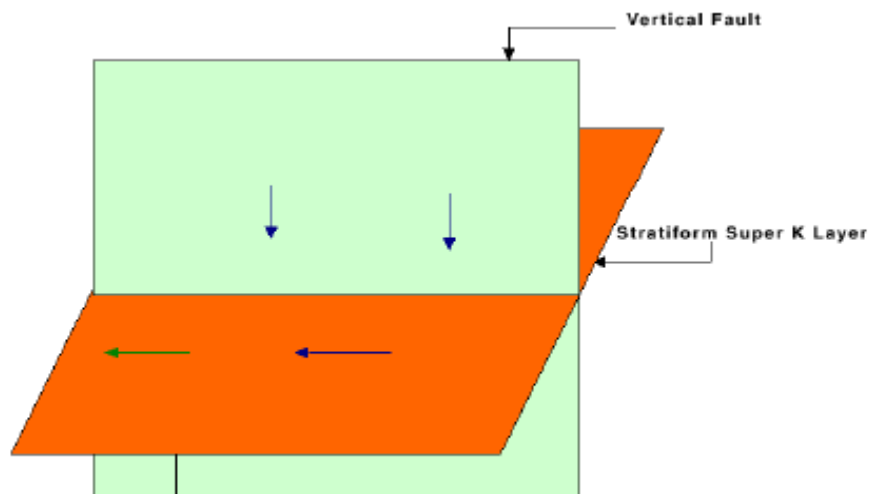


Fig. 2.11 - Horizontal and Vertical Flow in the Super-K

The Super-K permeability used in the model ranged from 40 to 70 darcies. Two relative permeability curves used, one utilizes rock curves and the second set utilizes straight lines for fractures and the Super-K zone. Only few cells were used to represent the aquifer and the pore volumes in those aquifer cells were adjusted to match the field observed pressure. The fast water movement was observed in Zone-3A and is believed to be related to fractures in the tight zone as presented in **Fig. 2.12**. The authors think that the faster water movement is due to capillary discontinuity between productive Zone-2B and the tighter Zone-3A. Large capillary difference between the two zones and with gravity forces, injected water will be imbibed by the tighter matrix (Zone-3A) and equal amount of oil will be displaced to the upper Zone-2B. With the use of this approach, the simulation results showed that water advanced faster in Zone-3A.

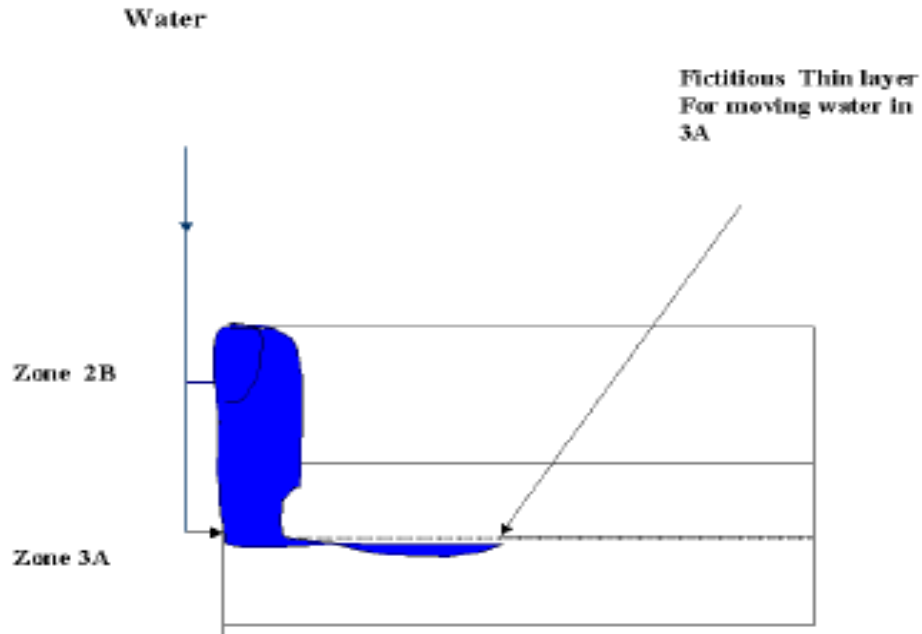


Fig. 2.12 - Fast Water Movement in Zone-3A Due to Fractures

After considering all facts and assumptions, a reasonable history match was obtained. Water production was matched adequately as can be seen in **Fig. 2.13**. Advancement of the flood front through the Super-K conduits is presented in **Fig. 2.14**. Fluid flow is matched accurately by using a dual porosity type grid and capillary discontinuity modeling concept.

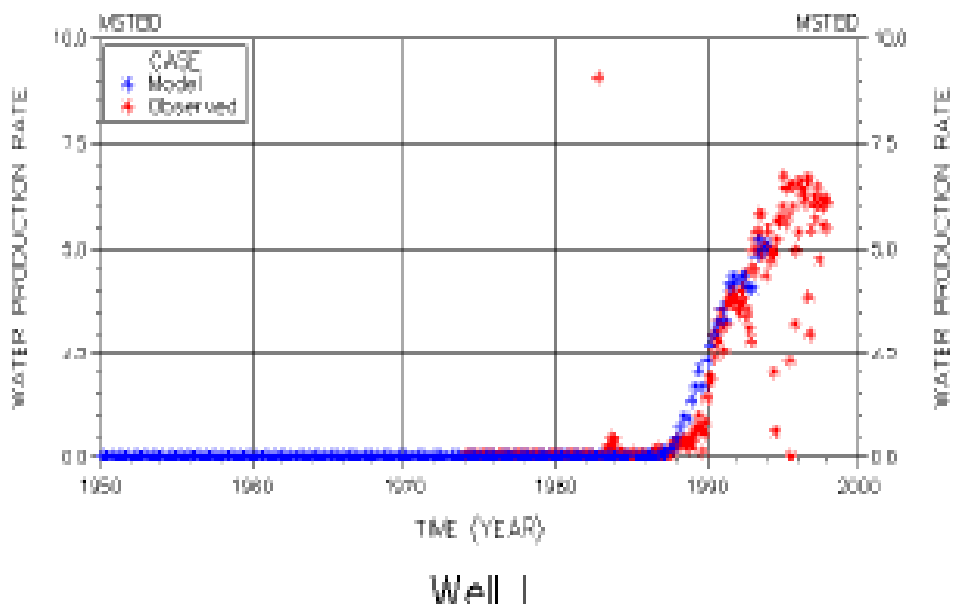


Fig. 2.13 - Water Production History Match

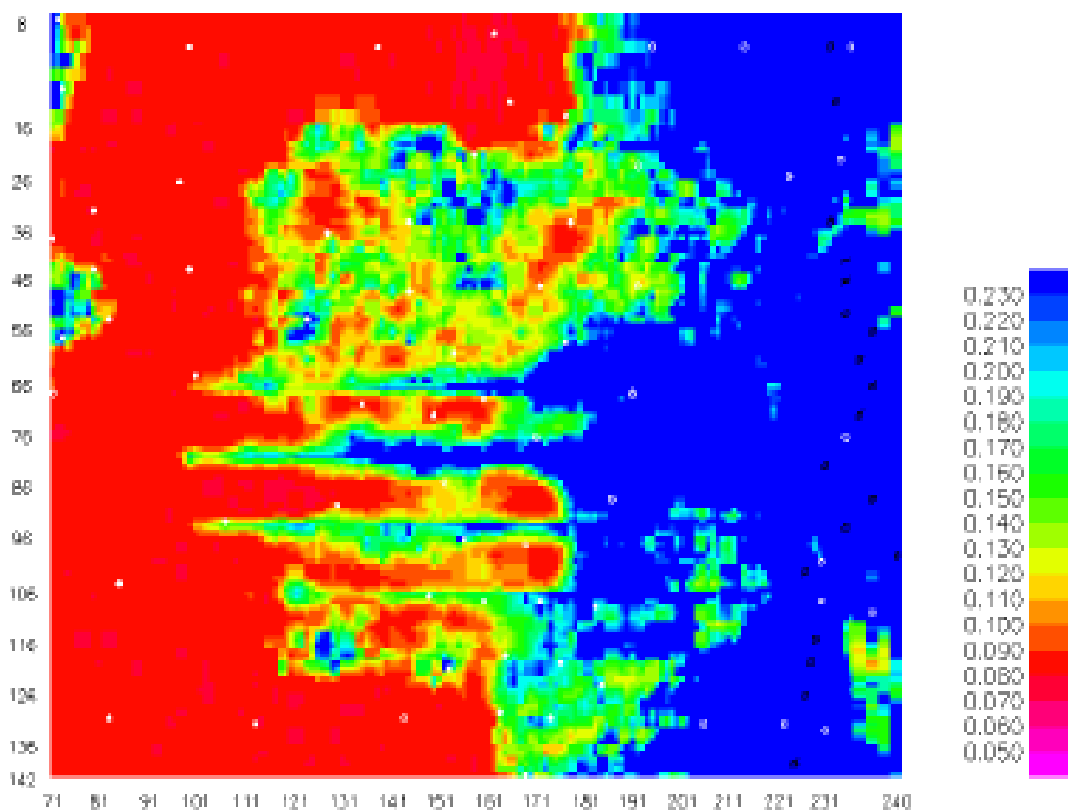


Fig. 2.14 - Advancement of the Flood Front through the Super-K

In conclusion, an overview of super high permeable zones was addressed above to understand the fluid flow mechanism in very thin layers called Super-K in a carbonate reservoir. The thin layers are likely to be bounded by impermeable layers in the Arab-D formation. The Super-K zones were found to have interconnection with faults and or fractures. Examples of production profiles were presented to identify the Super-K zones. Pressure transient test and simulation cases were highlighted for better understanding to the fluid flow mechanisms in the Super-K zones. Finally, it is critical to account for the Super-K layers in the simulation studies before a model can represent the actual reservoir behavior.

CHAPTER III

FRACTURE REVIEW

Reservoir characterization, modeling and simulation of naturally fractured reservoirs are unique due to the complexity and challenges of such reservoirs. It is not only the matrix and fractures that have to be characterized and modeled but also the interaction between matrix blocks and surrounding fractures has to be understood in a multiphase reservoir simulation. A naturally fractured reservoir (NFR) is characterized as a system of matrix blocks and each matrix block is surrounded by fractures. Usually the interconnected fracture system provides the main flow paths with high permeability and low storage volume, and the rock matrix is the main source of hydrocarbon with low permeability and high storage volume. Hence, oil production flows mainly from fractures to the wellbore. The physical mechanisms that are associated with matrix-fracture system include oil expansion, pressure or saturation diffusion, gravity imbibition or drainage, and viscous displacement or convection. Oil expansion and pressure diffusion are the most predominant mechanisms in NFRs.

An efficient approach in modeling NFRs has been through a dual porosity/dual permeability model, in which fractures and matrix systems are separated, each with its own set of properties. Mass transfer between matrices and fractures are modeled through “Transfer Function” that controls the interaction between matrices and fractures in a dual porosity model. Another important factor that takes place in transfer function calculation is the “Shape Factor”. The shape factor represents the geometry of the matrix elements and controls flow between two porous media.¹³

Since the fluid behavior of the Super-K layer involves interaction with fractures, the coming sections of this chapter will highlight some of the important work done to represent different shape factors and transfer functions used to represent the fluid transfer between the matrix and fractures in a dual porosity/dual permeability simulation model. The CMG™ simulator used in this research uses either the shape factor proposed by Warren and Root or Kazemi and Gilman. Their work is going to be presented in addition to the work of some other authors.

3.1 Transfer and Shape Factor

Warren and Root¹⁴ analytically investigated a one dimensional single phase unsteady state flow in fractures and quasi-steady state in matrix. Their model presented in **Fig. 3.1** was based on the following assumptions:

- The matrix containing the primary porosity is homogenous and isotropic, and is contained within a systematic array of identical, rectangular parallelepipeds or building blocks.
- The secondary porosity is contained within an orthogonal system of continuous, uniform fractures. The fractures are oriented so that each one is parallel to one of the principal axes of permeability; uniformly spaced and are of constant width. The fractures surround the building blocks.
- Formation fluid flows from matrix to fractures and the high conductive fractures carry the fluid to the wellbore column.

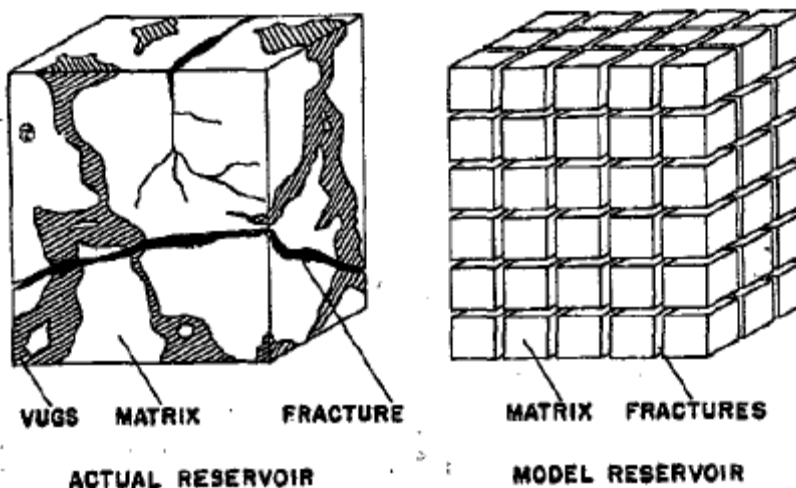


Fig. 3.1 - Warren and Root Fracture Model

To describe the communication between the primary and secondary media, a shape factor is needed. The shape factor reflects the geometry of the matrix elements and it controls the flow between the porous regions. The interporosity flow per unit volume, q , is given by

$$q = \sigma \frac{K_m}{\mu} (p_m - p_f) \dots\dots\dots 3.1$$

Warren and Root shape factor for uniformly spaced fractures while variations in the fracture width is allowed is given by the following formula

$$\sigma = 4n(n + 2)/l^2 \dots\dots\dots 3.2$$

Where n is the number of normal sets of fractures = 1, 2, 3 and L is the fracture spacing.

Kazemi *et al.* and Kazemi and Gilman^{15,16} solved for a multiphase flow in heterogeneous dual porosity reservoirs such as naturally fractured systems. They described stable, fully implicit, finite-difference simulator. The flow rates and pressures are solved simultaneously along with fracture and matrix fluid saturations and pressures

at all grid points. They also assumed that only the fractures produce into the wellbore and are the path of fluid flow from one grid block to another. For multiphase flow, three forces must be accounted for which are; gravity, viscous and capillary forces. The matrix blocks are further divided into grid blocks as in **Fig. 3.2** to get better definition of saturation distribution.

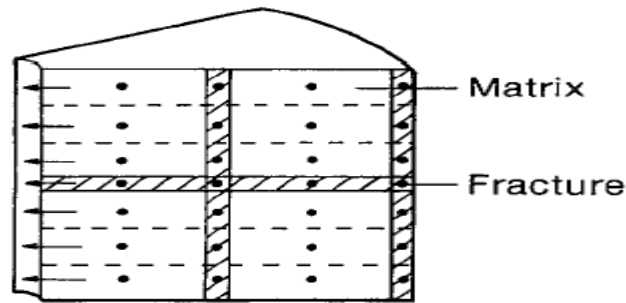


Fig. 3.2- Kazemi and Gilman Fracture Model

Kazemi *et al.* extended the Warren and Root model to multiphase systems to account for capillary and gravity forces. Their simulation equations to describe the flow in the dual porosity model for two-phase (oil and water) are as follows; for the fractures:

$$\Delta[T_{cf}(\Delta p_{cf} - g_{cf}\Delta D_f)] - T_{cma} * [(p_{cf} - g_{cf}D_f) - (p_{cma} - g_{cma}D_{ma})] + q_\alpha = \frac{V_b}{\Delta t} \Delta t \left(\frac{\phi S_\alpha}{B_\alpha} \right)_f \dots\dots\dots 3.3$$

And for the matrix:

$$T_{cma} [(p_{cf} - g_{cf}D_f) - (p_{cma} - g_{cma}D_{ma})] = \frac{V_b}{\Delta t} \Delta t \left(\frac{\phi S_\alpha}{B_\alpha} \right)_{ma} \dots\dots\dots 3.4$$

Terms in the equations are defined for the X-directional transmissibility for Cartesian coordinates as

$$T_{cfx} = 0.001127 \left(\frac{K K_{ra} \phi}{\mu_{\alpha} B_{\alpha}} \right)_f \left(\frac{\Delta y \Delta z}{\Delta x} \right) \dots \dots \dots 3.5$$

$$T_{oma} = 0.001127 K_{ma} \Delta x \Delta y \Delta z \sigma \left[\omega \left(\frac{k_r}{\mu B} \right)_{ma} + (1 - \omega) \left(\frac{k_r}{\mu B} \right)_f \right] \dots \dots \dots 3.6$$

And the shape factor is given by the following formula

$$\sigma = 4 * \left(\frac{1}{L_x^2} + \frac{1}{L_y^2} + \frac{1}{L_z^2} \right) \dots \dots \dots 3.7$$

The number of unknowns in equations 3.3 and 3.4 can be reduced by the use of the following saturation relationships in equations 3.8-3.11, which then give us four equations and five unknowns: fracture and matrix, water pressure, fracture and matrix water saturation, and wellbore flow rate.

$$S_{of} = 1 - S_{wof} \dots \dots \dots 3.8$$

$$S_{oma} = 1 - S_{wma} \dots \dots \dots 3.9$$

$$p_{of} = p_{wof} + p_{cf} \dots \dots \dots 3.10$$

And

$$p_{oma} = p_{wma} + p_{cma} \dots \dots \dots 3.11$$

The additional equation is the wellbore constraint which is giving by the following formula

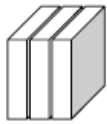


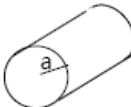

$$q_{\alpha} = A_{\alpha w} (p_{of} - p_{bh}) \dots \dots \dots 3.12$$

For radial flow into the wellbore, the coefficient $A_{\alpha w}$ is given by equation 3.13.

$$A_{\alpha w} = \frac{0.001127 (2\pi) \Delta z K_e}{\left(\frac{r_l^2}{r_l^2 - r_w^2} \right) \ln \left(\frac{r_l}{r_w} \right) - \frac{1}{2} + s} \left(\frac{k_r}{\mu B} \right)_{\alpha f} \dots \dots \dots 3.13$$

Many authors presented different shape factor formulas, which brought some confusion about which one is correct. Summary of an excellent study done by Mora and Wattenbarger¹⁷ at Texas A & M University to confirm the correct formulas for the shape factors by using numerical simulation (Gassim a single phase 1-D-2D and Eclipse 3D commercial reservoir simulator) under pseudo-steady state condition is presented in **Table 3.1** for different geometries: Slabs, Columns, Cubes, Cylinder and Spheres.

Table 3.1 – Shape Factor Values Based on Different Authors

Geometry	Constant Fracture Pressure					Constant Rate (pss)
	W & R	Kazemi	Zimmerman	Lim & Aziz	This Study	This Study
	12	4	$\pi^2 = 9.87$	$\pi^2 = 9.87$	$\pi^2 = 9.87$	12 *
	32	8	$2\pi^2 = 19.74$	$2\pi^2 = 19.74$	$2\pi^2 = 19.74$	28.43 *
	60	12	$3\pi^2 = 29.61$	$3\pi^2 = 29.61$	$3\pi^2 = 29.61$	49.48 *
			$18.17 \left(= L^2 \frac{23.11}{D^2} \right)$	$18.17 \left(= L^2 \frac{23.11}{D^2} \right)$	$18.17 \left(= L^2 \frac{23.11}{D^2} \right)$	$25.13 \left(= L^2 \frac{32}{D^2} \right)$
			$25.67 \left(= L^2 \frac{4\pi^2}{D^2} \right)$	$25.67 \left(= L^2 \frac{4\pi^2}{D^2} \right)$	$25.67 \left(= L^2 \frac{4\pi^2}{D^2} \right)$	$38.98 \left(= L^2 \frac{60}{D^2} \right)$

Based on the simulation results, when the boundary condition is constant pressure, the general formula for the shape factor given by Lim & Aziz was confirmed.

$$\sigma = \pi^2 * \left(\frac{1}{L_x^2} + \frac{1}{L_y^2} + \frac{1}{L_z^2} \right) \dots\dots\dots 3.14$$

And for the case of constant rate, an empirical shape factor has been derived.

$$\sigma = \frac{2.31 * n^2 + 9.5 * n + 0.19}{n} \left(\frac{1}{L_x^2} + \frac{1}{L_y^2} + \frac{1}{L_z^2} \right) \dots\dots\dots 3.15$$

In order to have a reasonable simulation results, one should understand the importance of crossflow between matrix blocks and fractures. The exchange of flow can occur by 1) compressible effects, 2) gravity, 3) capillary, 4) diffusion, and 5) viscous forces. The crossflow understanding and calculation is so important in observing the recovery performance in naturally fractured reservoirs. Transfer functions and shape factors are very important parameters in simulating NFRs using a dual porosity reservoir model.

3.2 Dual Permeability Modeling

Single porosity modeling is not efficient to represent the fluid flow mechanisms in a fractured reservoir where two media interact with each other. It is essential to use a dual porosity/dual permeability modeling for better representation to the interaction or fluid flow mechanisms between Super-K/Fractures and matrix cells. Three popular approaches are used to model field-scale flow in naturally fractured petroleum reservoirs. The approaches are: dual-porosity, discrete fracture network and dual permeability modeling. In a dual porosity modeling, there is no matrix-to-matrix flow, but there is matrix-to-fracture flow.

The dual-porosity models ignore any viscous displacement from the matrix; however methods were developed by some authors that account for this displacement mechanism. The discrete fracture network relies on 3-dimensional mapping of fracture

planes. It requires very precise description of fracture network and has been widely applied in single-phase systems because of the large computational efforts required. In the dual permeability idealization of the reservoir, the matrix blocks communicate with each other; therefore there is matrix-to-matrix flow in addition to matrix-to-fracture flow.

In this model, the reservoir is assumed to be composed of a set of vertical columns of matrix blocks surrounded by interconnected vertical fracture planes as presented in **Fig. 3.3**. The capillary pressure forces interact with the gravity forces to elevate or oppose matrix drainage.¹⁸ Since in the reservoir, there is fluid flow between matrix to matrix with fractures enhancing the flow, dual-permeability modeling has been chosen to understand the fluid flow mechanisms between different media.

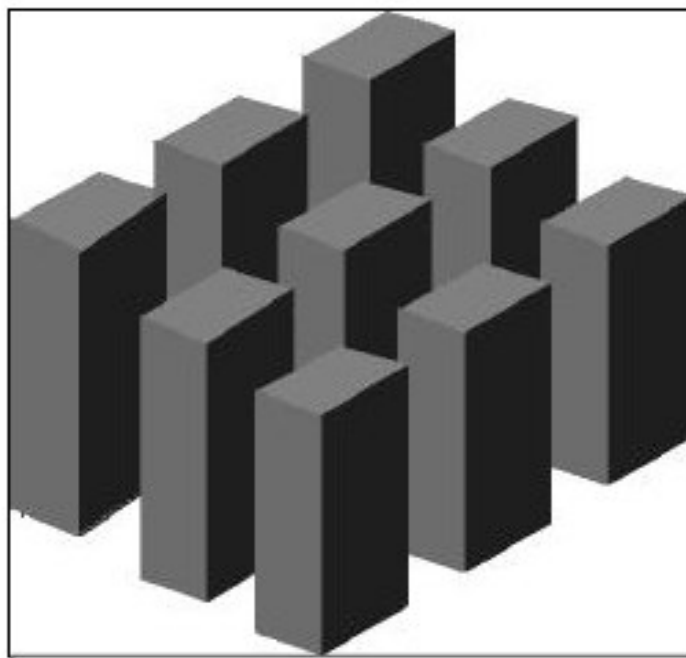


Fig. 3.3 - Interconnected Vertical Fracture Planes

CHAPTER IV

HYPOTHETICAL HISTORY MATCHING

In a conventional reservoir, it is easy for reservoir engineers to collect the data needed (reservoir geology, rock and fluid properties, results from well logs and formation evaluation...etc) for reservoir performance assessment. In fractured reservoirs however, collecting a reasonable data and predicting reservoir performance is more difficult than for a conventional reservoir. For a better modeling and reservoir development, one need precise description of reservoir properties including fracture mapping in terms of size, conductivity, connectivity and frequency distribution and then turning this information into a consistent fracture network characterization.¹⁸

So, to achieve a real history match for the whole field or even for a smaller sector of the field, one should know that the reservoir is the most heterogeneous reservoir in the world and each layer changes in properties from one to another. This makes it a very difficult job to history match production or pressure profiles. For this reason, a small sector in the Crestal area was selected with four imaginary injectors placed at the water flood front which is considered to be the boundary region for the model.

The purpose of the work in this chapter was not to develop a good representative history match to the reservoir parameters but rather to create a reasonable model that can test the interaction between the Super-K layer, natural fractures and the rest of the reservoir matrix. In the next sections, the simulation model will be discussed in details and sensitivity studies (mechanistic- cause and effect) will be conducted to study the

interaction between different Super-K and fracture parameters with the rest of the reservoir matrix.

4.1 Simulation Model Construction

In this section, building the simulation model will be discussed in details. The commercial CMG™ builder was used to construct the simulation model. The builder is shown in Fig. 4.1.

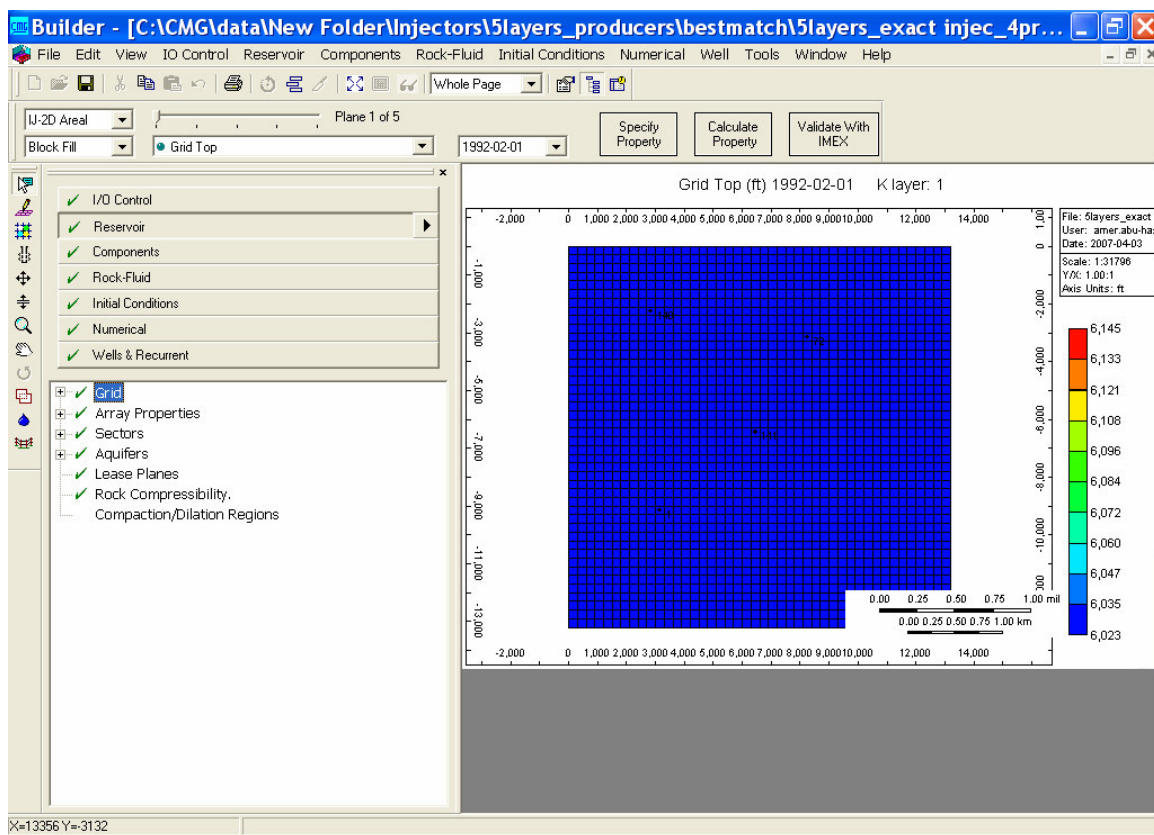


Fig. 4.1 – CMG™ Builder Used for Simulation Runs

The dimension of the reservoir small sector model was chosen to be 44 x 44 x 5 (9680 blocks) with 300 ft block width and five different layers. The simulation type is dual permeability to account for the fluid flow between the matrix blocks. The model

consists of four regions as presented in **Fig. 4.2**. The first region includes the matrix blocks. The second region is the fractures sector which is concentrated in the middle of the reservoir model. The third one is the Super-K layer located in the third layer inside the fracture network and the last one is the boundary region as a box located before the last block in each side of the model made to account for reservoir volume and help slow the depletion process. Two weak aquifers are located in the fifth layer at both edges of the model covering 23 blocks in each side. Each aquifer is about 20 ft thick and of a 100 ft radius. This aquifer represents a real case scenario since the reservoir has a weak aquifer that was not enough to pressure support the reservoir. Injectors were drilled at the reservoir boundary to maintain the pressure.

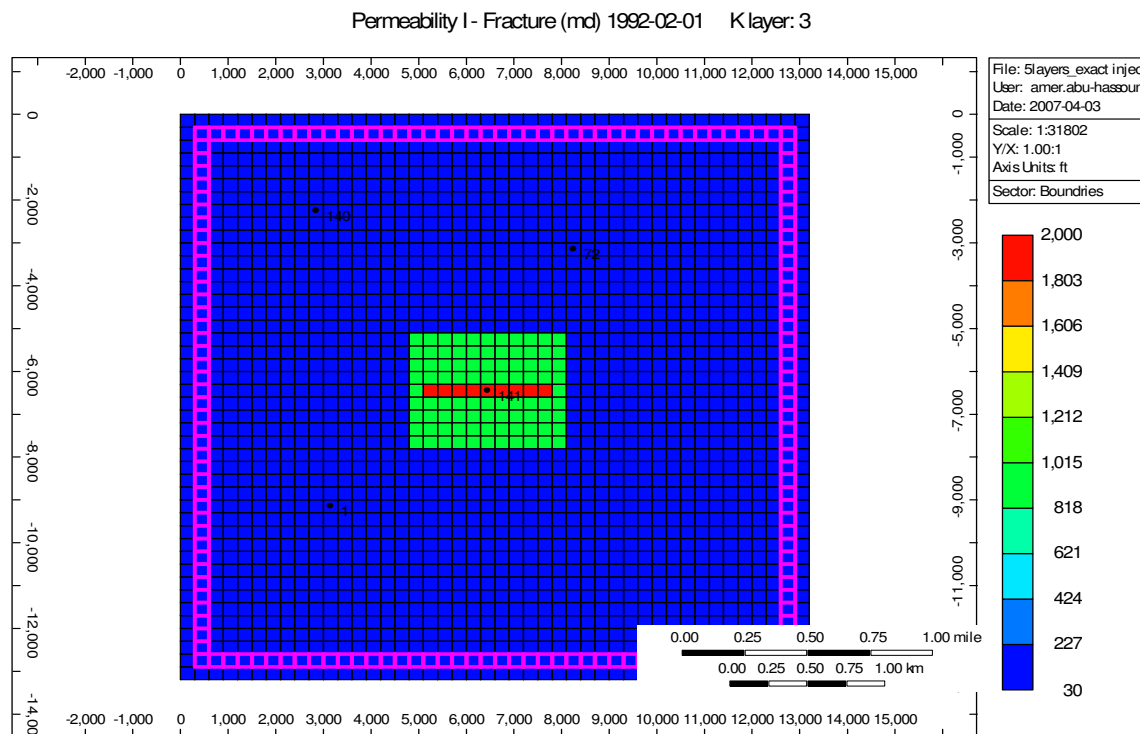


Fig. 4.2 - Four Regions in the Model: Matrix (Blue), Boundary Sector (Pink), Super-K Sector (Red) and Fractures Sector (Green)

The model has four vertical producers completed in the top four layers including the subject well P-141. Since the weak aquifers were not enough to pressure support the reservoir, four injectors were placed at each corner of the model for reservoir pressure maintenance as will be seen in the pressure matching section in this chapter. The tabulated reservoir data and figures are presented in **Appendix A**.

4.2 Producer P-141

The wells (producers and injectors) were located in such away they represent the right location on the real reservoir. P-141 is the subject well which intersects the Super-K layer in the third layer. P-141 was drilled as a vertical well in the Crestal area (the center of the reservoir) and had a complete loss of circulation at 6,090 ft where the Super-K layer is found based on a PLT run shown in **Fig. 4.3**. The well was producing dry oil at an average rate of 15,000 bbls/day with 70 % of the flow coming from a 4' interval (the Super-K layer thickness). In 1998, it was decided to plug-in the Super-K zone for better sweep efficiency and to control the water movement. A liner was run across the Super-K zone and the wellbore extended as a 6-1/2" deviated open-hole across the entire reservoir. However, after putting the well on production, P-141 production rate reduced dramatically to an average rate of 3,000 bbls/day with 1 % water cut.

The Super-K layer is assumed to extend for about 2700 ft in the third layer of the model. Three more producers (P-1, P-140, and P-72) were selected to give a better representation of the fluid flow in the model. A final step was to account for the sharp pressure drop from 1990 to 1992. As part of increasing the reservoir pressure strategy of maintaining the bottom-hole pressure, water injectors were drilled at the flanks of the

reservoir. Four injectors (I-121, 135, 77, & 90) were placed at the four corners of the model and were enough to provide a good pressure support to the simulator.

All the required data were entered into the simulator model (including estimated values of production and injection rates from the actual field data) and after several runs, a reasonable bottom-hole pressure history match of P-141 well pressure is achieved between years 1991 to 1998 as noticed in **Fig. 4.4**. After 1998, P-141 was shut-in for a workover job and was drilled as a slanted well across the entire reservoir, however when the well was put on production, the oil production drastically decreased from 11,000 bbls/day to ~ 3,000 bbls/day. This drop in production and the shut-in of P-141 for one year while maintaining the same water injection rate caused the pressure to increase in the reservoir as noticed in the same figure after year 1998.

The total production from all the wells also decreased due to lower demand which helped the reservoir pressure to increase. These changes were hard to match, so critical assumptions to P-141 completion profile were chosen. It was assumed that the well was kept vertical and the Super-K was producing but with exponential decline rate factor as will be explained in the next section.

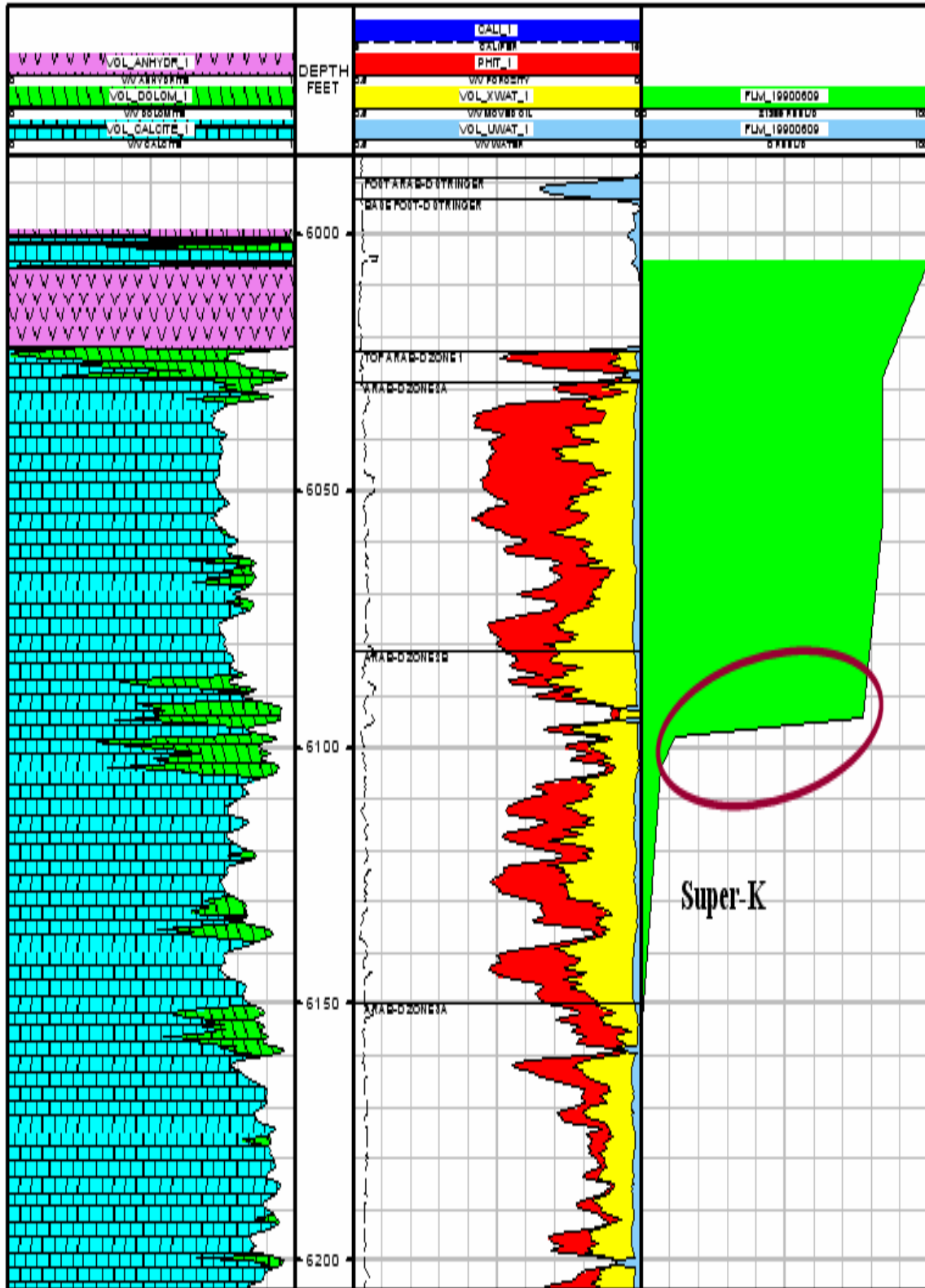


Fig. 4.3 - Well P-141 Production Logging Profile Showing Super-K Zone

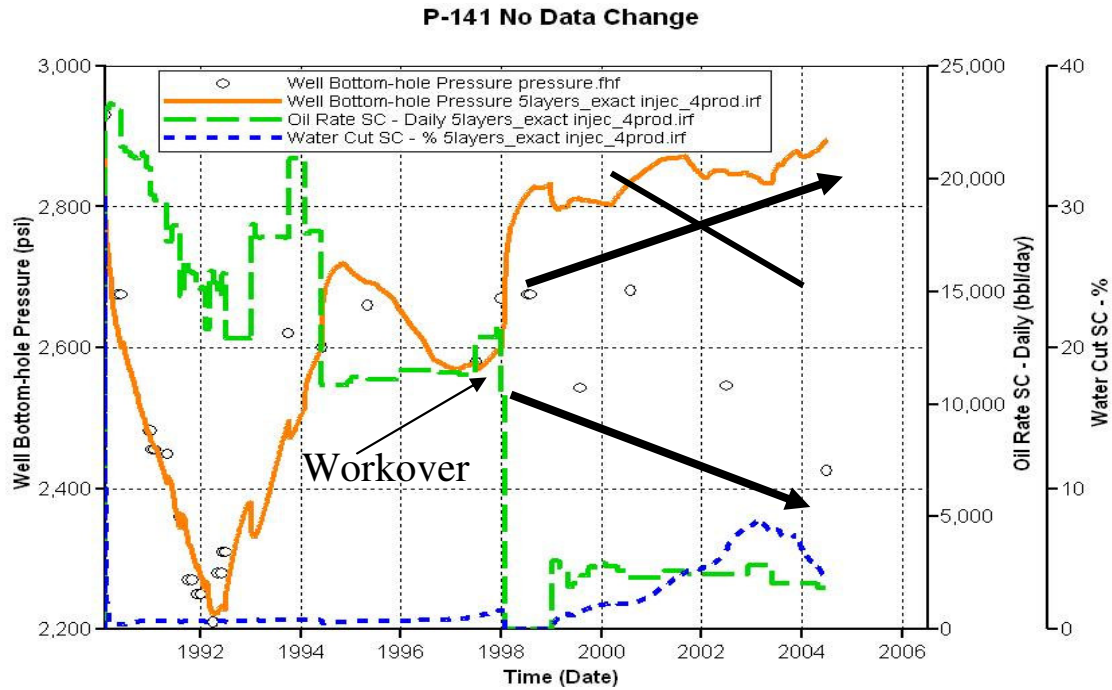


Fig. 4.4 - Good History Match Until 1998

4.3 Changes to Oil Rate

A simple calculation to achieve the exponential decline rate from all the producers showed that the reservoir is declining at a rate of 10 % per year. So, another simulation run including a 10 % decline to the P-141 well production rate after 01/1998 yielded a better match as shown in **Fig. 4.5**. This step showed the significant impact of keeping the Super-K layer opened to achieve a better history match. Though the pressure history match improved, there was a slight increase in W.C. after year 2000 from 7 % to 10 %.

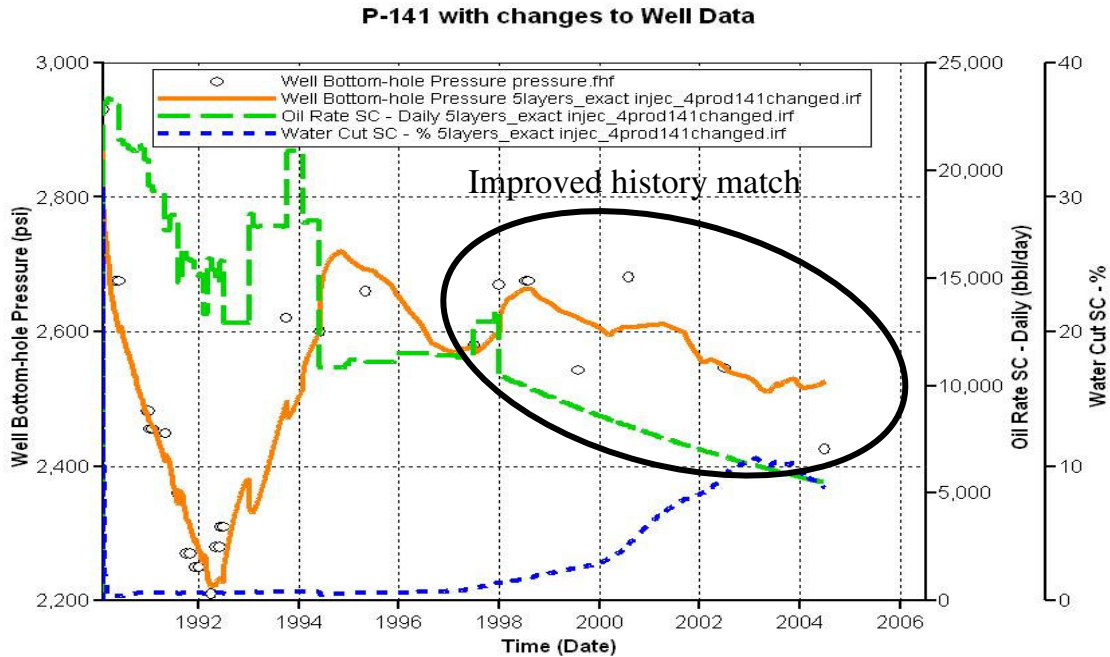


Fig. 4.5 - Improved History Match After Year 1998

4.4 Model Limitation and Errors

Since there have been a lot of data assumed, the model is still considered hypothetical and may not represent the actual fluid flow behavior in that small sector of the field. The history match was achieved after assumptions made to the rate and completion geometry of P-141 which does not reflect the actual completion history of the well. There is no fracture data (fracture spacing, length, width, permeability, porosity...etc) available from FMI logs or core data that can represent the actual fracture behavior in the reservoir. All of the fractures data has been assumed based on the available literature information which can introduce some errors to the simulation model.

CHAPTER V

SENSITIVITY STUDIES

The purpose of this chapter is to examine the interaction between Super-k layer and fractures with the rest of the matrix blocks. Parameters like fracture spacing, fracture length, Super-k extension, intersecting between fractures and Super-K will be changed in to understand the Super-K behavior which will help determining the best completion practice in the future. Fractures have significant impact on early water breakthrough. Fractures if connected to a water source can vertically bring water prematurely to the wellbore causing the well to produce huge amount of water. The situation gets worse if the fractures are connected to a high permeability layer (Super-K) with high horizontal permeability. As a result, water production will be higher with reduction to the recovery factor.

In this chapter, several runs will be conducted to examine the effect of fractures and Super-K layer on water production. All the sensitivity cases were run using the best match case where well geometry of P-141 is vertical and a 10 % decline rate is used after 1998.

5.1 Fracture Length

The fractures are varied in three different ways in the model. The effect of fractures will be studied when they are placed at the top two layers; when intersecting all layers including the fifth layer where water is injected and last will be placed in all layers but will not intersect the third layer where the Super-K zone is located.

5.1.1 Fractures at the Top Layers

In this case, the fractures are only connected to the first top two layers. Since the fractures are not connected to the Super-K zone or close to the water source, the water production in this case is steady and water cut is low as noticed in **Fig. 5.1**.

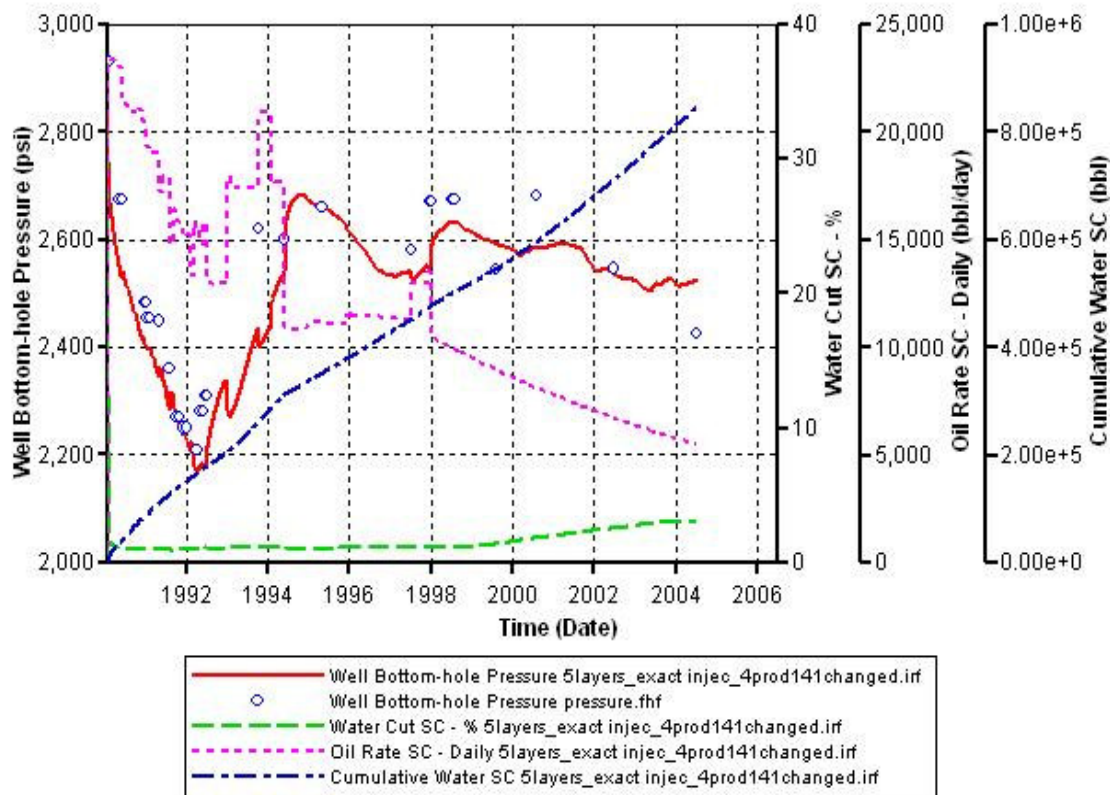


Fig. 5.1 - Run Results of Fractures at the Top Layers

5.1.2 Fractures Intersecting All Layers

The fractures are connected to all layers including the fifth layer where the water is injected. If the water approaches producer P-141, one would expect the water to breakthrough quickly. In this study, the fractures are linked to layer-5 in the model and also intersecting the Super-K zone in the third layer. As noticed in **Fig. 5.2**, the water

broke through prematurely due to the fact that fractures act as water conduits. Also the calculated pressure is lower than the actual data because of water production.

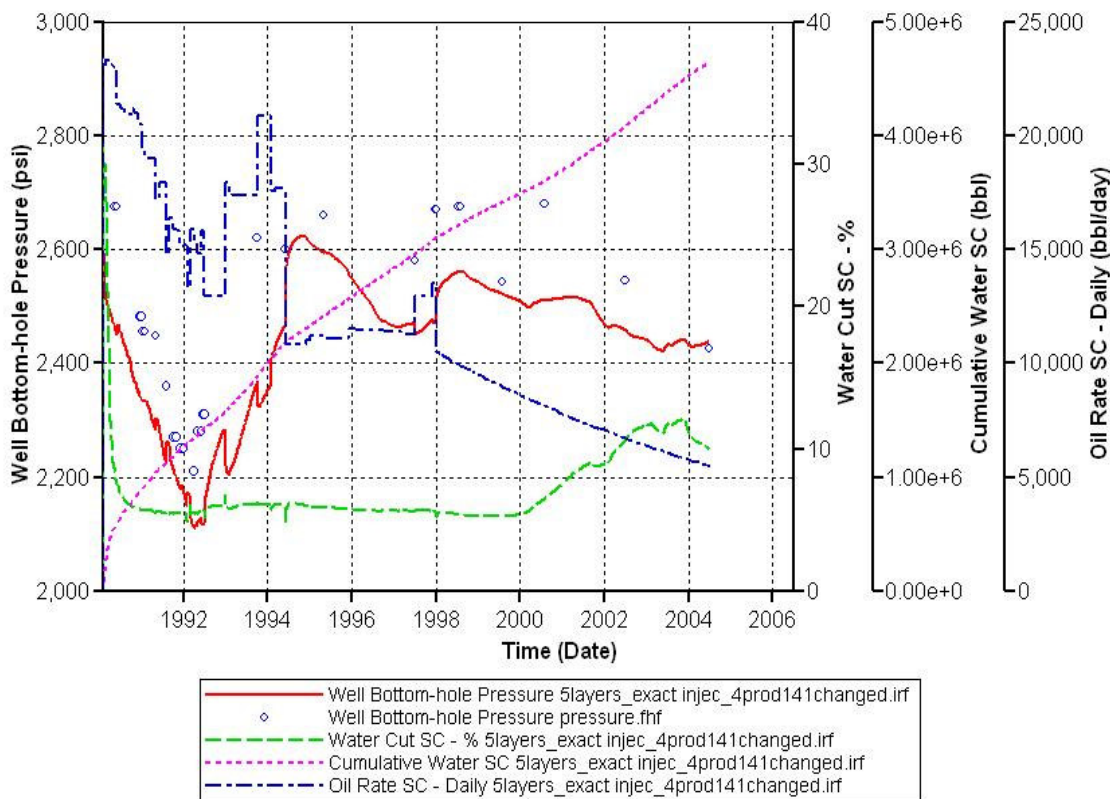


Fig. 5.2 - Fractures Intersecting All Layers Run

5.1.3 Fractures in All Layers but Not the Super-K

In this case fractures intersected all layers except the Super-K interval to investigate if the Super-K layer will have any effect on water production if the fractures are present. As seen in **Fig. 5.3**, the water cut is less than the case where the fractures intersect all layers but still water broke through prematurely. The bottom-hole pressure match followed the same trend of the real pressure data. In this case, the Super-K zone

did not contribute much in bringing water to the wellbore if compared to the fractures contribution.

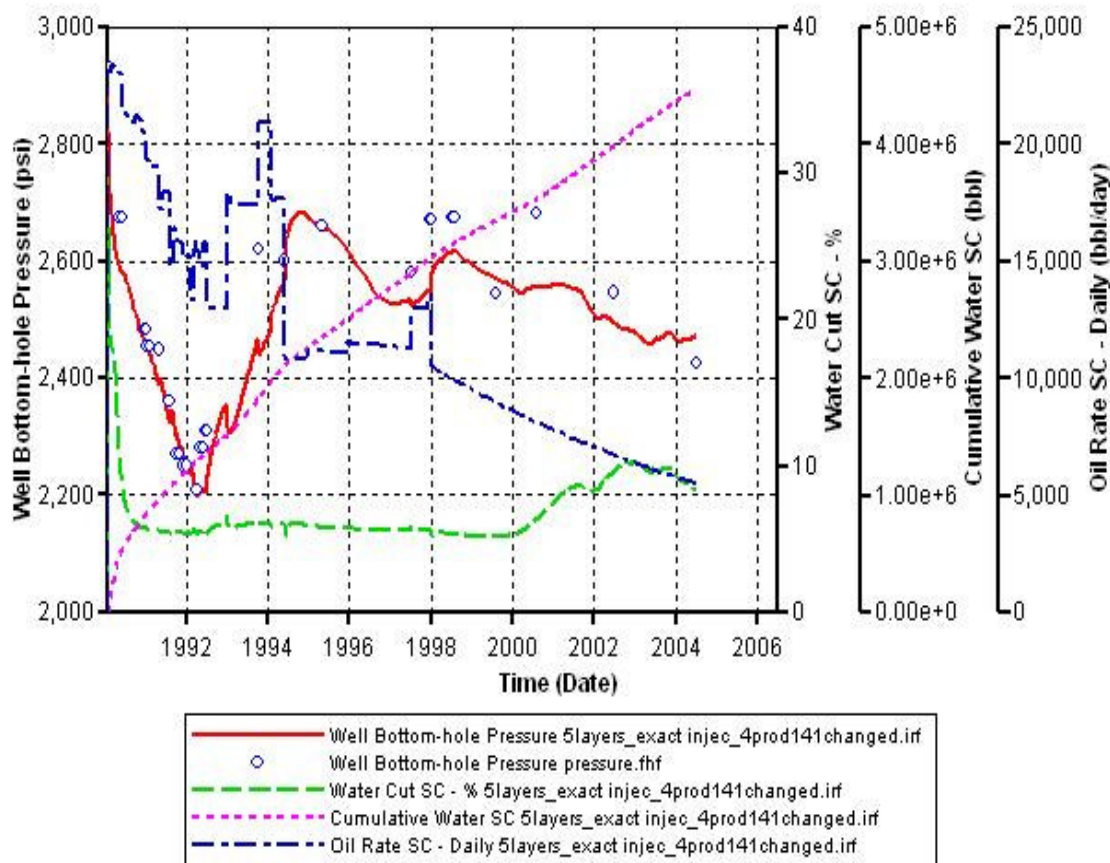


Fig. 5.3 - Fractures Not Intersecting the Super-K Layer

Another plot is prepared to compare the water production from all the cases to point out the significant of fracture length in the simulation model. **Fig. 5.4** shows that if fractures are away from the water source, then water production is way lower than if fractures were connected to the fifth layer as noticed from the case where fractures only intersect the top two layers. Also, the Super-K zone was not a primary factor to cause pre-mature water breakthrough.

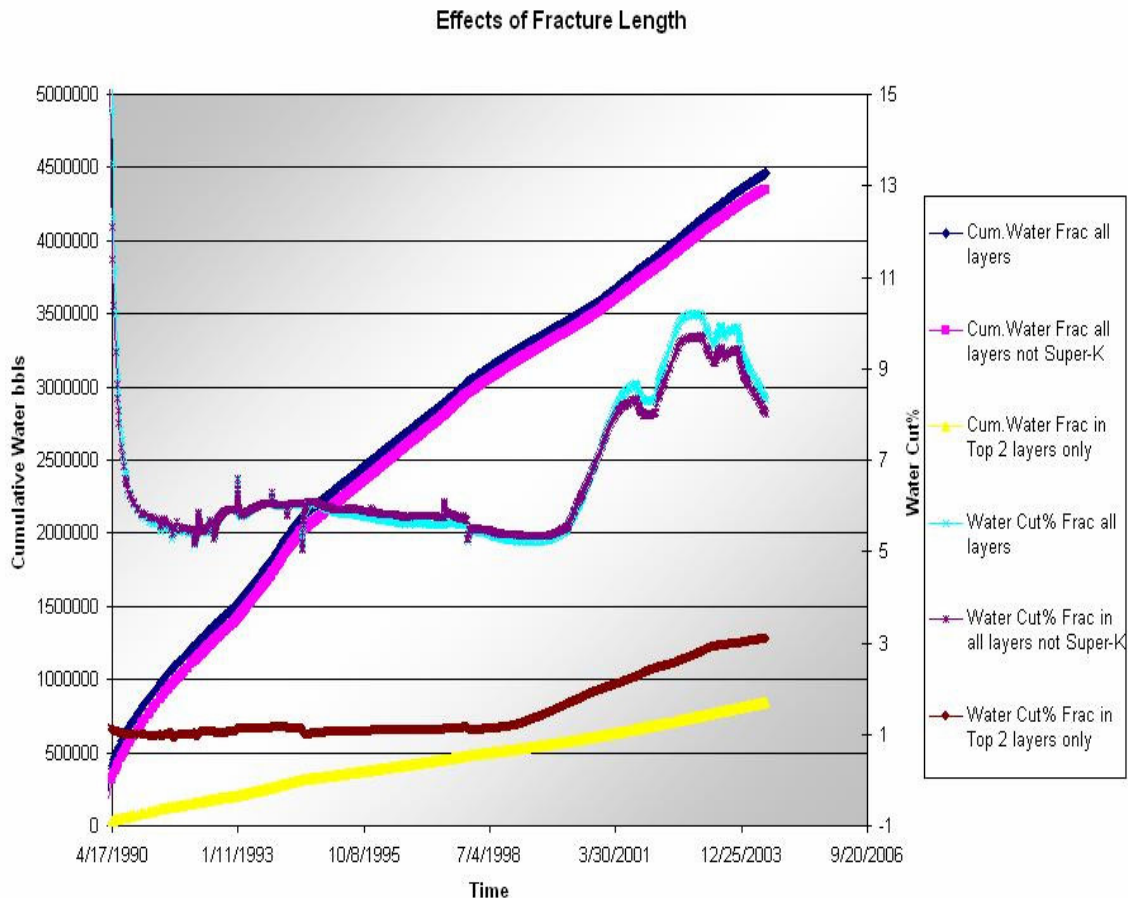


Fig. 5.4 - Comparison Plot to the Three Runs

5.2 Super-K Length

The Super-K length is varied in the model to see if the Super-K zone will affect the water channeling to the wellbore. The modeling is done with fractures embedded in the model and compared to the results for another case with no fractures. Different lengths are run for 300 ft and 10,200 ft of Super-K lengths. Two runs are presented in **Figs. 5.5** and **5.6** below.

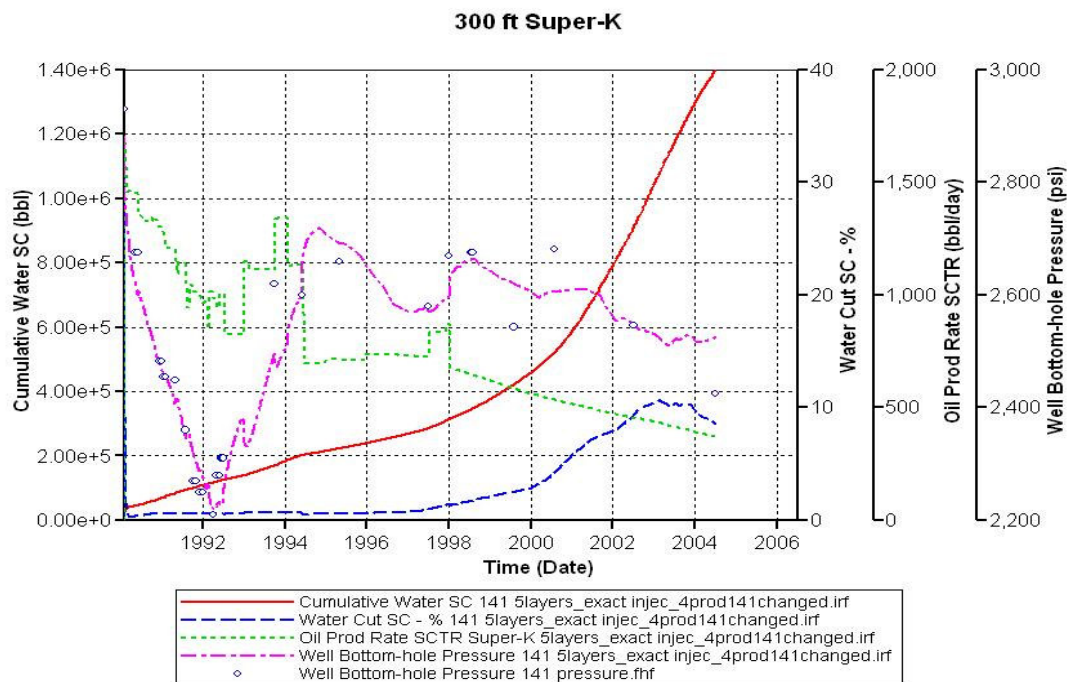


Fig. 5.5 - Run Results of the 300 ft Super-K Length

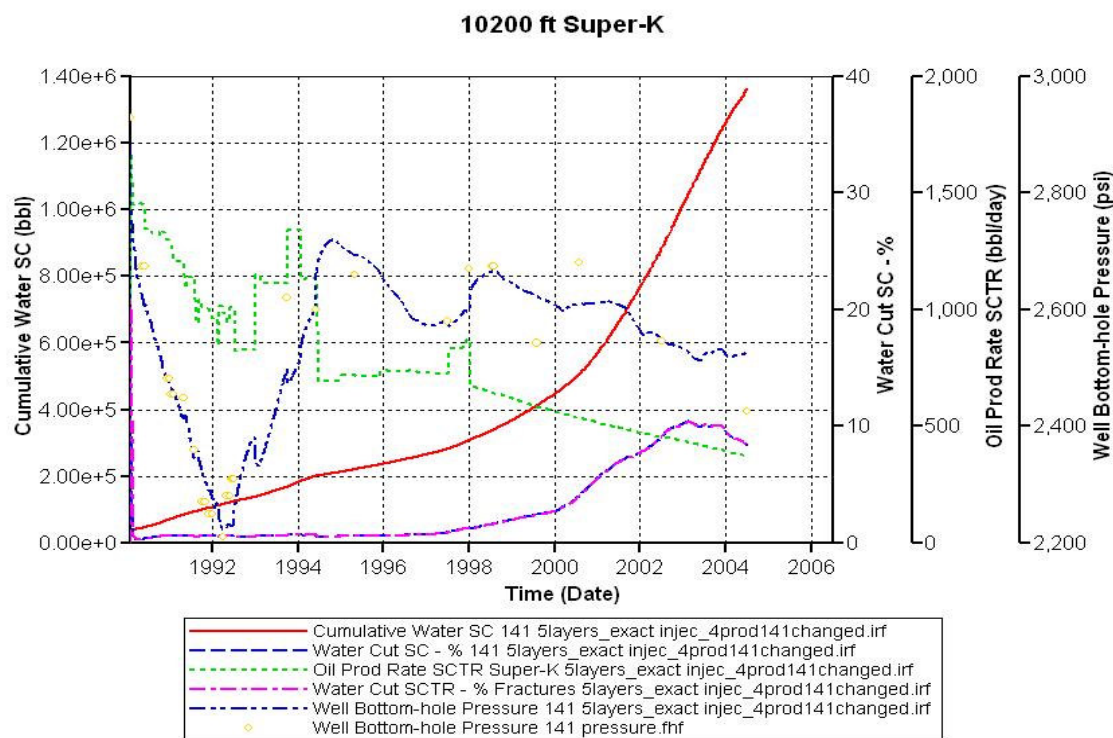


Fig. 5.6 - Run Results of the 10200 ft Super-K Length

As noticed in the plots, there was no effect in varying the Super-K length on water production or pressure profile because fractures dominate the flow since the water cut in the fractures matches the calculated water cut produced from the wellbore. Another comparison is made to compare the results shown above by varying the Super-K length with no fractures in the model. The result of running the 10,200 ft Super-K length is presented in **Fig. 5.7** below.

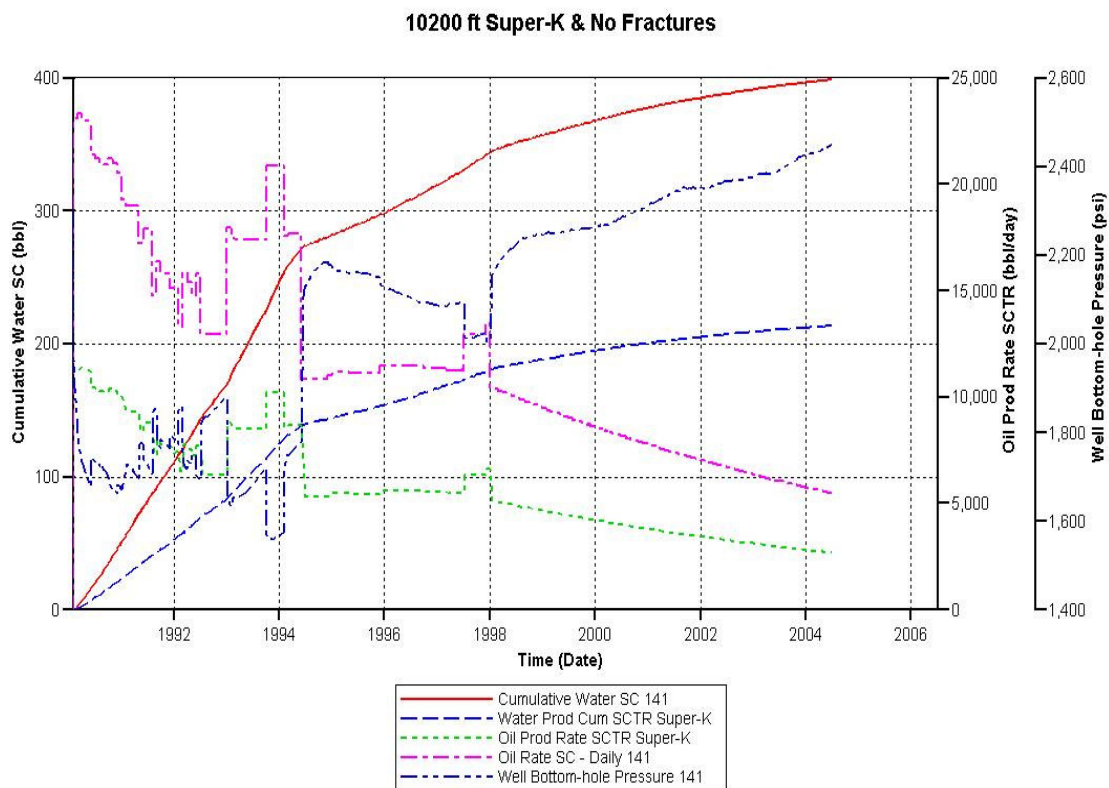


Fig. 5.7 - Run Results of the 10,200 ft Super-K Length, No Fractures

Analyzing this figures yielded the following results:

- Almost half the water production was coming from the Super-K but still very low compared to the case which has fractures embedded in the model.

- Also, the calculated pressure profile does not follow the real field pressure as seen in previous plots when the fractures were accounted for in the model.

The cumulative oil and water production from the 300 ft and 10,200 ft Super-K length is presented in **Fig. 5.8** for the case with no fractures in the model.

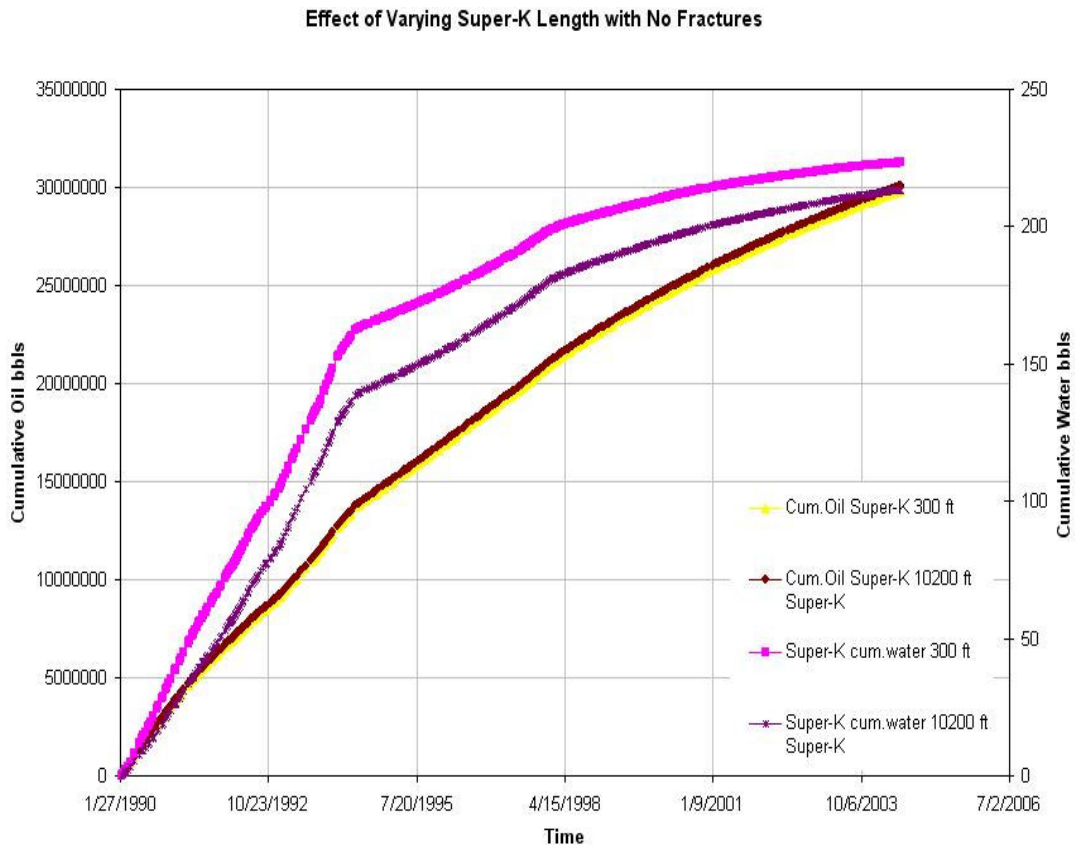


Fig. 5.8 - Comparison Plot of Cumulative Production for the Model, No Fractures

The cumulative oil production result for the 300 ft and 10,200 ft Super-K length is close to each other. The well has a very low water production in the case where fractures are not present in the model. **Fig. 5.9** shows how slow water approaches well P-141 in layer-5 by end of the simulation run with 10,200 ft of Super-K length compared with **Fig. 5.10** where fractures are present for the same Super-K length. The figures clearly show

the importance of the fractures in bringing water prematurely to the wellbore, shortening life of the well and leaving behind un-recovered oil.

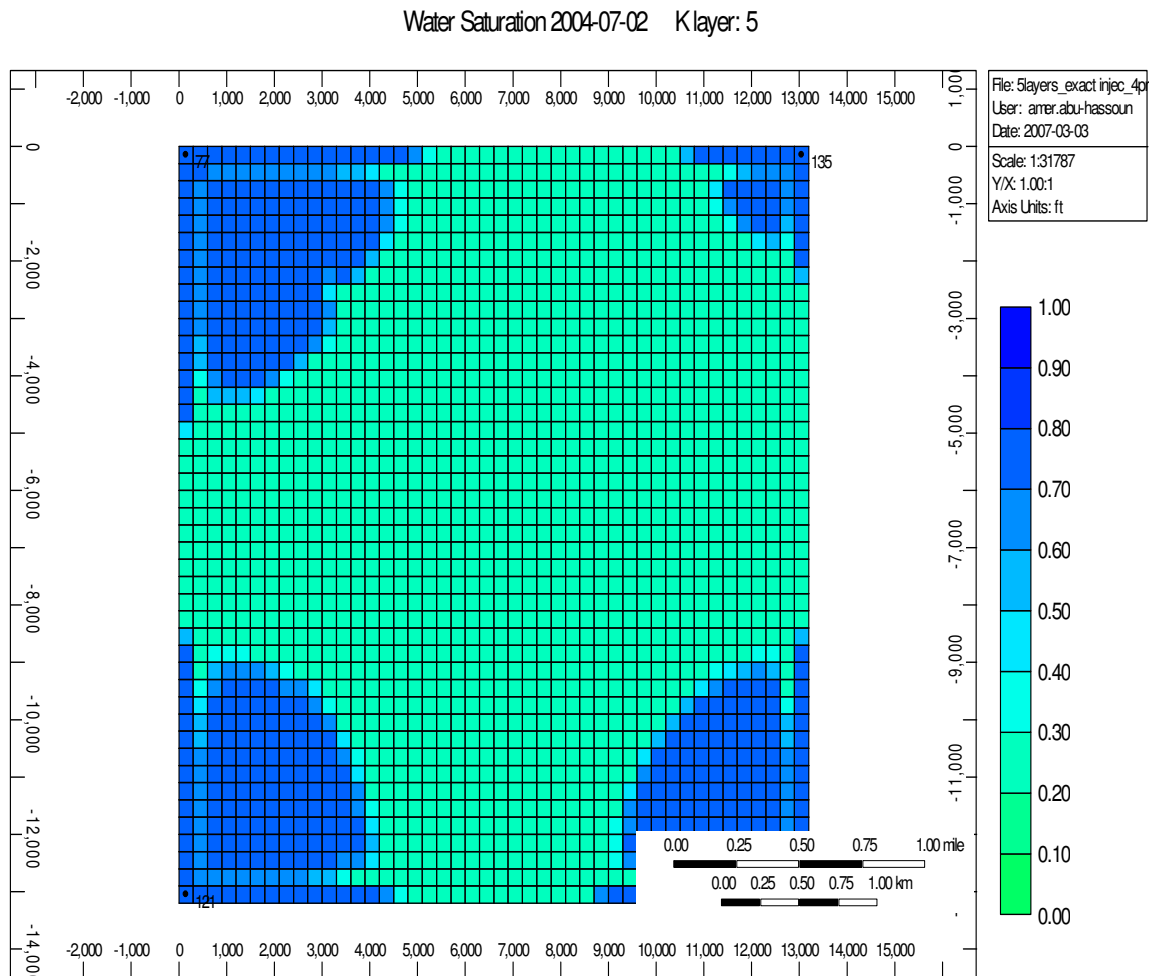


Fig. 5.9 - Water Slowly Approaches P-141 in Layer-5 by End of Simulation Run

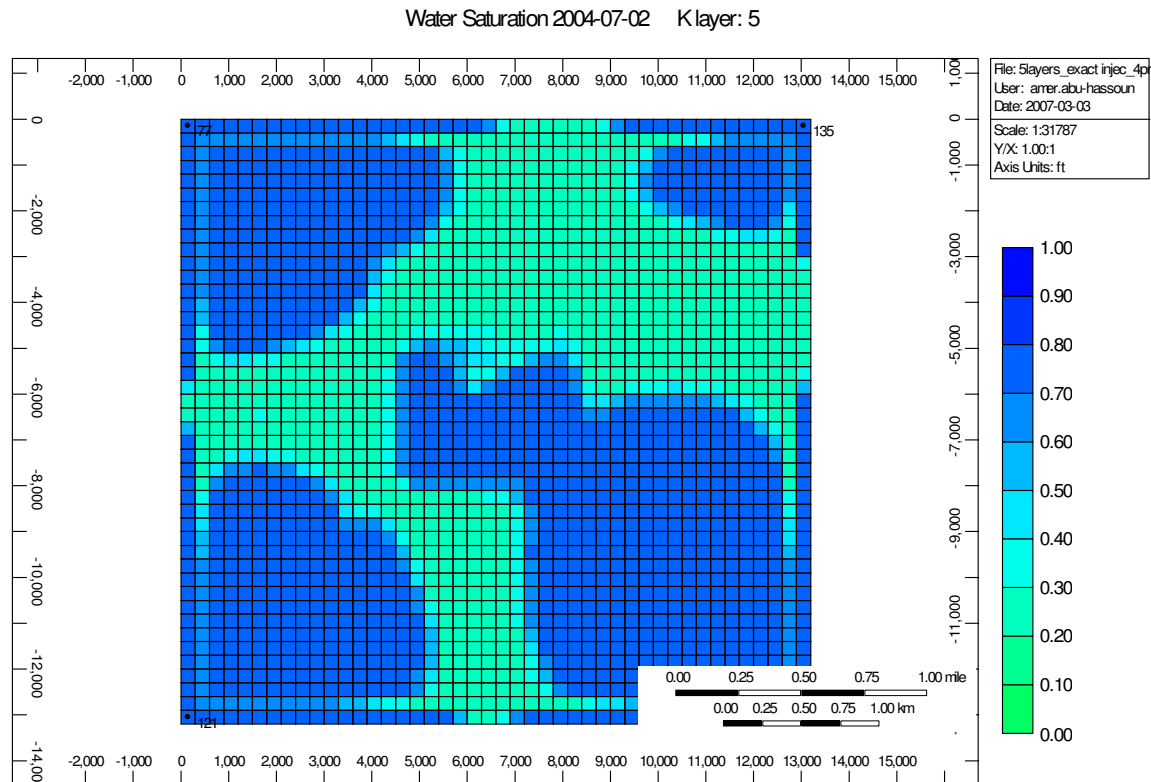


Fig. 5.10 - Fractures Presence Cause Quick Water Channeling

5.3 Super-K Porosity

In order to get the right porosity value, it is necessary to examine the rock in the laboratory. The Super-K porosity could be moldic, vuggy connected or interconnected porosity or could be channels that have high porosity. Since, the right porosity value for the Super-K is not available; a sensitivity study has been conducted by varying the Super-K porosity (45% and 75%) to see the effect on production profile. The Super-K and fractures permeabilities are 2,000 mD and 1,000 mD respectively. Cases were run to investigate the effect of varying Super-K porosity on production profiles. The results are plotted in the **Figs. 5.11** and **5.12** below for 45% and 75% Super-K porosity, respectively.

In these two cases, changing the Super-K porosity did not affect the production profiles and the fractures still dominate the flow.

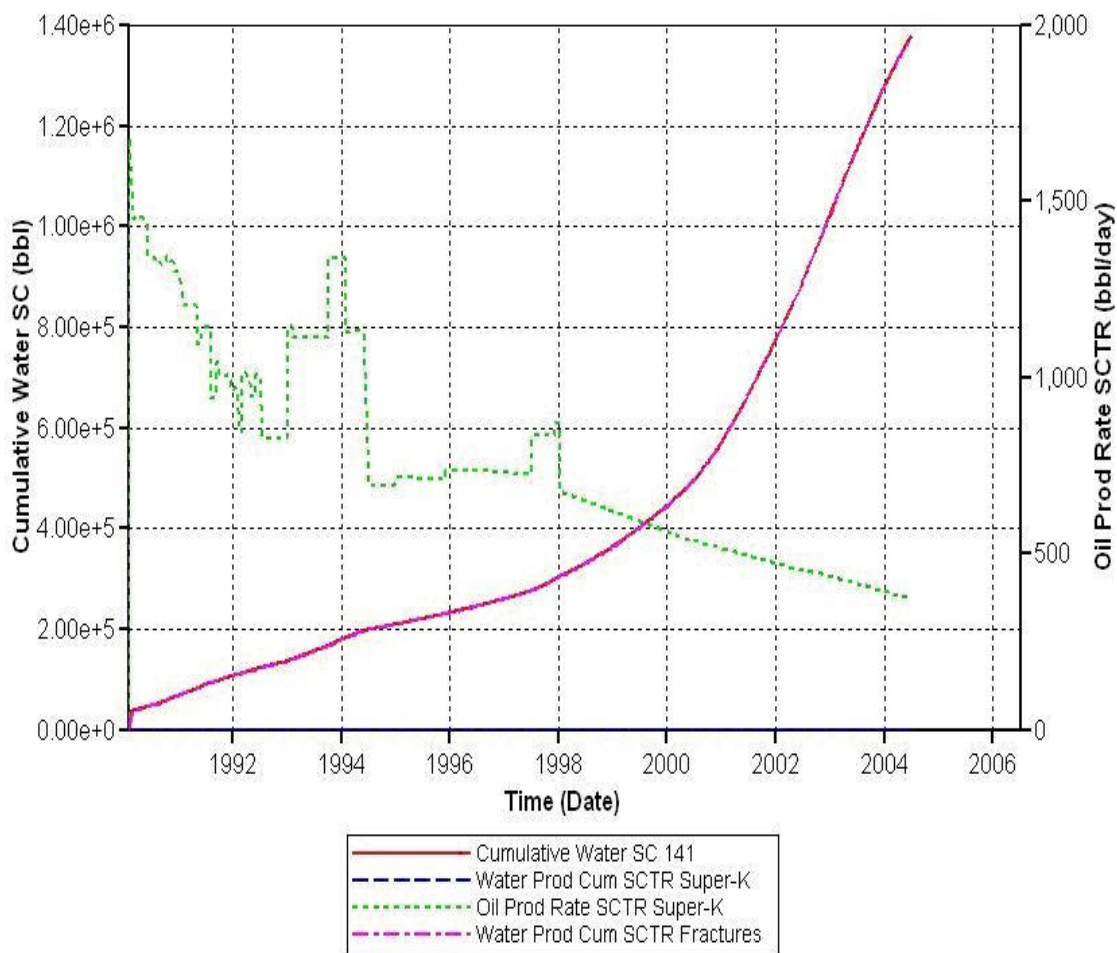


Fig. 5.11 - 45% Super-K Porosity Results

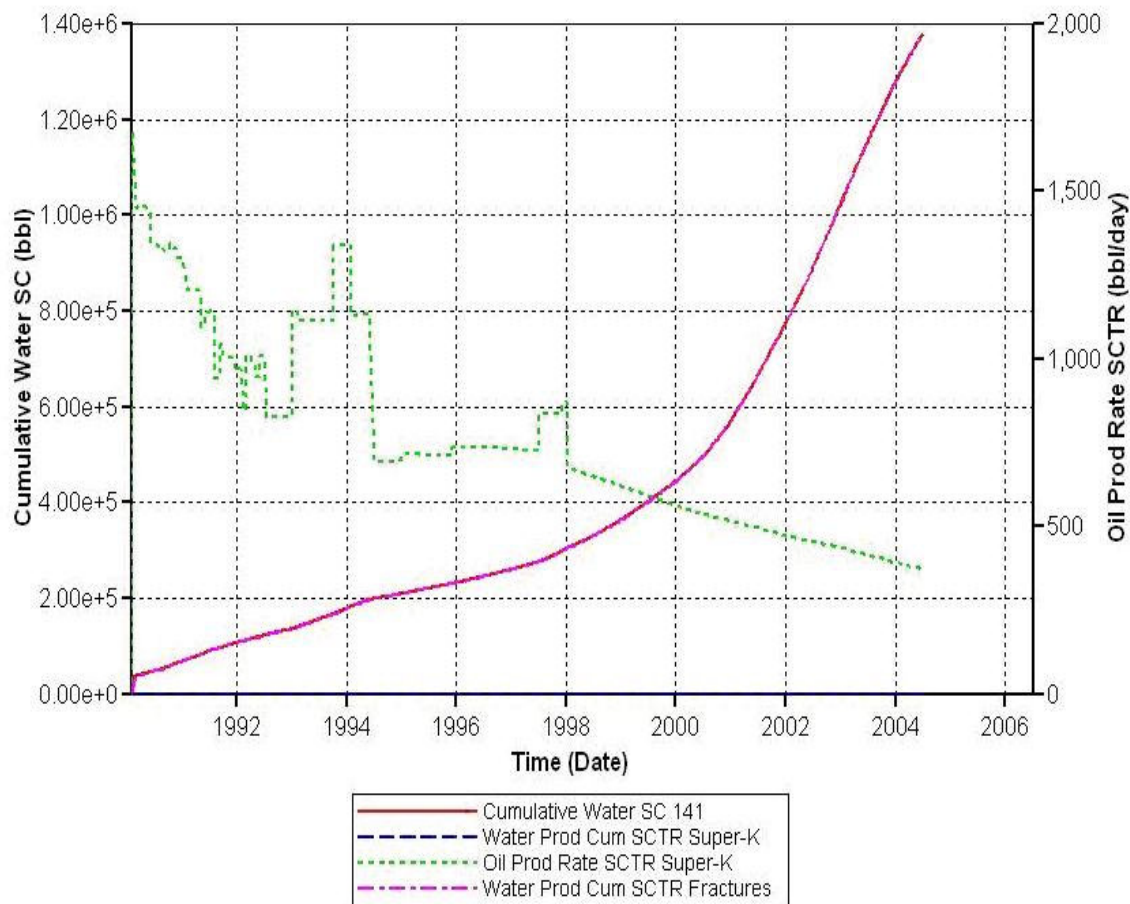


Fig. 5.12 - 75% Super-K Porosity Results

5.4 Fracture Spacing Effect

Several runs were made to visualize the effect of varying fracture spacing on production profiles. The fractures are assumed to be concentrated in an 11 x 9 rectangle with 300 ft cell width as seen in **Fig. 4.2**. Producer P-141 is in the middle of the rectangle intersecting the fractures. The runs are made for several fracture spacing to see the effect of varying the spacing on production profiles. In one case, the fractures are modified only in the I-direction in the fractures sector model. Furthermore, another case is run, where

the fractures are included in the entire model. Finally, fracture spacing was modified in all directions equally ($I = J = K$).

5.4.1 Fracture Spacing: I-Direction

The model runs include changing fracture spacing in the I-direction only while the J and K-directions are kept equal to 300 ft. The simulation runs are for the following fracture spacing: 1, 10, 300, and 1,000 ft. Two of the results are presented in **Figs. 5.13** and **5.14** below.

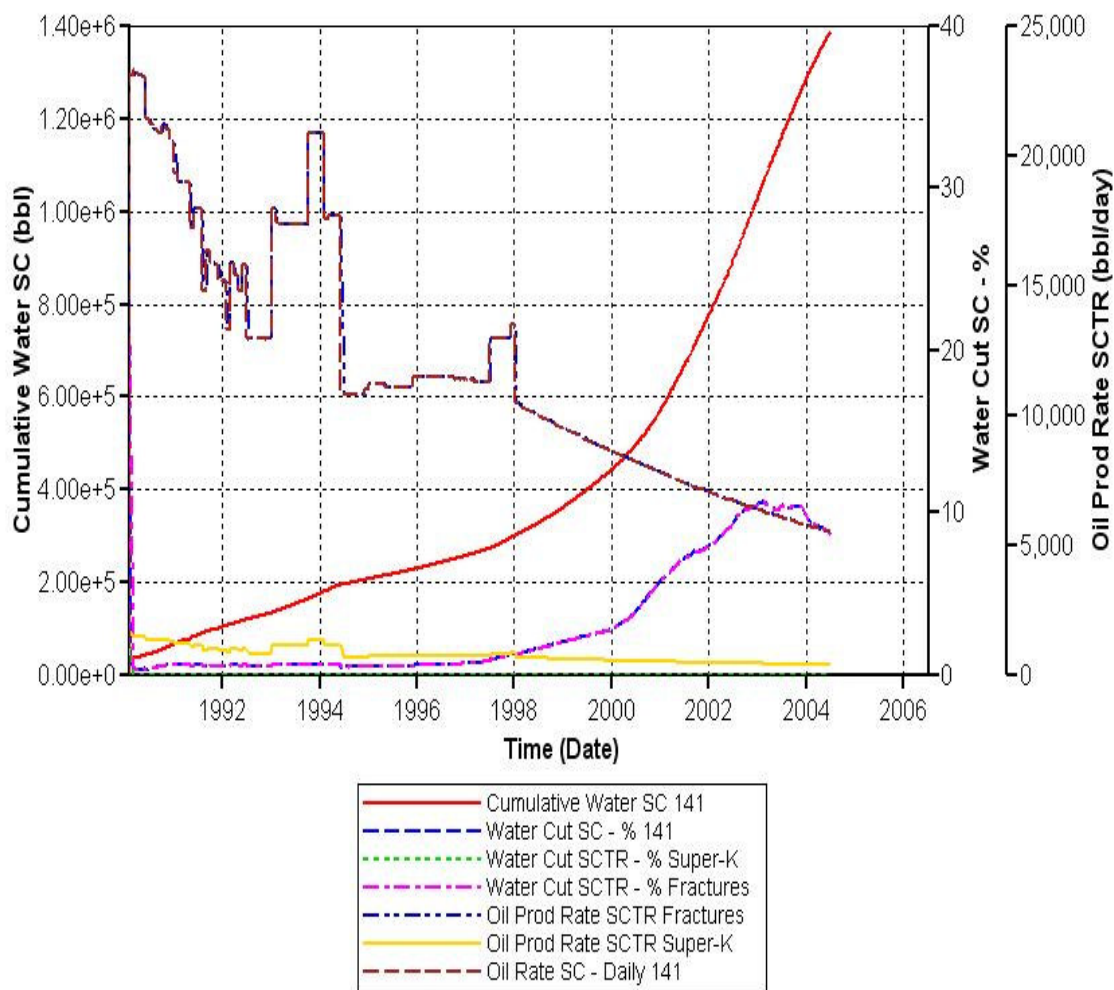


Fig. 5.13 – 1 ft Fracture Spacing Run Results

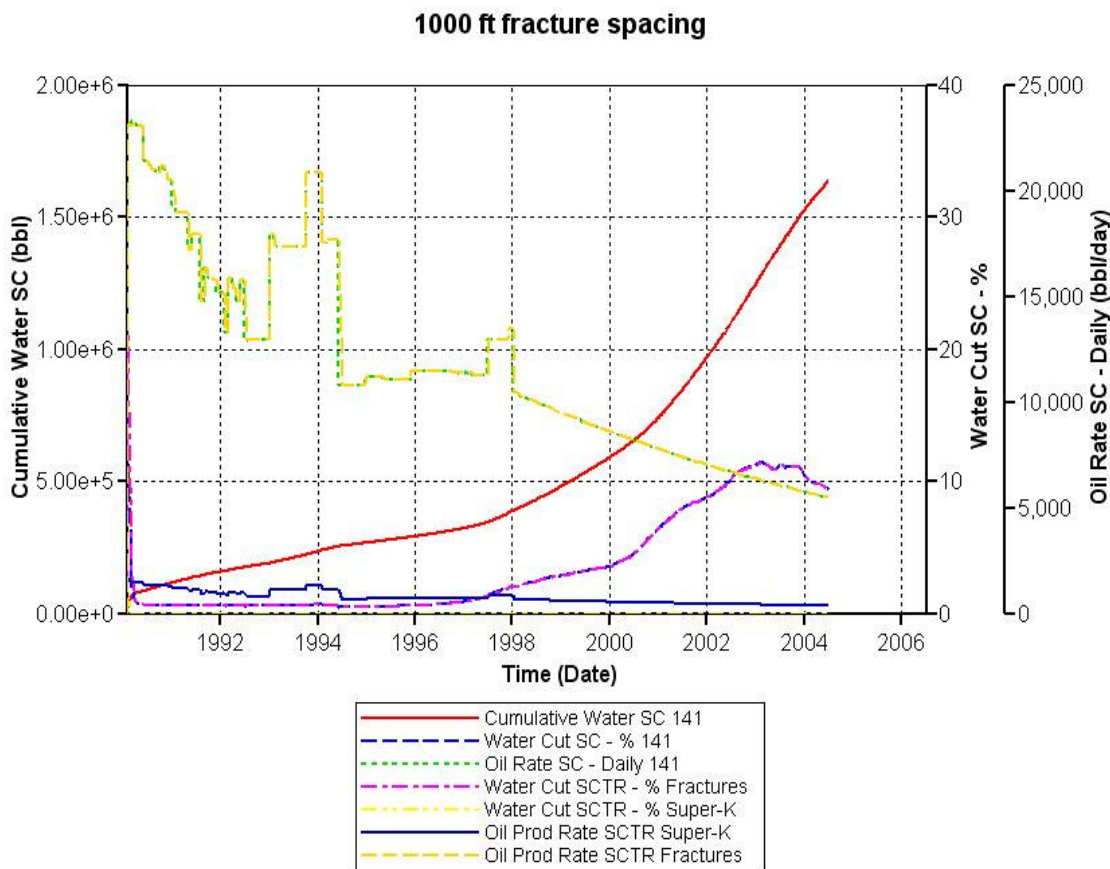


Fig. 5.14 – 1,000 ft Fracture Spacing Run Results

The cumulative produced water, water cut % and oil rate for producer P-141 in the fracture sector and the Super-K sector are plotted versus time. As noticed from previous results, the Super-K layer did not contribute to bringing water to the wellbore as the water produced from the Super-K zone is low and almost negligible. As observed from the plots, all the water was coming from the fractures as the water cut from the fractures matched the water cut from the wellbore. Unexpectedly, the produced oil from the Super-K zone is much lower than that produced from the fractures. A comparison plot with cumulative water produced and water cut % was prepared to compare the results for

different fracture spacing. As seen in **Fig. 5.15**, the greater the fracture spacing is, the higher the water production.

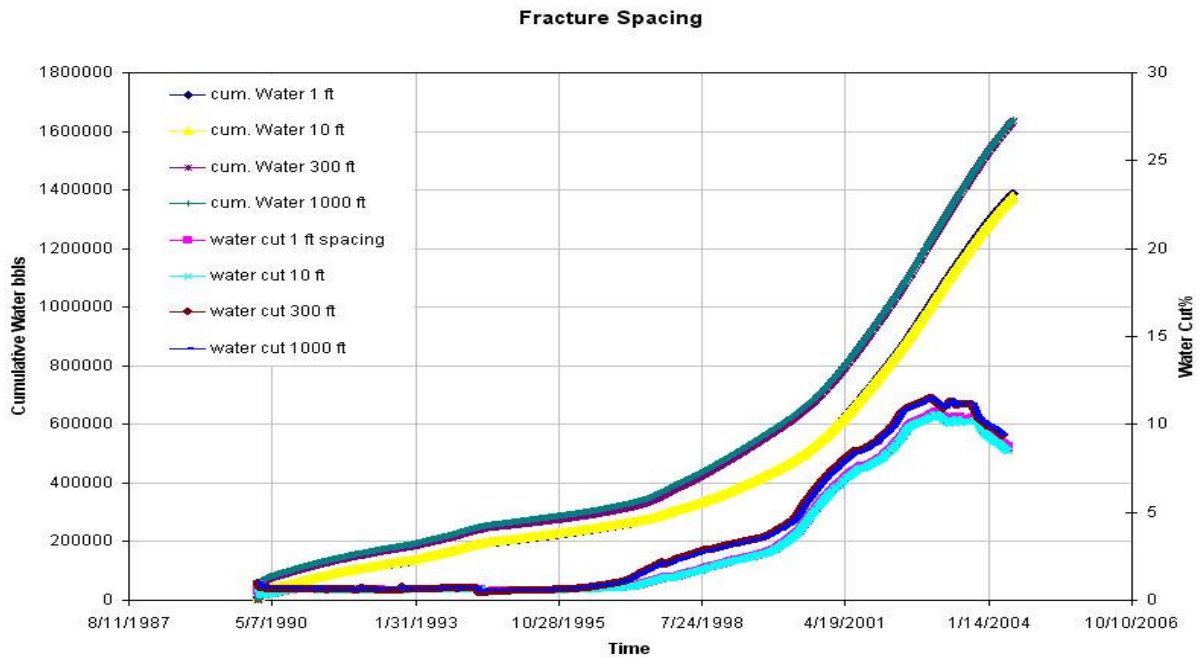


Fig. 5.15 - Different Fracture Spacing Comparison to Produced Water

According to the results in **Fig. 5.16** by the end of 1999, the water started invading the fractures from top of layer-5 to bottom of layer-4. The water approached the fractures from injector # 90 as observed in the same figure. This water production behavior can be witnessed by the sharp increase in water production after that year.

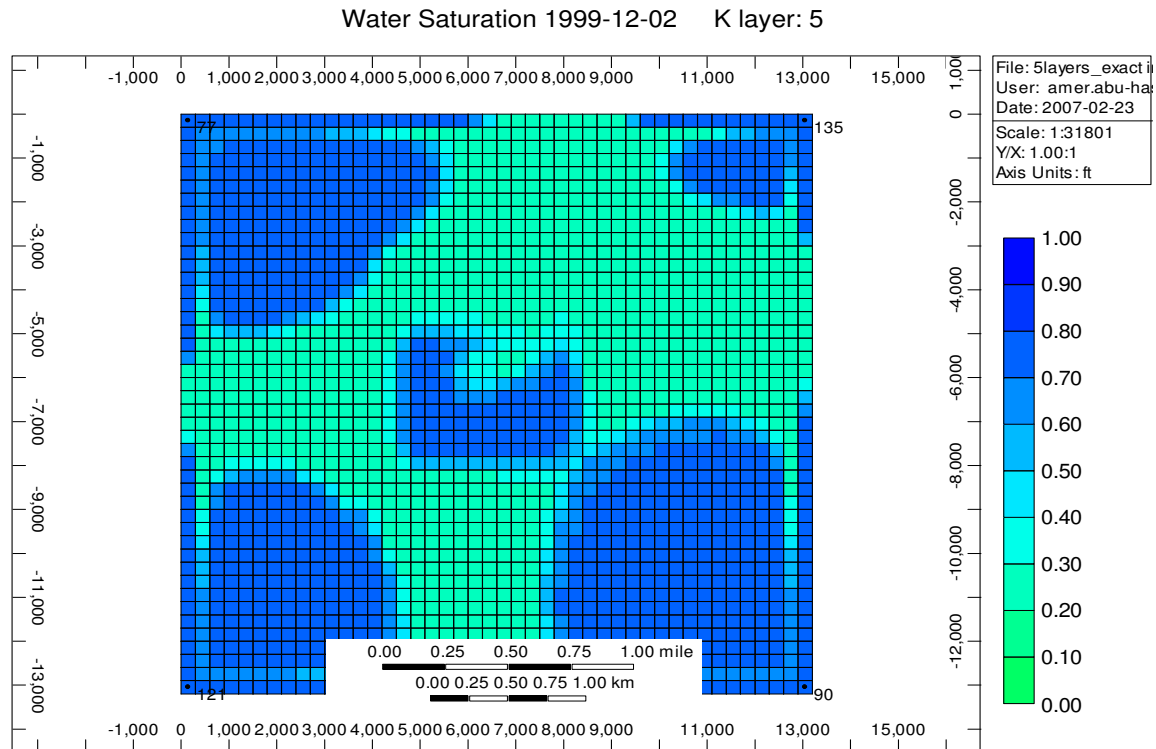


Fig. 5.16 - Water Invasion After 1999 from Top of Fifth Layer

5.4.2 Fractures in the Entire Model

Fractures in this case are found in layers 1 through 4 and distributed through out the entire model except at the boundary where the injectors are located. The fractures in the J and K-direction are kept equal to 300 ft. The modification in fracture spacing is in the I-direction only. Several runs are made to change the fracture spacing to see the effect on the pressure and production profiles. The runs were made for 1 ft, 10 ft, 100 ft, and 500 ft spacing. Two of the results are plotted in **Figs. 5.17** and **5.18** below.

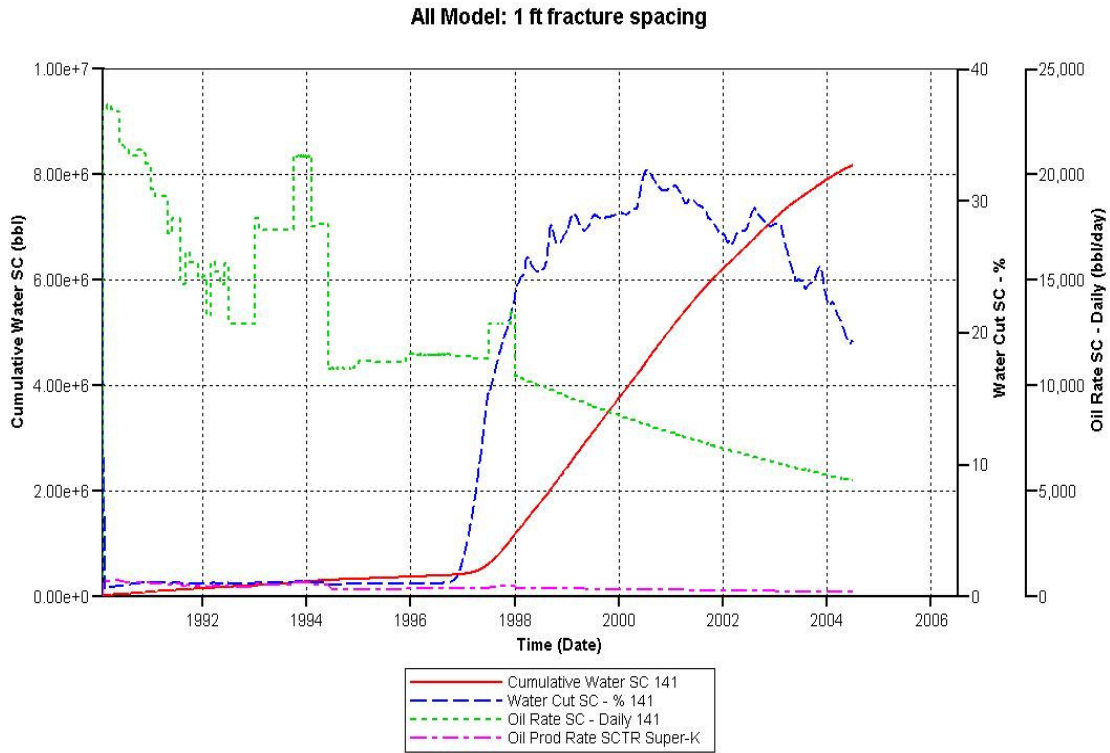


Fig. 5.17 - Fractures in Entire Model: 1 ft Fracture Spacing

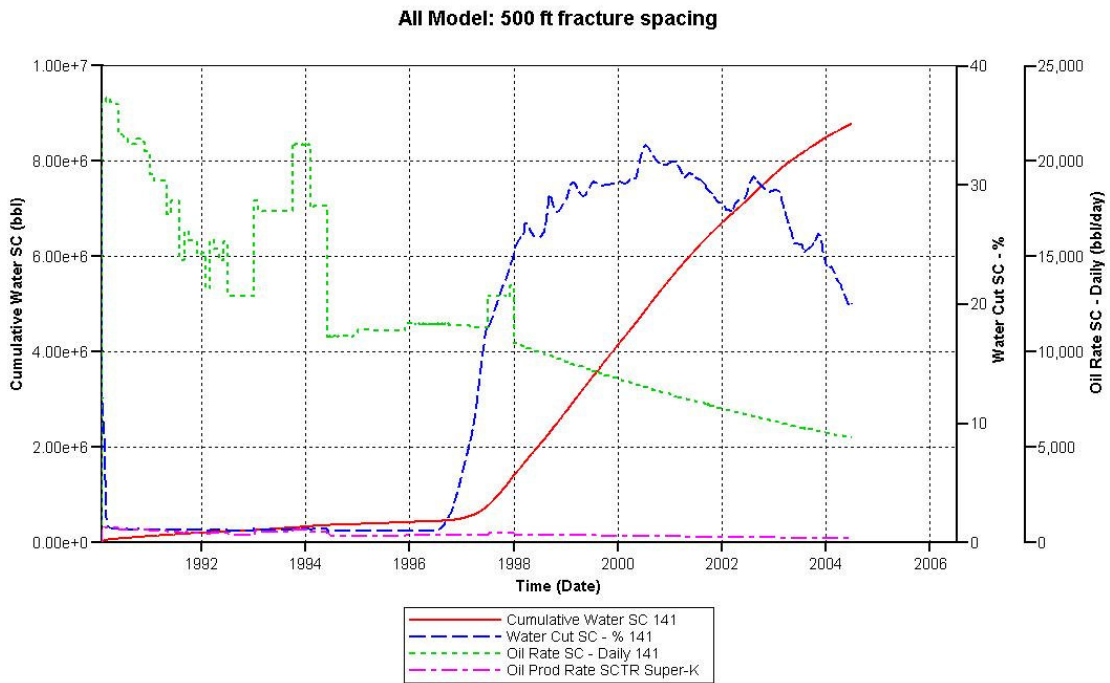


Fig. 5.18 - Fractures in Entire Model: 500 ft Fracture Spacing

For the 500 ft fracture spacing run, the water cut and cumulative water was higher. By the end of year 1997, the water invaded the fractures that intersected producer P-141 from the top of the fifth layer as seen in **Fig. 5.19** below.

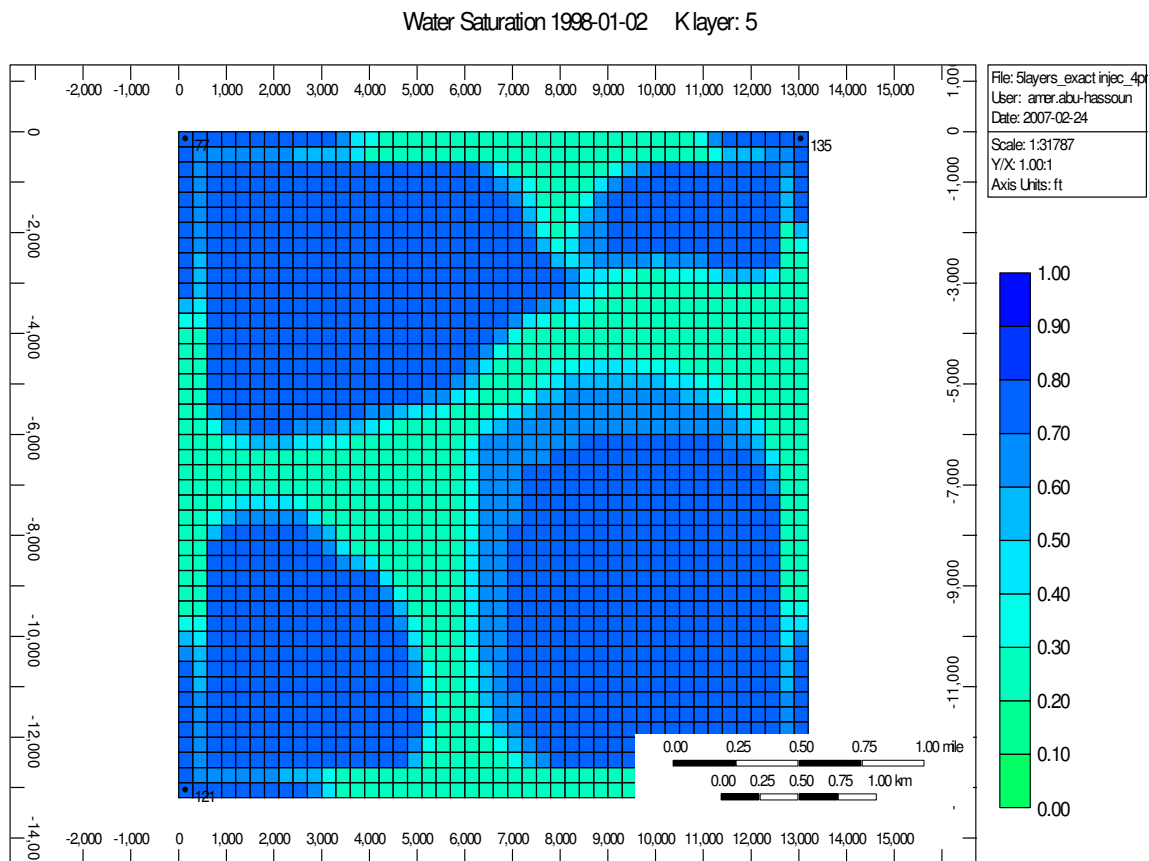


Fig. 5.19 - Water Breakthrough by the End of 1997

At the end of the simulation period, it can be seen that the oil is swept from most of layer-5 as seen in **Fig. 5.20**, but the rest of the layers are not swept yet as can be seen in **Fig. 5.21**.

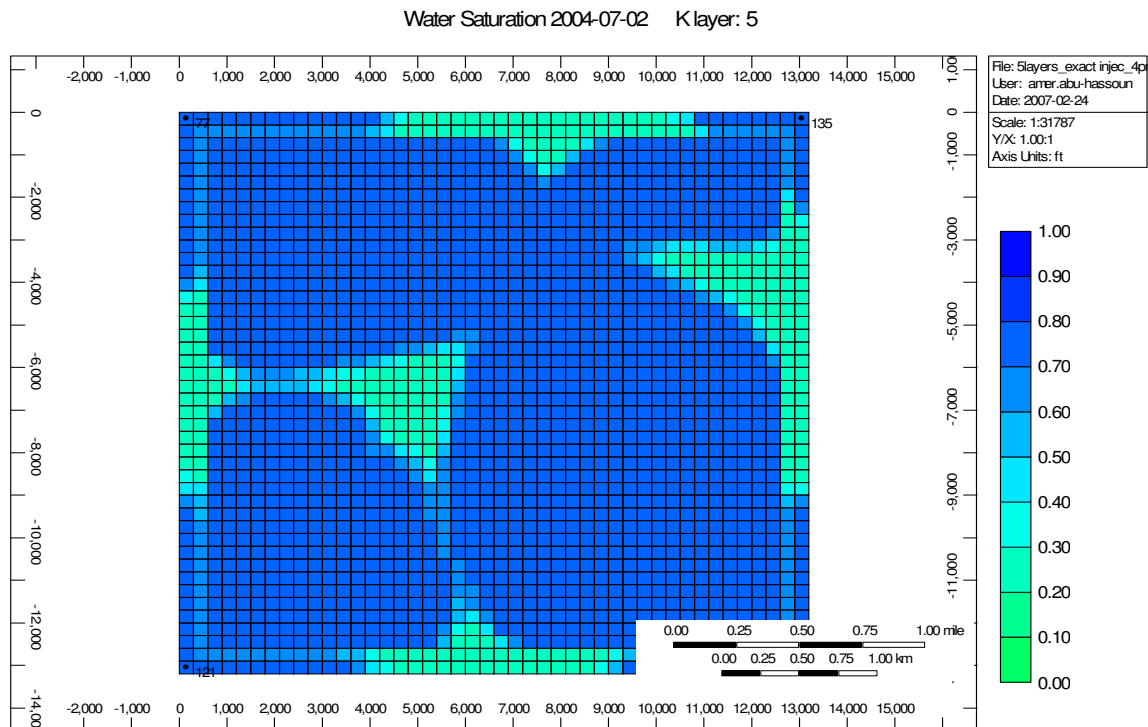


Fig. 5.20 - Oil Swept from Most of Layer-5

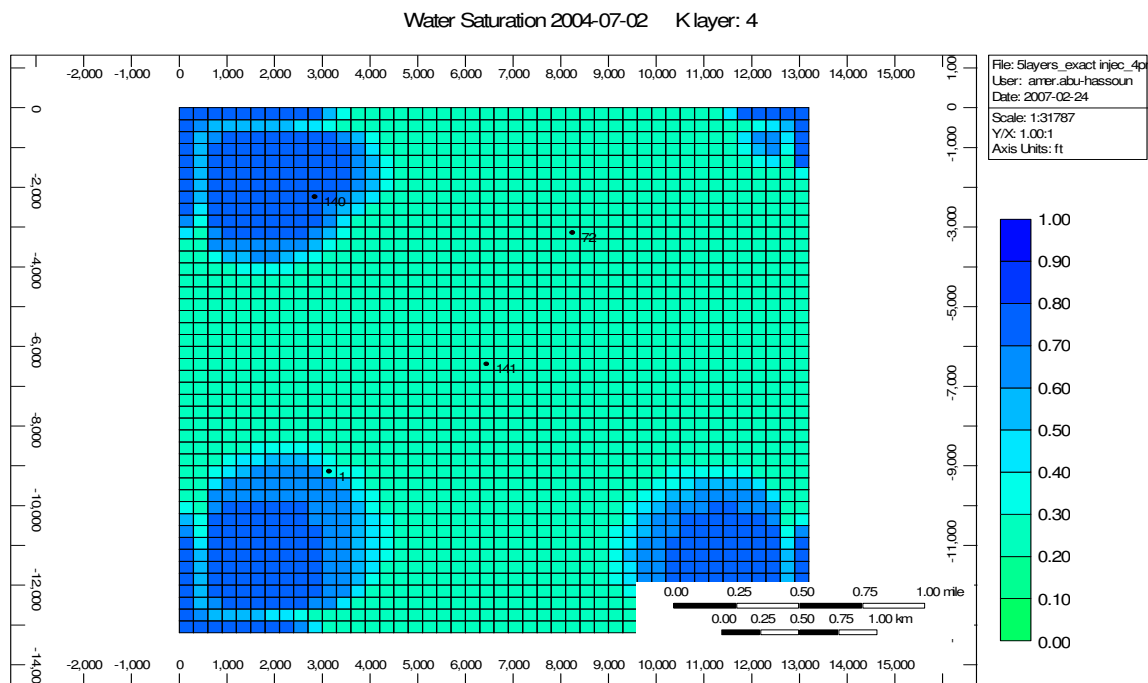


Fig. 5.21 - High Oil Potential in Layer-4 by End of Simulation Run

Fig. 5.22 shows water production comparison from producer P-141 only for fractures covering layers 1 to 4 through out the entire model for different fracture spacing. As noticed from the plots, the water production increases for greater fracture spacing.

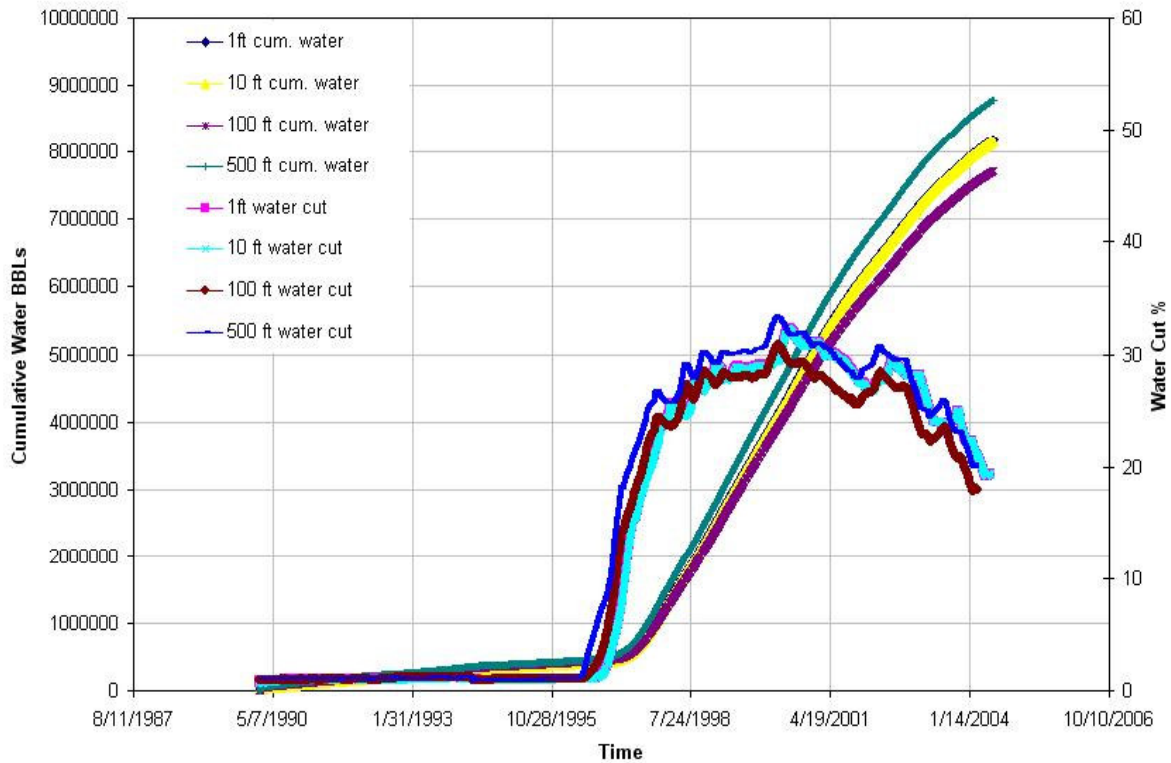


Fig. 5.22 - Comparison of Water Production of Fractures in the Entire Model

5.4.3 Fracture Spacing I = J = K

Fracture spacing is made equal in all directions ($I = J = K$) in the fracture sector only. The water production is plotted and compared to the results obtained from previous results of varying only the spacing in the I-direction while keeping $J = K = 300$ ft. The results are presented in **Fig. 5.23**. Based on the results obtained, the cumulative water production increases if the spacing are equal in all directions ($I = J = K$).

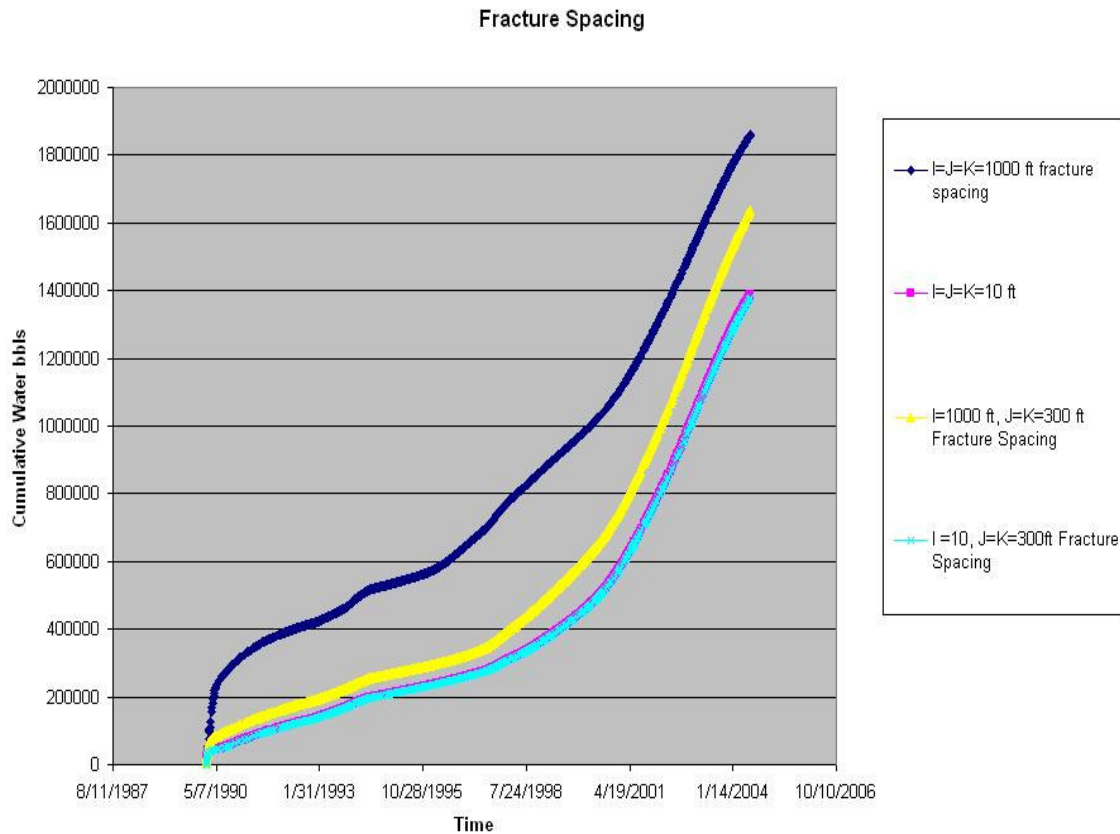


Fig. 5.23 – Comparison Plot for Equal and Different Fracture Spacing

5.5 Super-K Permeability Variation

The Super-K zone has proven to be a secondary conduit to high water production if fractures are present. In this section, the Super-K permeability is varied to see if that will affect the production behavior where the fractures are present. The Super-K permeability is varied as 10, 25, 50 and 70 darcies. The first case is run for the Super-K intersecting fractures. The results for changing the Super-K permeability are presented for permeability values of 10 and 70 darcies only. The results are presented in **Figs. 5.24** and **5.25**.

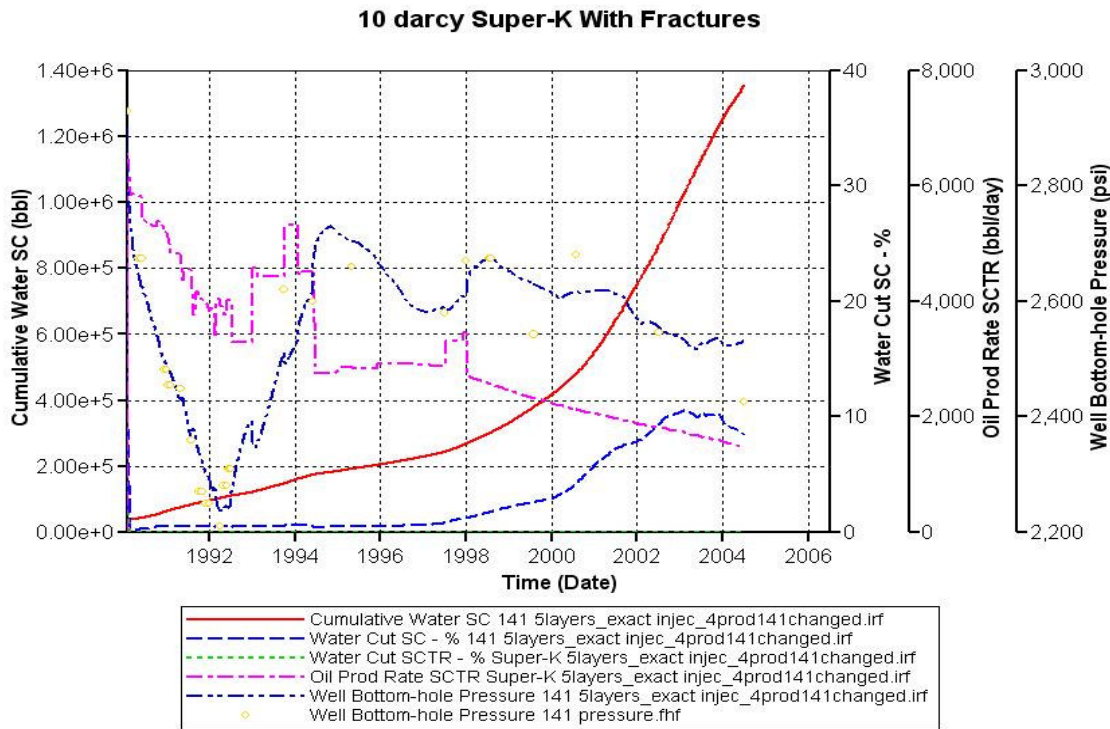


Fig. 5.24 - Simulation Results of 10 Darcies Super-K Permeability

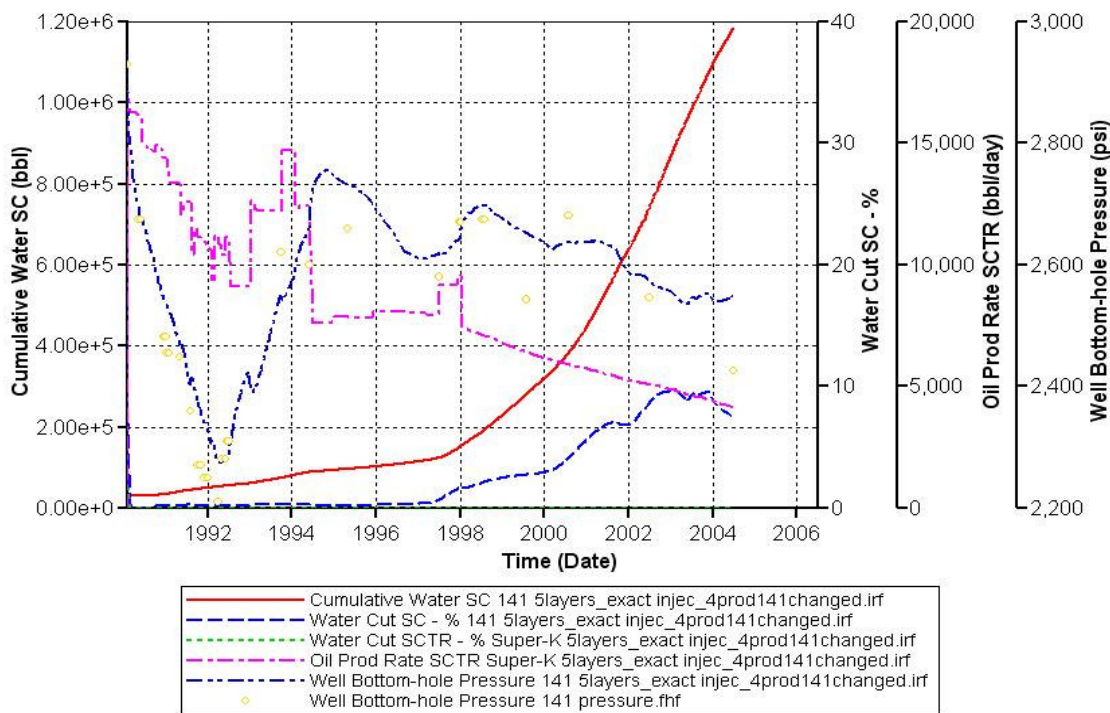


Fig. 5.25 - Simulation Results of 70 Darcies Super-K Permeability

As expected from a high permeability layer, the oil production from the 70 darcies run is higher. This means as the Super-K permeability gets higher; the well tendency to conduct higher oil rates is expected. The cumulative water production is less in the 70 darcies run compared to the 10 darcies run. A comparison plot to the cumulative Super-K oil production and the wellbore cumulative water production for all the cases is shown in **Fig. 5.26**.

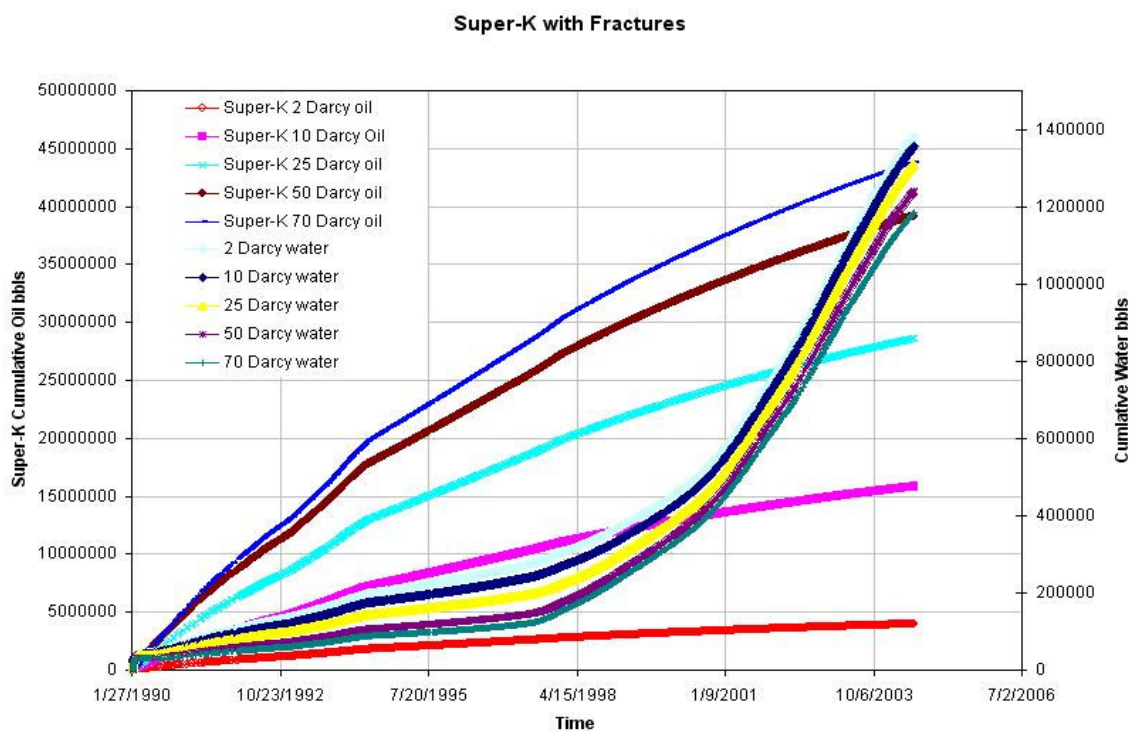


Fig. 5.26 - Comparison Plot to Super-K Layer Intersecting Fractures

The plot shows that as the Super-K permeability increases, the cumulative oil also increases but the cumulative water decreases. In the next runs, the fractures were not considered in the model to evaluate the production from the Super-K layer alone. Again,

the runs are presented for the 10 and 70 darcies of Super-K only and a comparison plot will be highlighted later. The results are shown in **Figs. 5.27** and **5.28**.

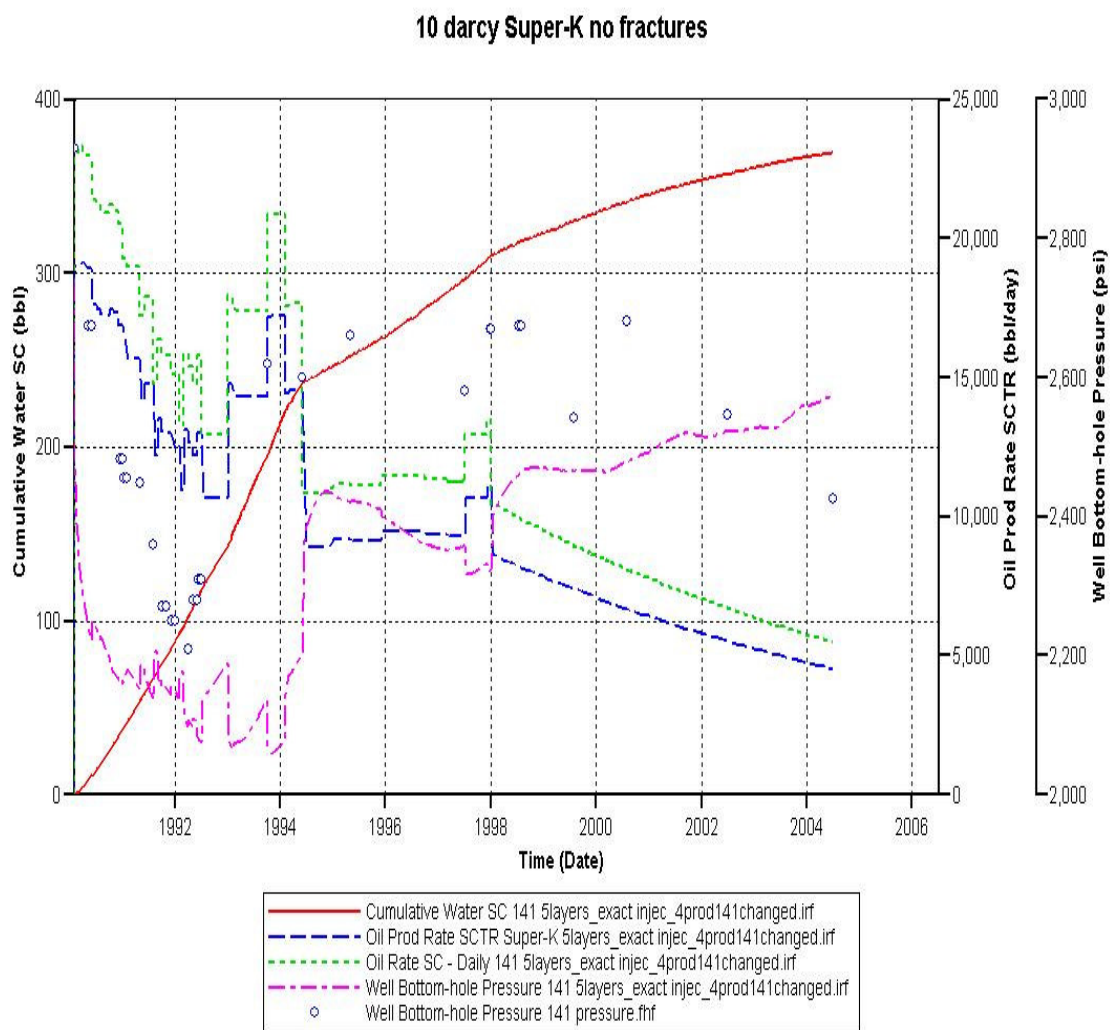


Fig. 5.27 - Simulation Results of 10 Darcies Super-K Permeability Model with No Fractures

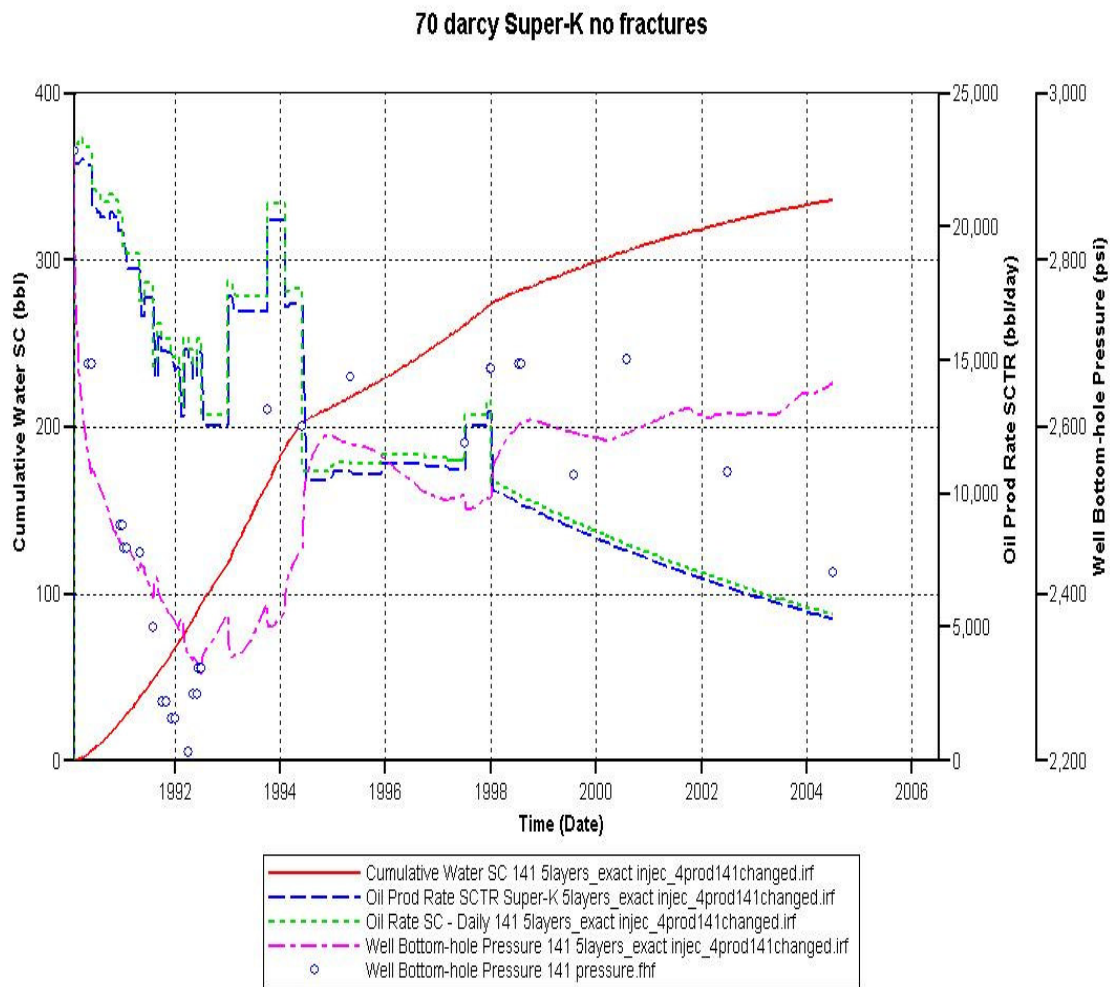


Fig. 5.28 - Simulation Results of 70 Darcies Super-K Permeability Model with No Fractures

As noticed, the pressure profile is shifted up in the 70 darcies run compared to that for the 10 darcies. Also, the oil production is higher for the 70 darcies case. For both runs the water production is very low and almost negligible. This result also proves that the main source of water production was fracture conductivity as seen earlier. A production comparison plot of the cumulative oil and water is presented in **Fig. 5.29** below.

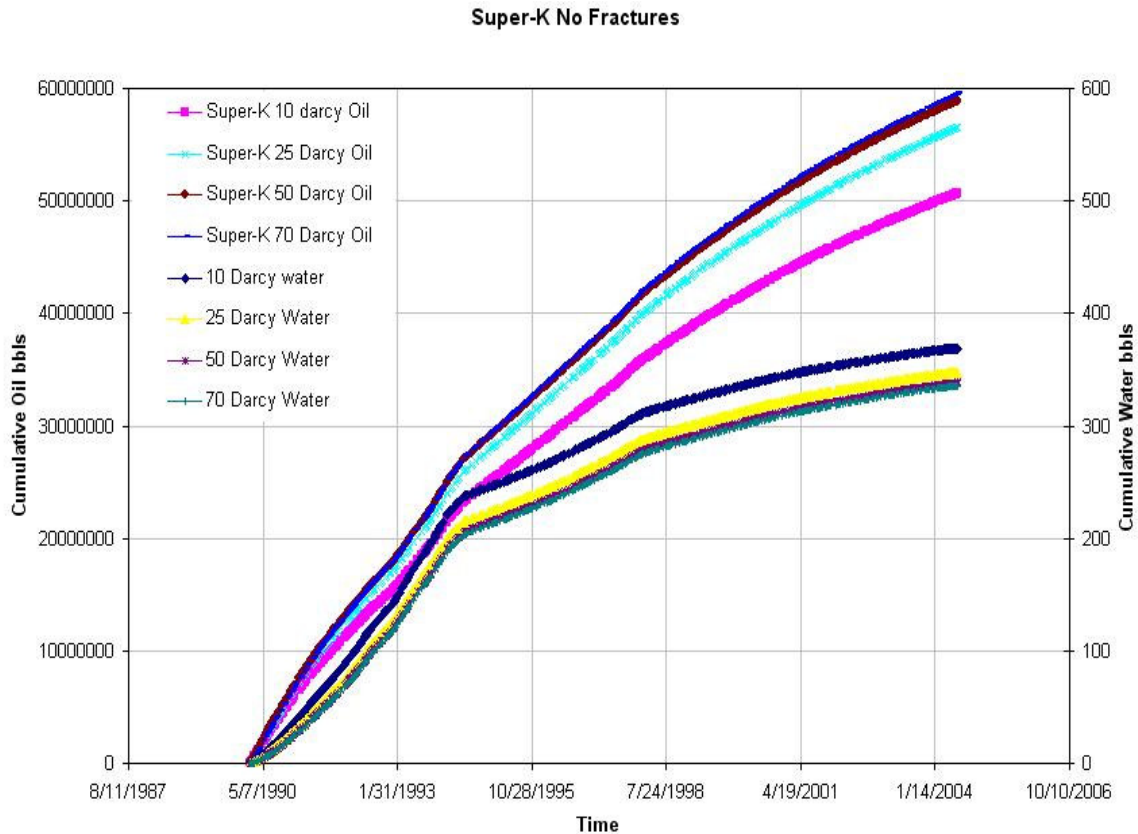


Fig. 5.29 - Comparison Plot to Different Super-K Permeability with No Fractures

The plot shows that as the Super-K permeability increases, enhanced oil production is anticipated through the high permeability layer (70-80 % of total produced oil) and less cumulative water is produced. This case is more representative to the real field case since the well is producing at 1 % water cut only. Super-K layer may not be directly connected to faults or fracture clusters but perhaps connected to matrix fractures and small fissures. The 25 darcies permeability of the Super-K zone gives almost 60 % of the total flow and is more realistic to the producer P-141 flow profile.

5.6 Fracture Porosity

The previous sensitivity studies were based on the fact that the model has fractures and the fracture porosity is assumed to be 1 %. In this section, the porosity is

changed to examine how the fractures will respond to such a variation. The model is calculated for porosity values of 0.1 %, 5 %, 10 %, and 15 %. The results for 0.1 % and 15 % are presented in **Figs. 5.30** and **5.31**, respectively.

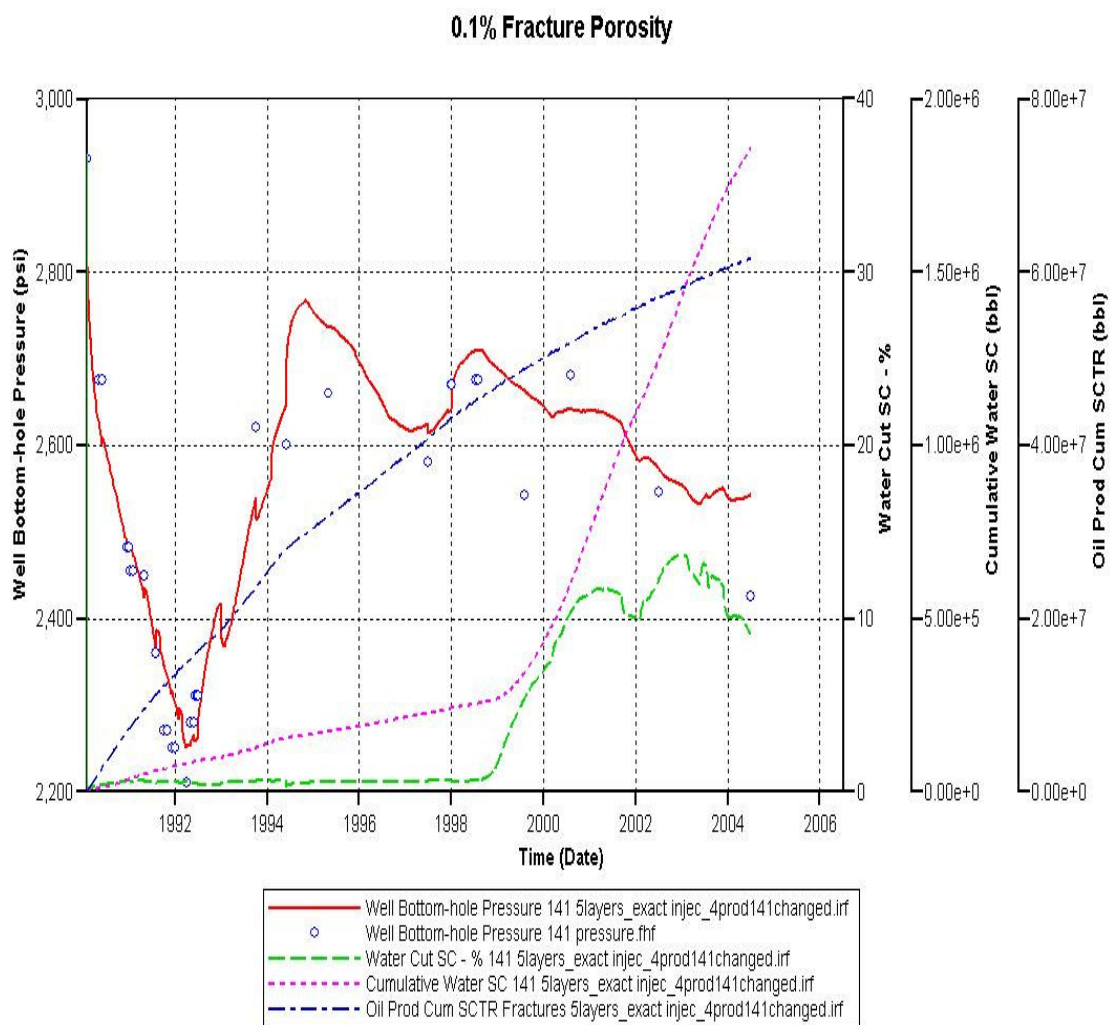


Fig. 5.30 - Simulation Results for 0.1 % Fracture Porosity

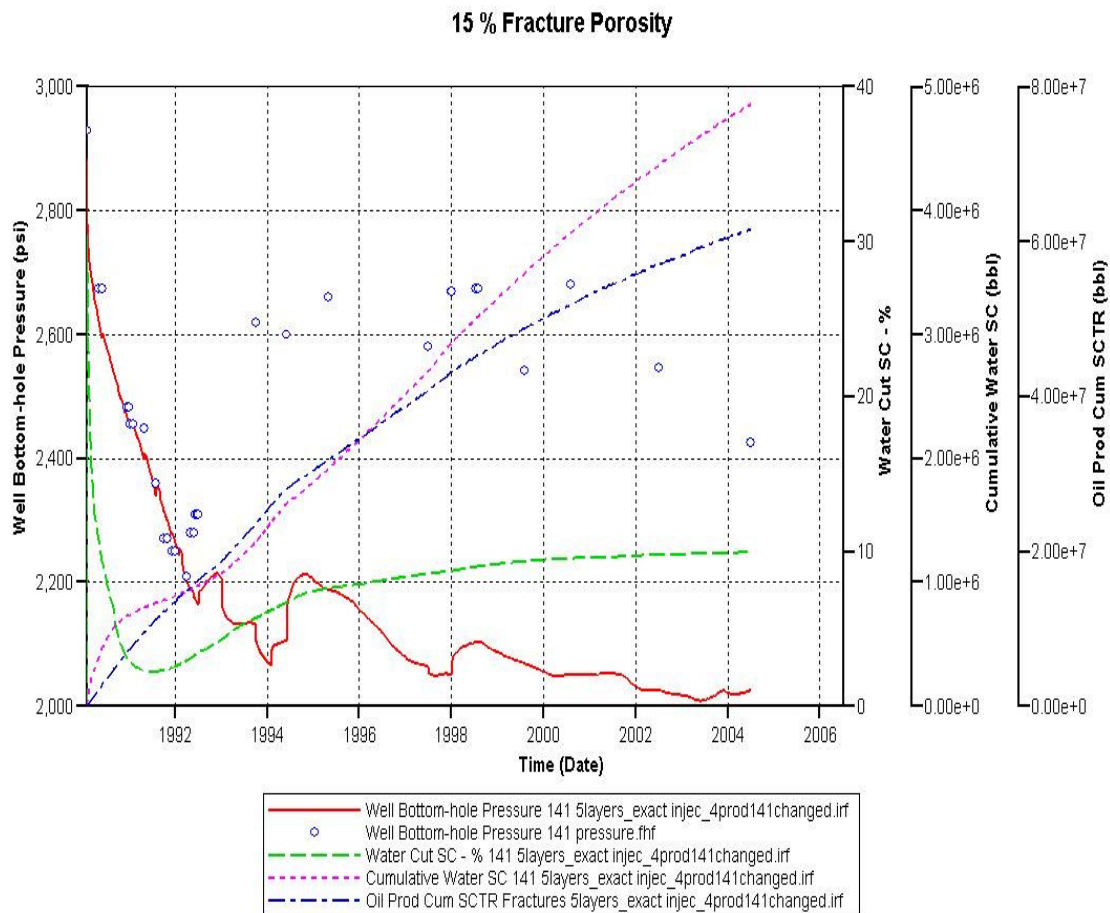


Fig. 5.31 - Simulation Results for 15 % Fracture Porosity

From the above results, the fracture porosity variation has affected both production and pressure profiles. As the fracture porosity increases, higher water rate is conducted. The bottom-hole pressure decreases even if the injectors are still injecting water for pressure maintenance. 1 % fracture porosity gave a better representation of how the well bottom-hole pressure responded as seen in Chapter IV. In analyzing the water saturation for the 15 % fracture porosity case, the fifth layer almost all was saturated with water by the end of year 1991 as can be seen in **Fig. 5.32**. The figure explains why the water cut starts increasing by the end of 1991.

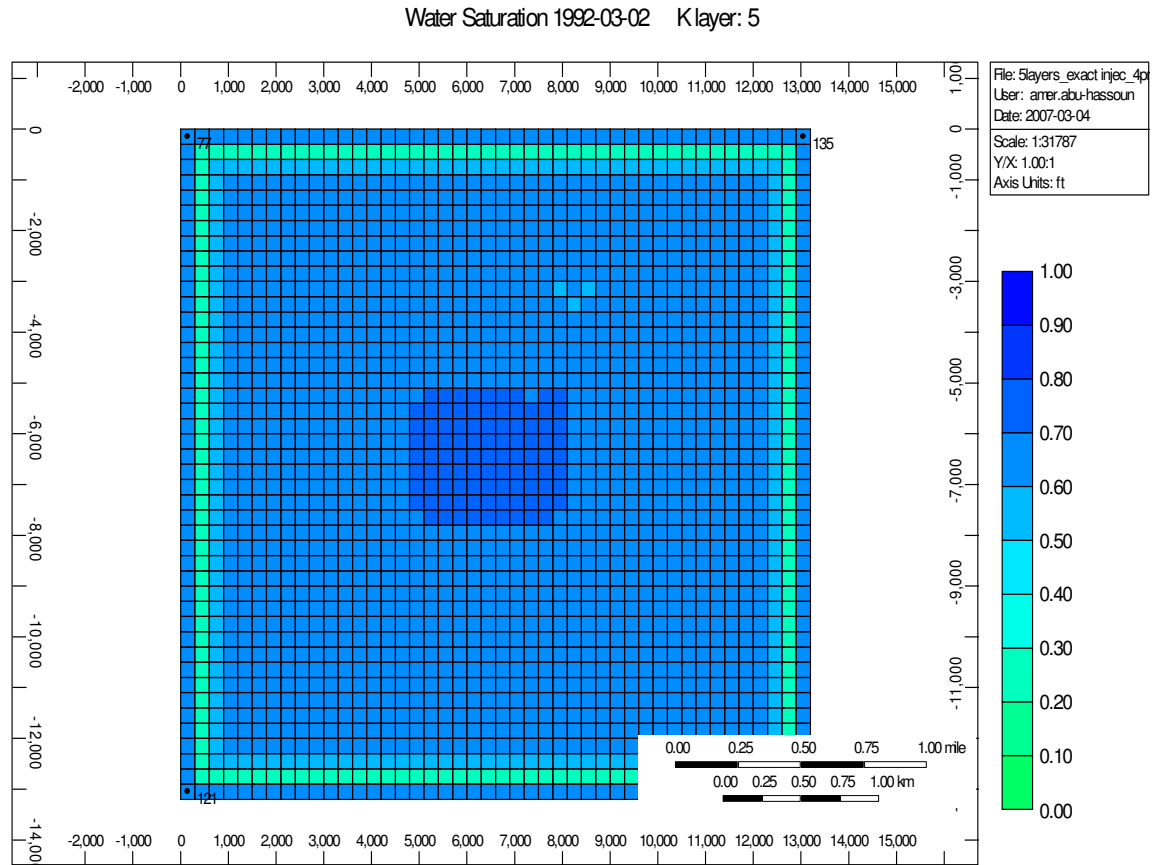


Fig. 5.32 - 2-D Diagram Shows Water Cut Increase at the Center by End of 1991

A comparison plot is made to compare the effect of varying fracture porosity on cumulative water production and pressure profile. **Fig. 5.33** shows that as the fracture porosity increases, higher water rate is being produced but the bottom-hole pressure decreases. The data used in the hypothetical history matching with 1 % fracture porosity was more realistic and gave a better history match.

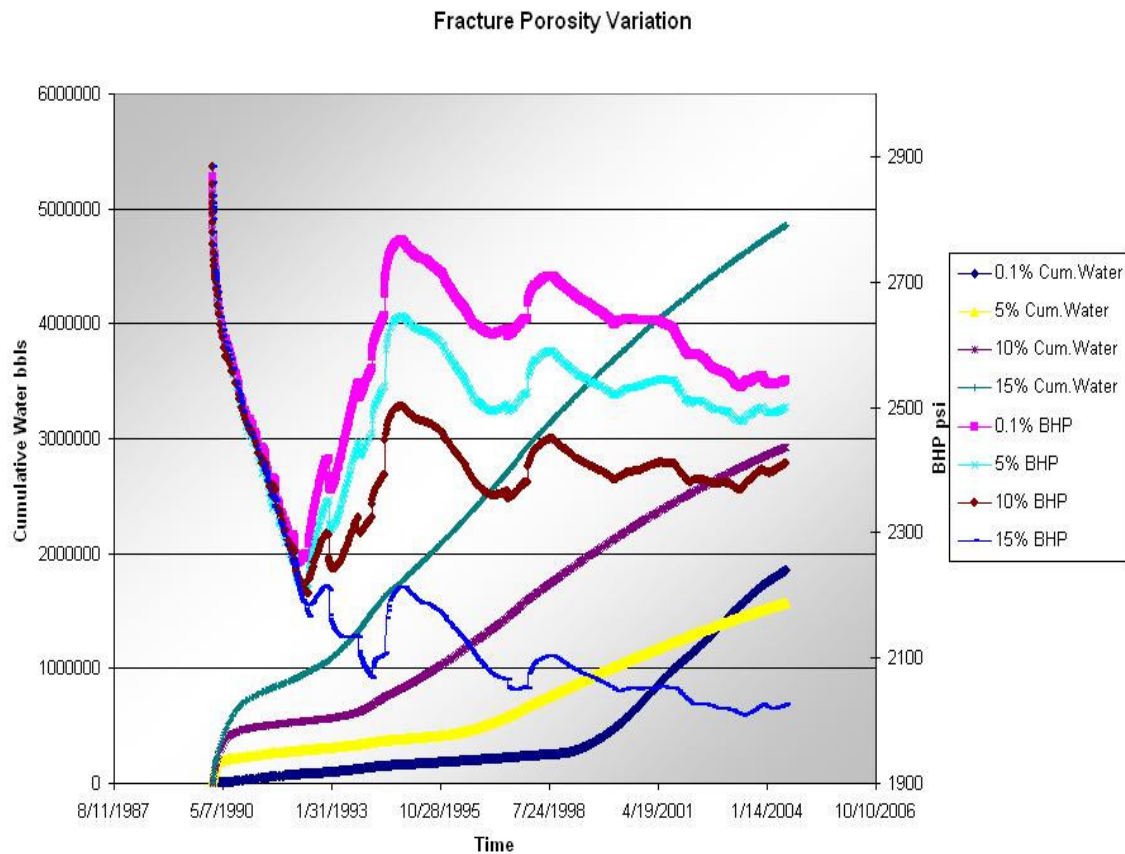


Fig. 5.33 - Comparison Results of Different Fracture Porosity

5.7 Fracture Location

The Super-K in this section is tested with the fractures placed at different positions away from producer P-141 drainage area and the fractures do not intersect the Super-K zone. This study presented different fracture location scenarios. The first scenario has the fractures located at three different locations in the model as in **Fig. 5.34** and the result for this run is shown in **Fig. 5.35**.

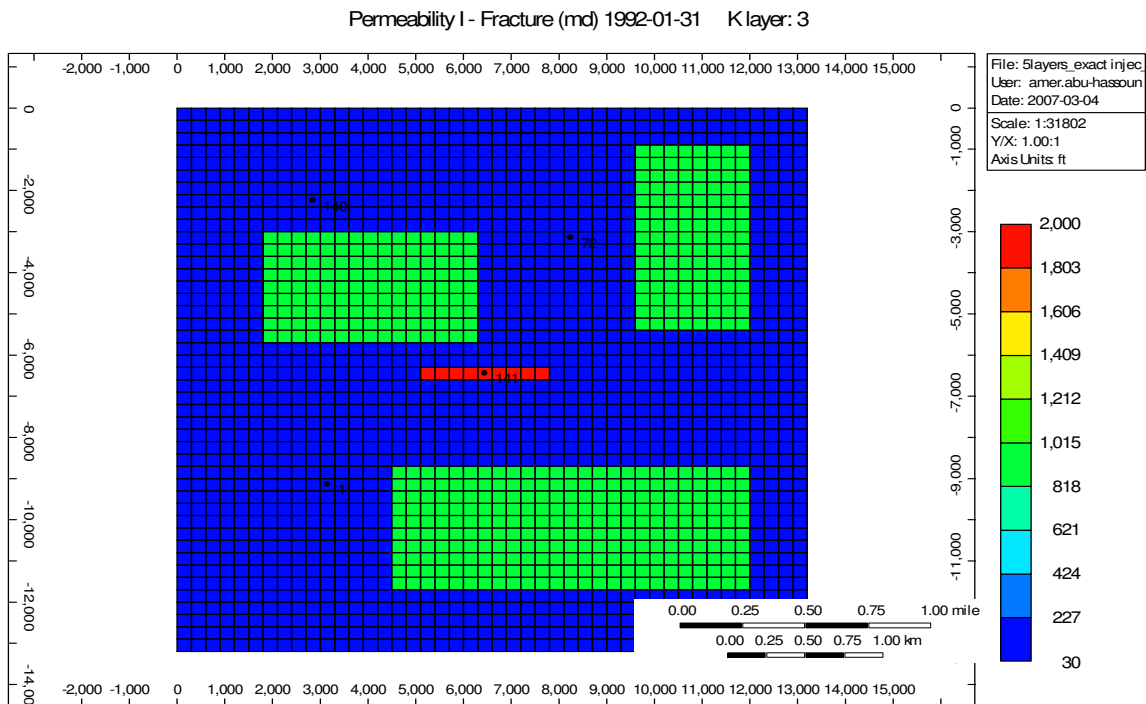


Fig. 5.34 - Three Different Locations of Fractures in the Model

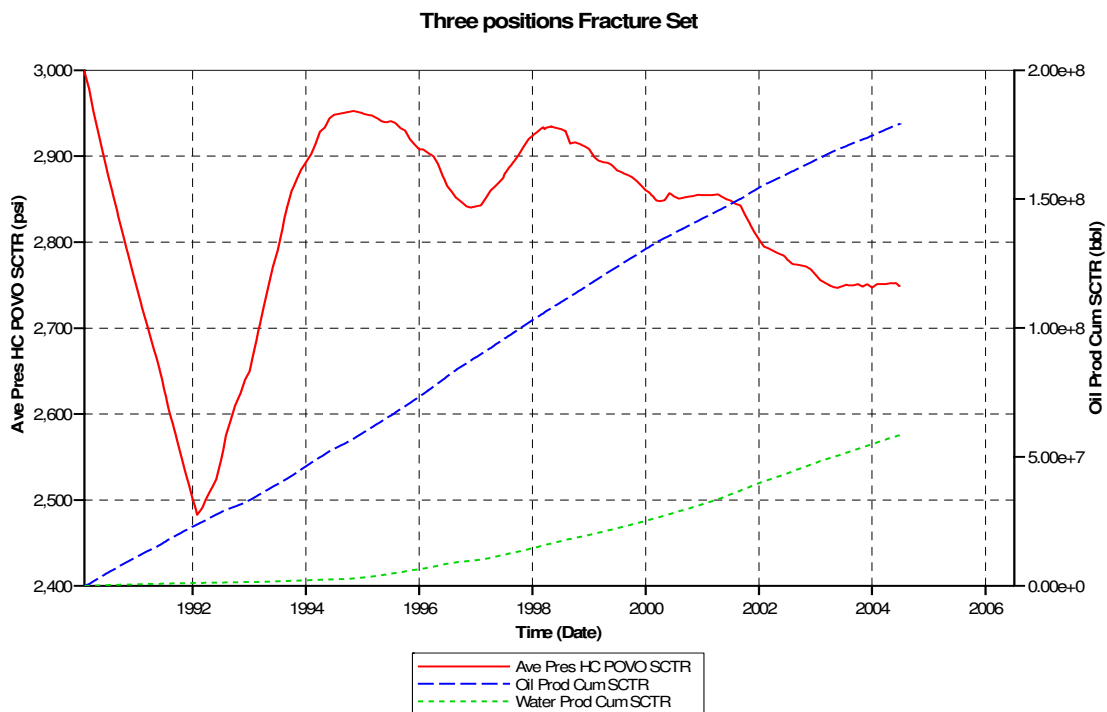


Fig. 5.35 - Results of Running Fractures at Three Locations

Figs. 5.36 and **5.37** show how water moved in the model in the three different fracture locations scenario by the end of the simulation period. The water advanced more in the lower part of the model since the fractures are more concentrated at the lower section of the reservoir model. The fractures will be examined at three different individual positions located in different portion of the reservoir.

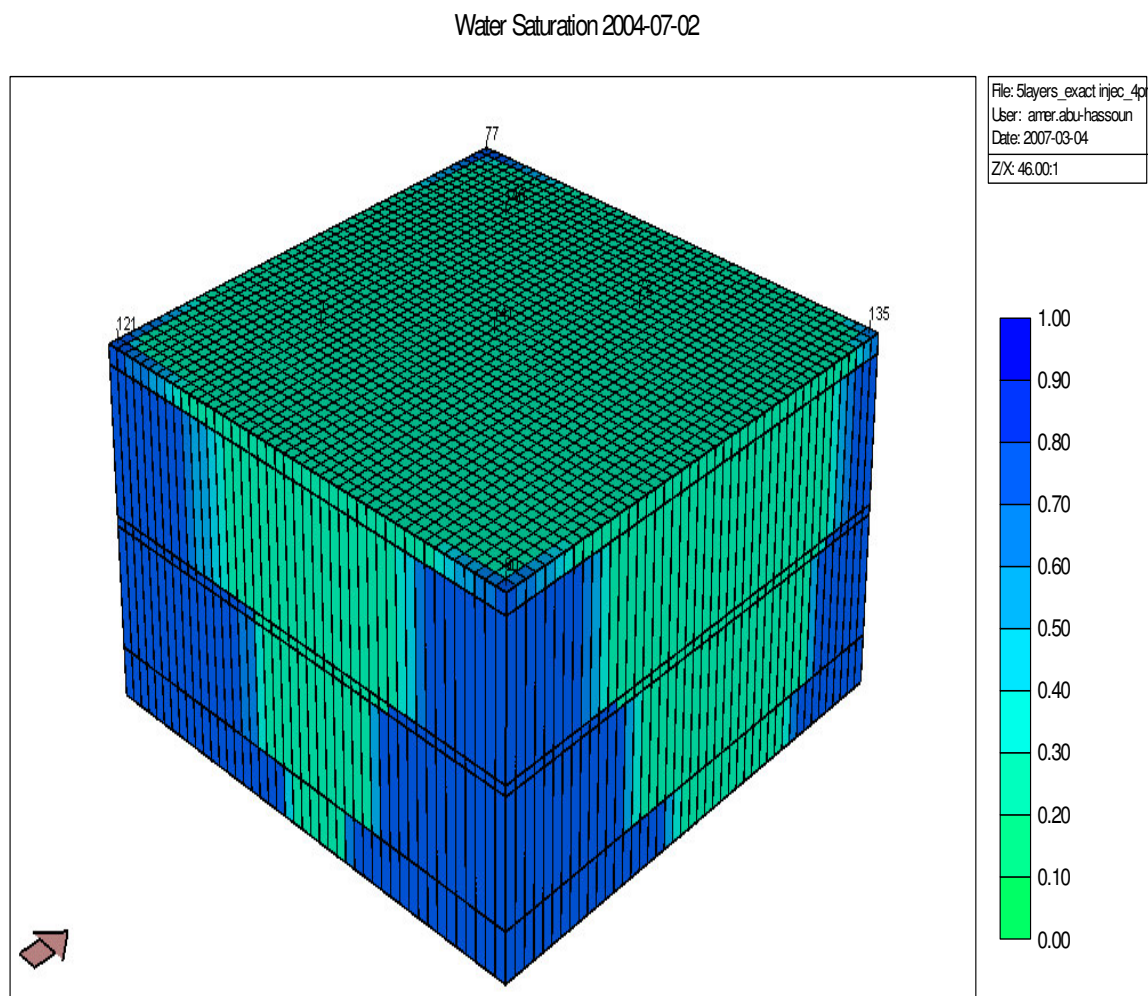


Fig. 5.36 – 3-D Diagram Shows Water Movement

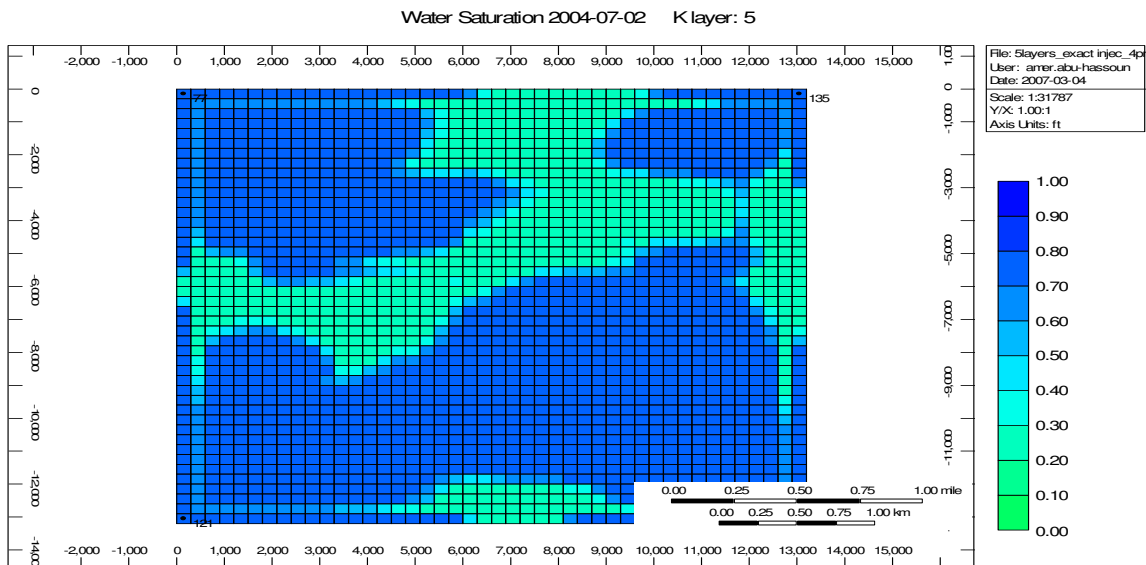


Fig.3.37 - Water Movement in Fifth Layer

5.7.1 Position: 1

The first position and the results are plotted in **Figs. 5.38** and **5.39**, respectively.

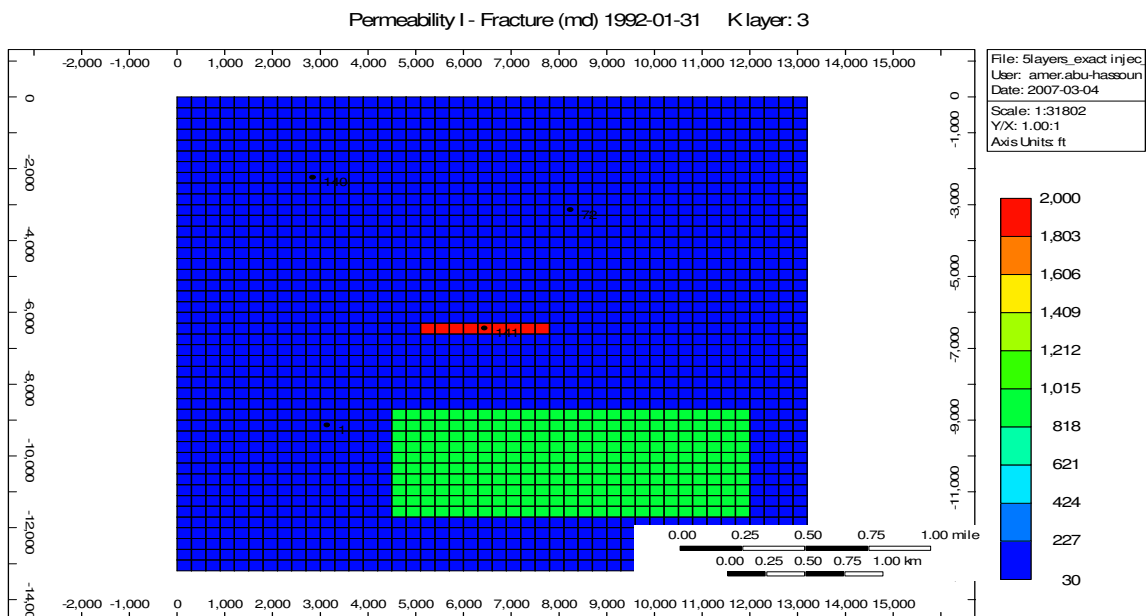


Fig. 5.38 - First Fractures Position (Green), Super-K Layer in Red

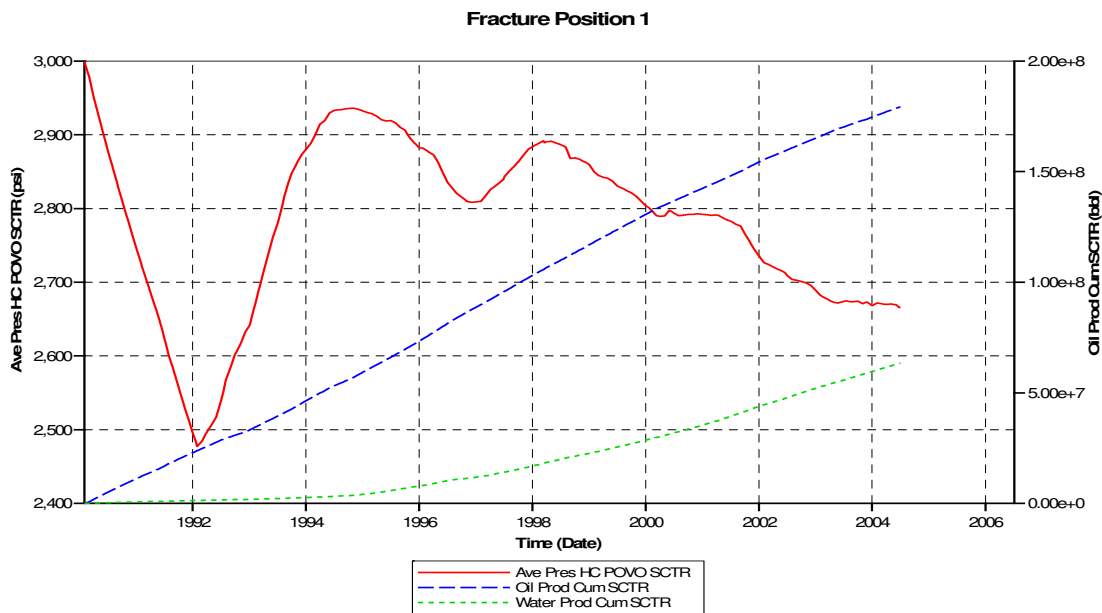


Fig. 5.39 - Results of First Fracture Position Run

5.7.2 Position: 2

The second position is shown in **Fig. 5.40** and the result is presented in **Fig. 5.41**.

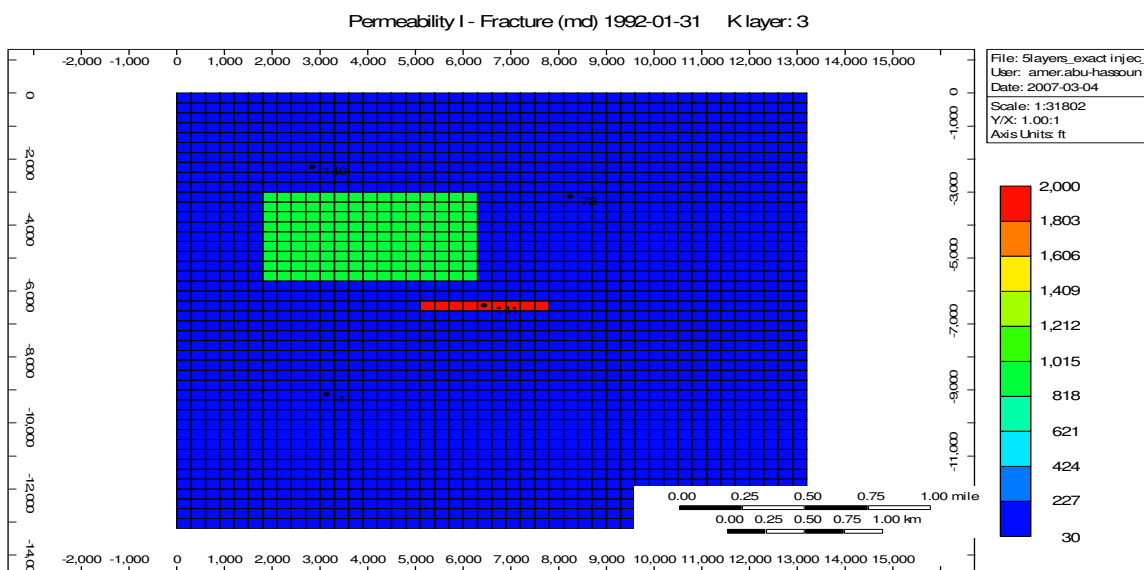


Fig. 5.40 - Second Fracture Position (Green), Super-K Layer in Red

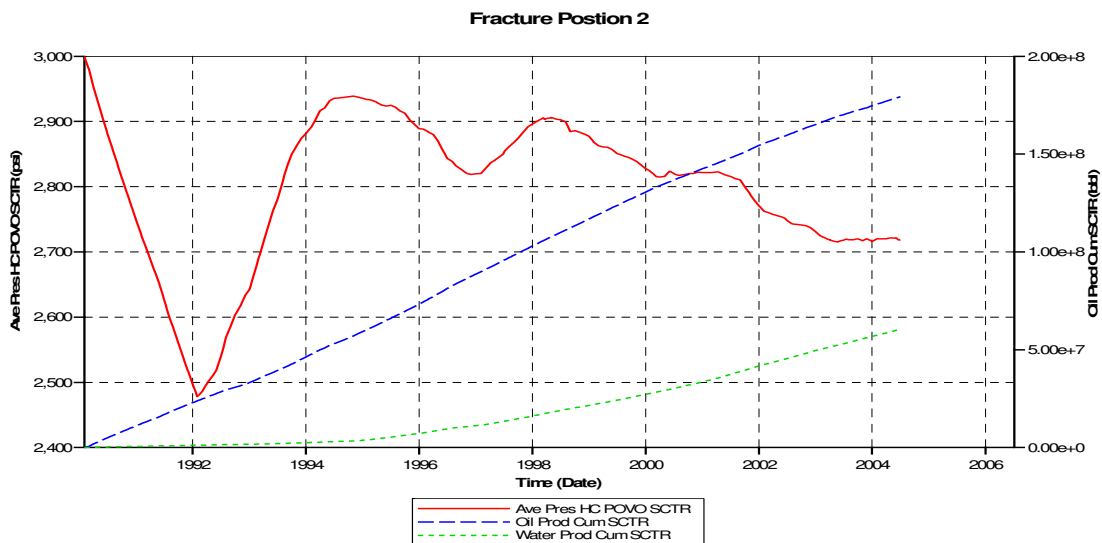


Fig. 5.41 - Results of Second Fracture Position Run

5.7.3 Position: 3

The last fracture network position is placed according to **Fig. 5.42** and the results are shown in **Fig. 5.43**.

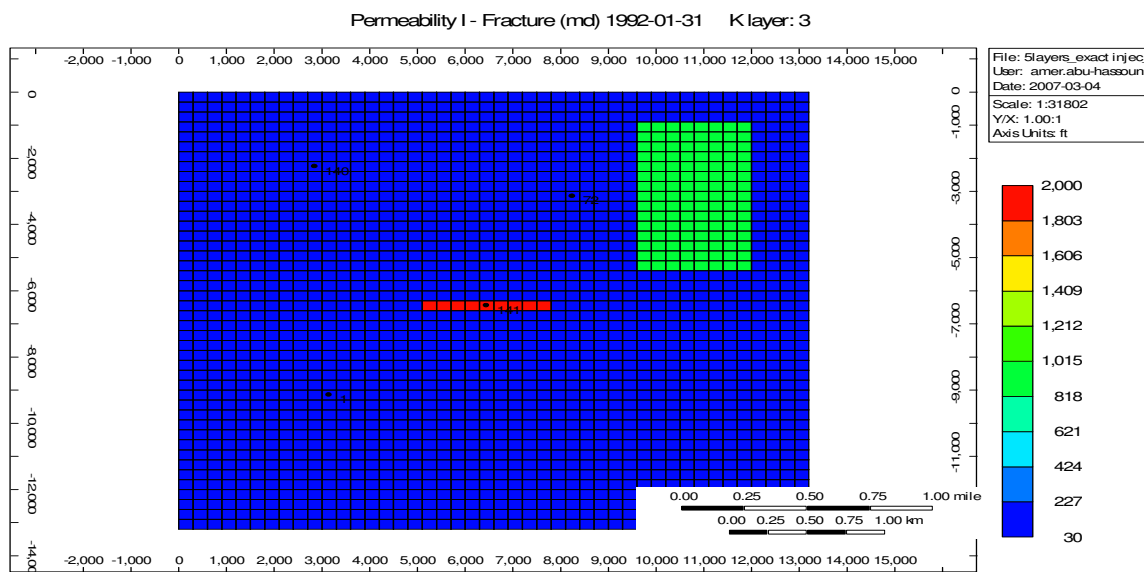


Fig. 5.42 - Third Fracture Position (Green), Super-K Layer in Red

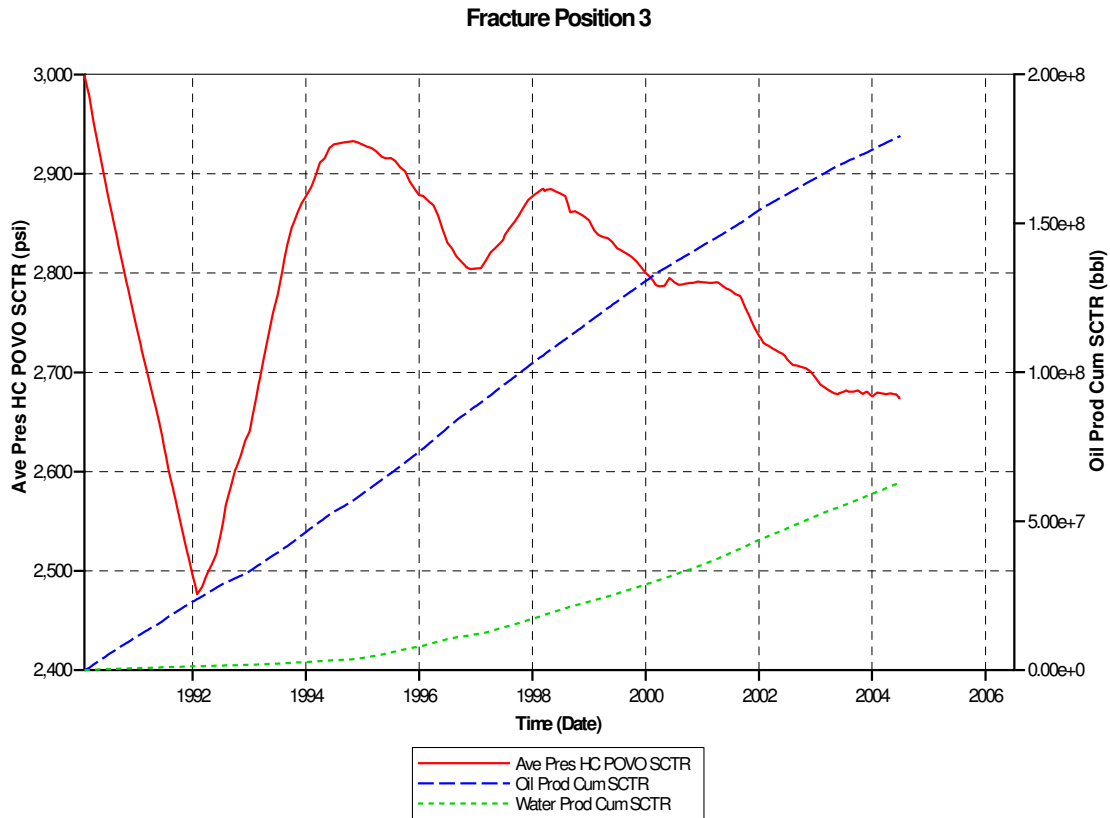


Fig. 5.43 - Results of Third Fracture Position Run

As the fracture position changes, the average field pressure profile and the water cut also changes but the cumulative water is the same for all fracture positions. As observed from the three plots, the fracture locations affected the water production differently and each position had different calculated bottom-hole pressure profile for producer P-141.

CHAPTER VI

WELL COMPLETION GEOMETRY

The completion geometry of producer P-141 is changed and the results will be analyzed to help identify the best completion strategies in the field. The completion is changed from vertical to a horizontal well. The horizontal producer in this scenario is completed in the third layer intersecting the Super-K zone as can be seen in **Fig. 6.1** below.

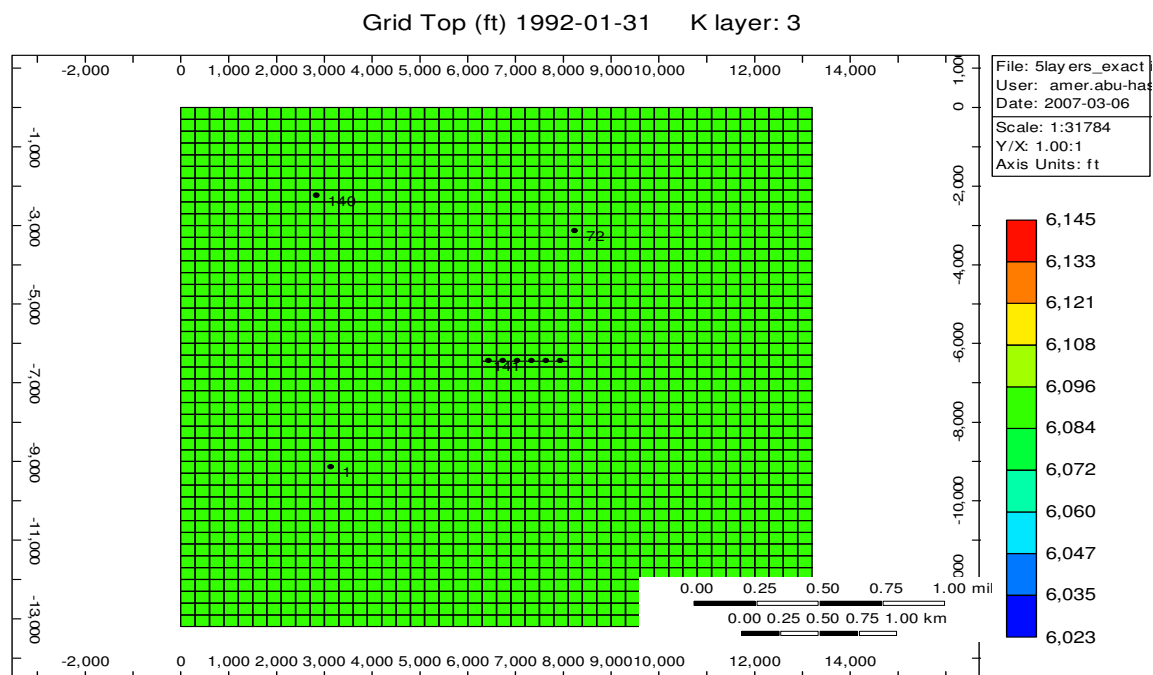


Fig. 6.1 - Horizontal Producer Placed in Third Layer

The horizontal hole extends 1,600 ft in the model and run with the 6-1/2” horizontal hole intersecting the fractures and the Super-K zone. The horizontal well is run again with the horizontal wellbore completed away from the fractures. The results of

running the simulator for the horizontal producer are presented in the **Figs. 6.2** and **6.3** below.

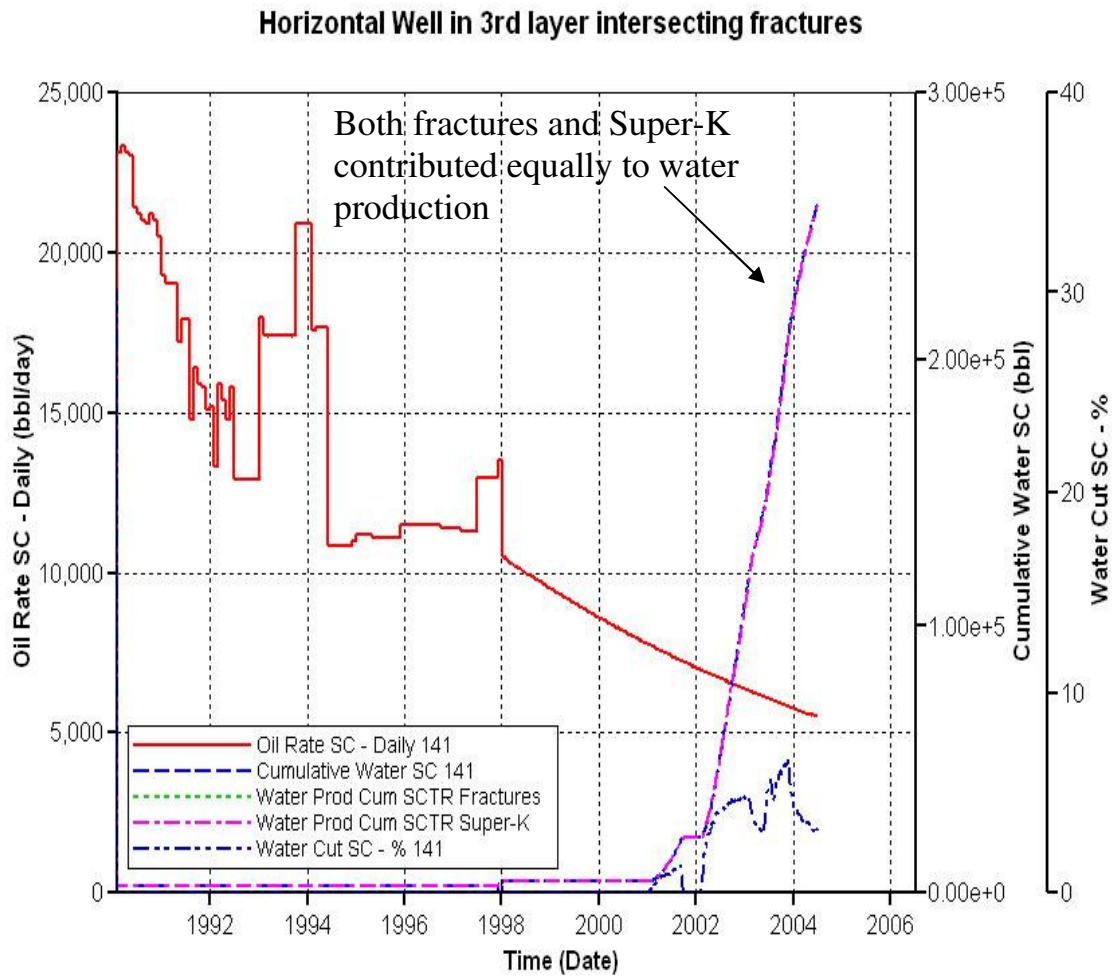


Fig. 6.2 - Simulation Results for a Horizontal-Hole Intersecting Super-K and Fractures

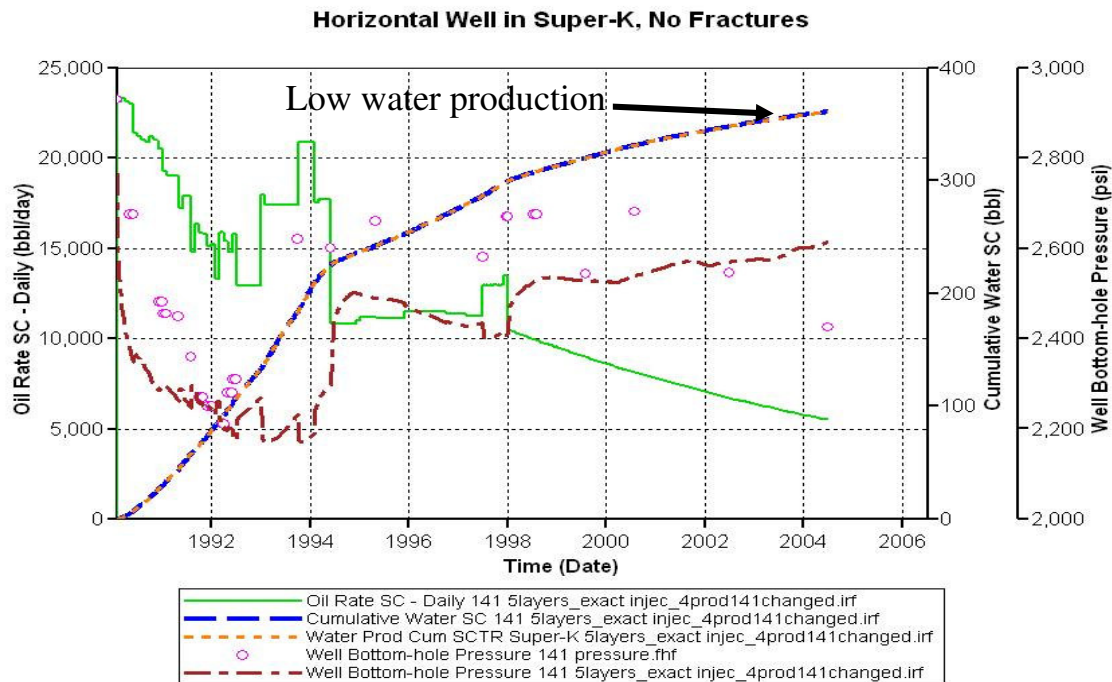


Fig. 6.3 - Simulation Results for a Horizontal-Hole Intersecting Super-K, No Fractures

As noticed from the figures above, the produced water is almost negligible in the case the horizontal well is completed in the third layer and no fractures exist. This indicates again that the fractures play a significant role in early water breakthrough problems in the area. The bottom-hole pressure profile in the case of fractures presented a good match to the pressure field data but in the case where there are no fractures; the pressure increased after year 1998. The completion will be changed in the next section to investigate the Super-K behavior with the horizontal well drilled above the Super-K zone and another run with the horizontal well completed inside the Super-K zone. Both cases are run with fractures and without fractures in the model.

The reason behind completing the horizontal well in the second layer is to compare the results with those obtained from completing the horizontal hole inside the Super-K layer for better completion practices. The results are plotted for two cases, one with fractures and another without fractures as presented in **Figs. 6.4** and **6.5**, respectively.

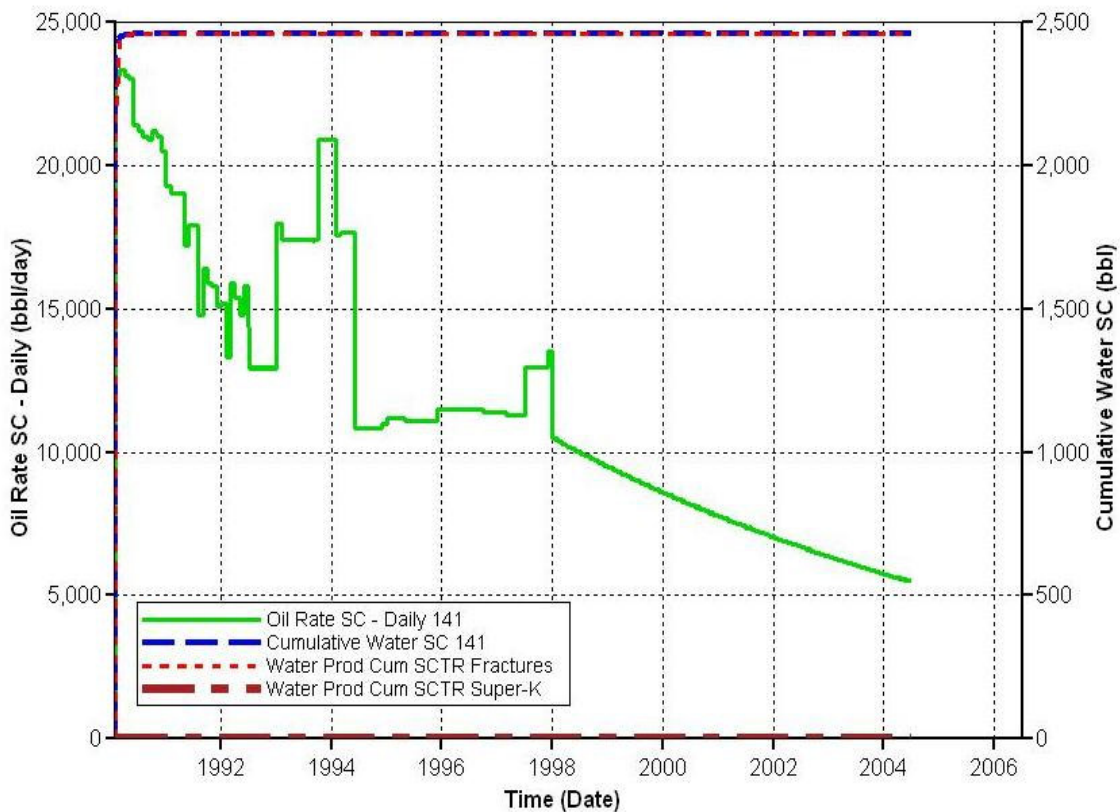


Fig. 6.4 - Simulation Results for a Horizontal-Hole above Super-K with Fractures Presence in the Model

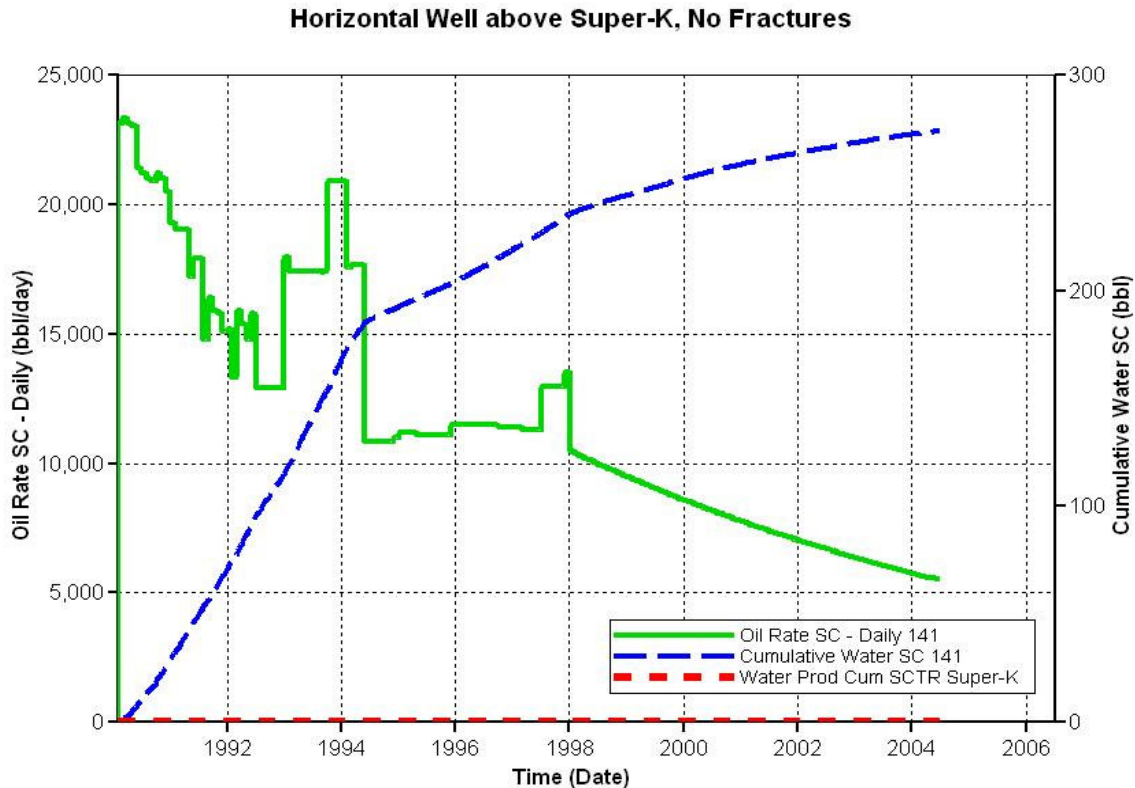


Fig. 6.5 - Simulation Results for a Horizontal-Hole above Super-K; No Fractures

Both figures show low water cut % and the calculated bottom-hole pressure came below the field pressure data in the case where there are no fractures the model. The Super-K zone did not contribute to the production profile for both cases. All the figures indicate that it is essential to include the fractures in the model if they exist in the field. The pressure and water cut is higher in the case with no fractures while the horizontal well intersects the Super-K zone.

CHAPTER VII

PREDICTION

In order to make a good reservoir engineering decision, it is important to predict how oil and water production and pressure profiles will most probably look like in the future. Prediction analysis is going to help modifying or improving completion strategies. In this chapter, a quick review of some cases will be discussed and based on the results; recommendations for best completion strategy will be concluded in the next chapter. The highlighted cases for this prediction study are as follows: best hypothetical history match case for vertical well, vertical well intersecting a Super-K zone and fractures are in three different positions, horizontal well intersecting a Super-K zone with fractures and without fractures, and horizontal well not intersecting a Super-K zone with fractures and another without fractures.

7.1 Case: 1

In this case, the same model achieved for best hypothetical history match is used but changes to the simulation time have been made. The well was assumed to be choked in July 2004 to give a rate of 5,450 bbls/day until the end of the simulation run. The simulation time is extended until the end of year 2039. The result of this run is presented in **Fig. 7.1**.

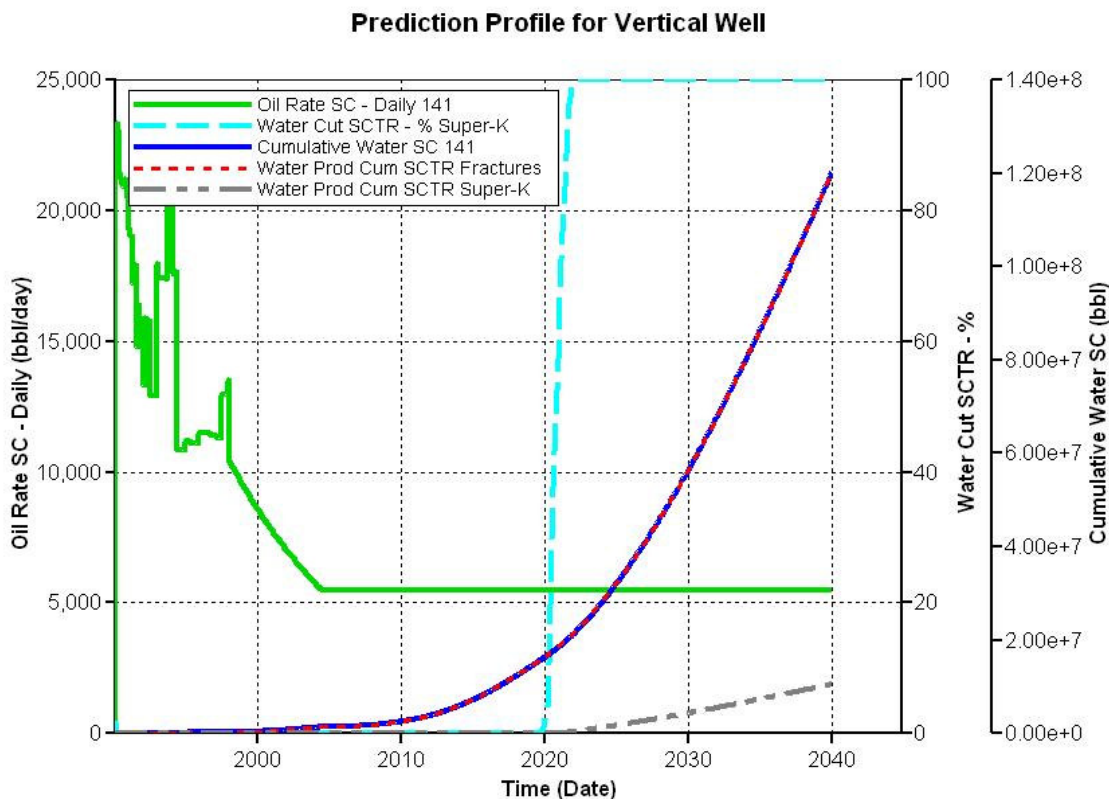


Fig. 7.1 - Case 1: Prediction Run

The source of water production is clearly the fractures rather than what is believed to be caused by the Super-K zone since the produced water from the fractures matches the water produced from the wellbore. The Super-K zone started producing water after year 2020 when the water reached layer three. The well shows a good capability of producing even after year 2040 when the water cut reached more than 80%. The BHP starts increasing after 2004 which means that the water injection in the area is more than what the producers need for pressure support. **Fig. 7.2** shows the water encroachment in producer P-141 by the end of the simulation run. Layers 5, 4 and 3 are almost swept but there is still capacity for oil production from Zone-1 and 2.

Water Saturation 2040-01-01 J layer: 22

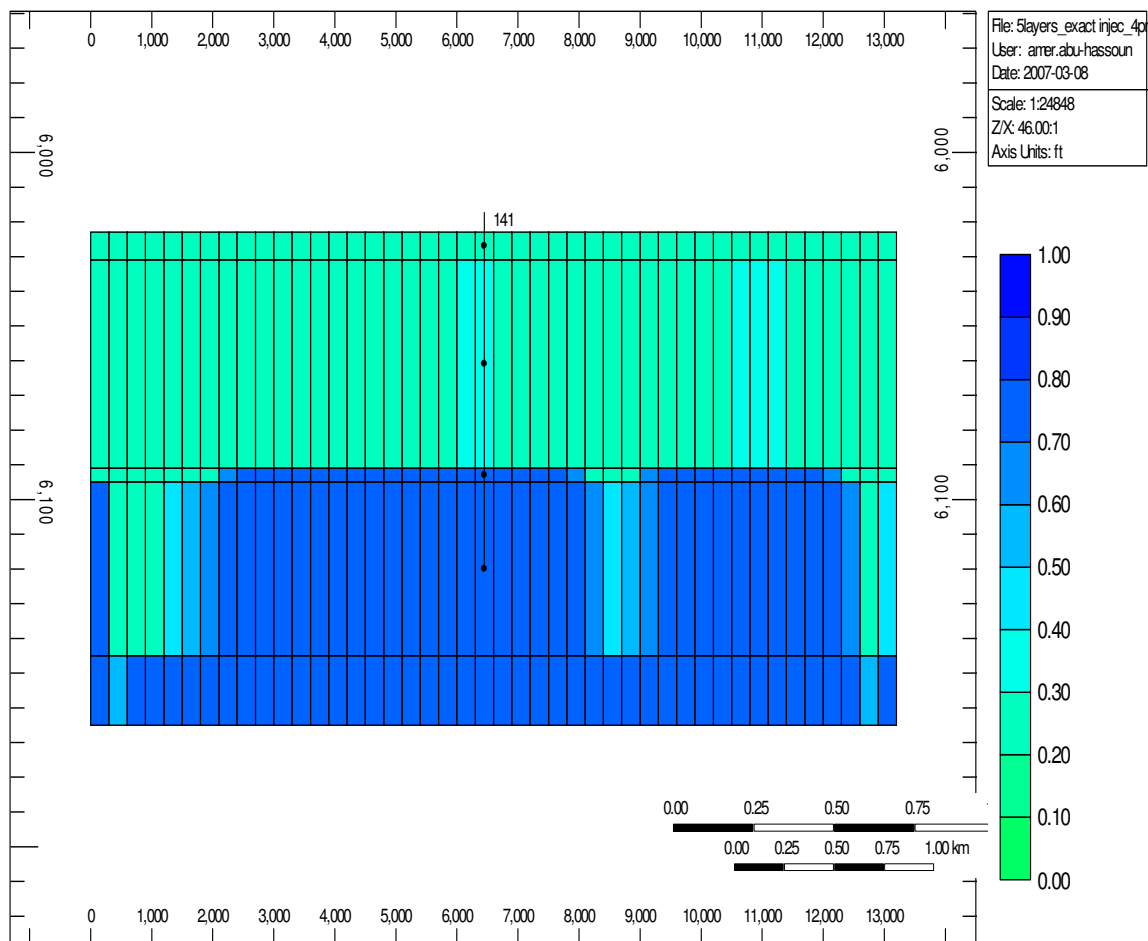


Fig. 7.2 - Water Encroachment near P-141 by End of Simulation Run

7.2 Case: 2

The fractures are located in three different positions as seen in **Fig. 5.34**. This case best describe how a vertical well intersecting a Super-K zone will behave if fractures are not connected to the Super-K zone. The results are presented in **Fig. 7.3**.

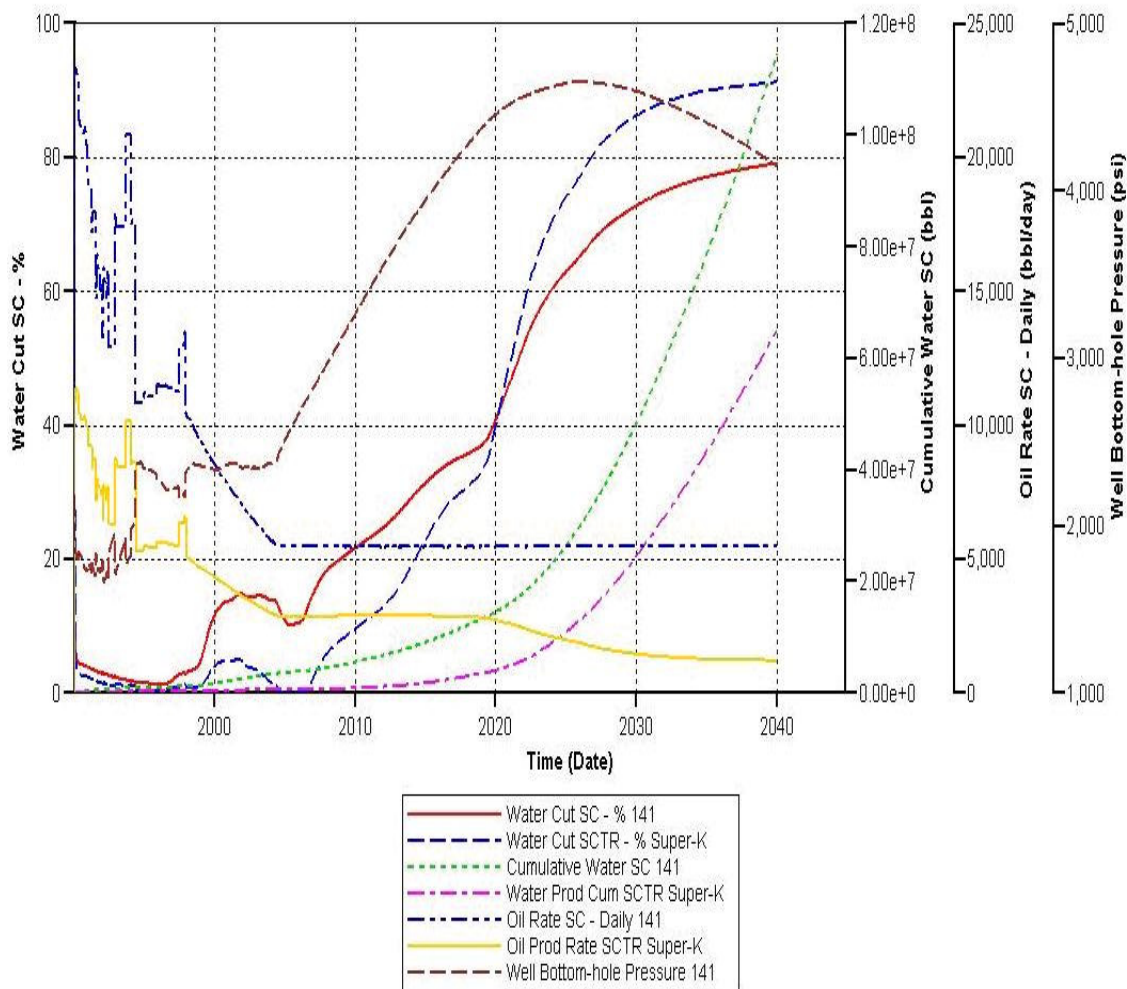


Fig. 7.3 - Case 2: Prediction Run

The Super-K contributed more to the flow in this case. As noticed, half of the production (oil and water) was coming from the Super-K layer. The water cut % in the Super-K zone started increasing gradually after 2008 and not sharply as seen in the best match case. **Fig. 7.4** shows how the oil is swept from layers 5, 4 and 3 but oil is still not recovered from layers 1 and 2.

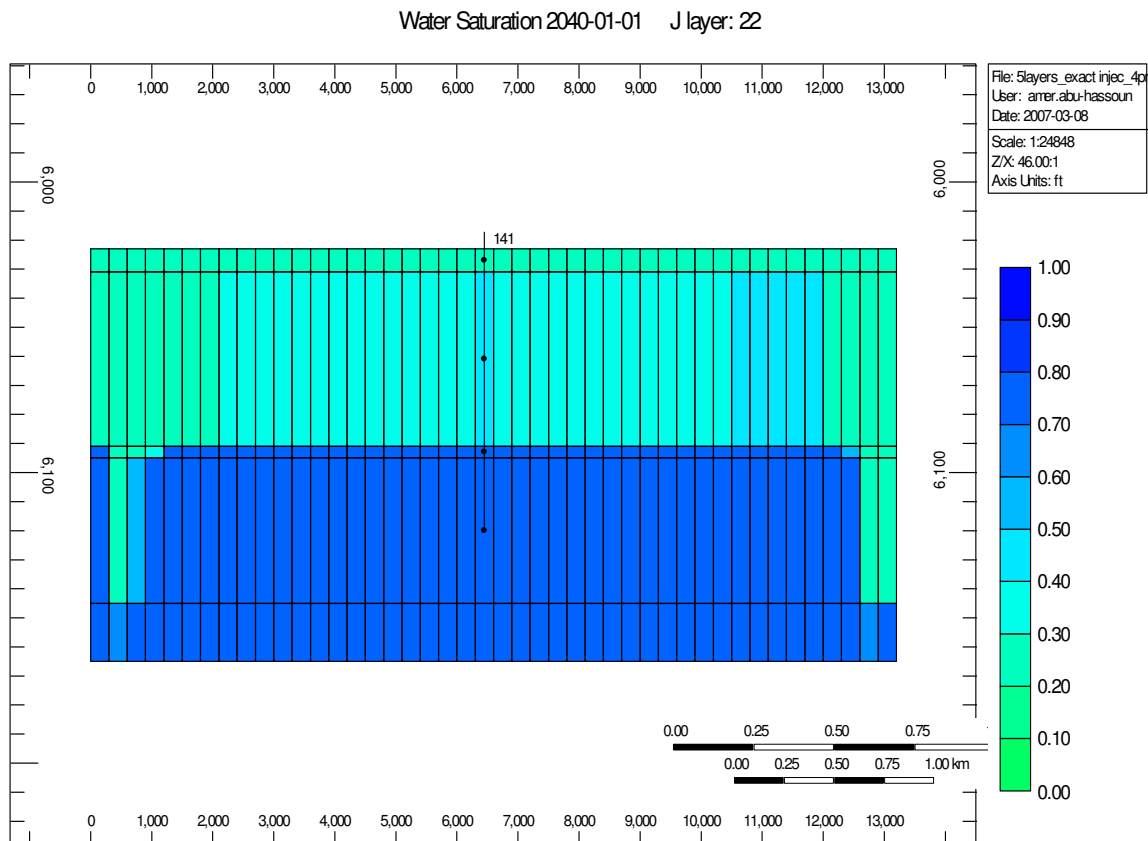


Fig. 7.4 - Good Oil Potential in Layers 1 and 2

7.3 Case: 3

In this scenario, the 1800 ft horizontal well is placed across the entire Super-K section with the fractures intersecting the Super-K zone. The result for this case is presented in **Fig. 7.5**. The figure shows that the oil and water production from the horizontal hole is all produced from the fractures and the Super-K zone. The Super-K layer acts like a horizontal pipe with vertical flow coming from the vertical fractures.

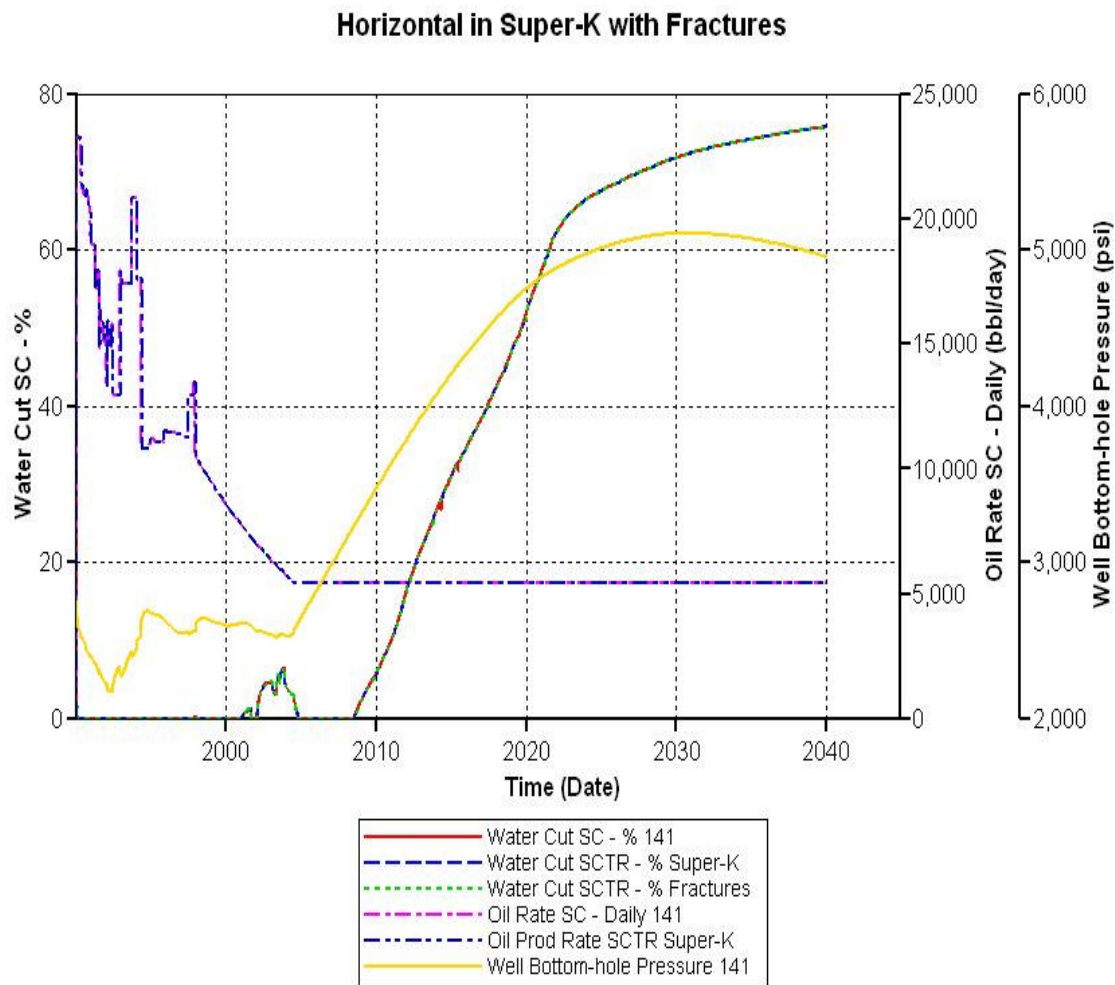


Fig. 7.5 - Case 3: Prediction Run

7.4 Case: 4

This case discusses the same horizontal well presented in case 3 but there is no fractures intersecting the wellbore or the Super-K zone. The result is shown in **Fig. 7.6**.

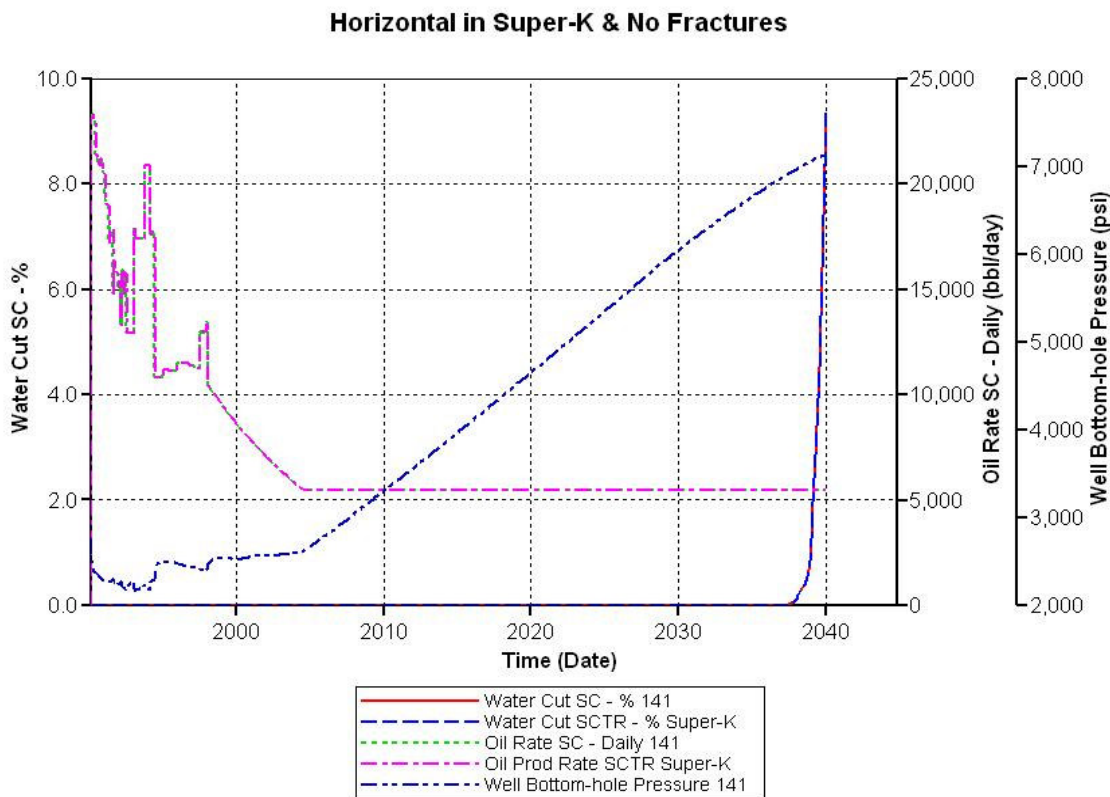


Fig. 7.6 - Case 4: Prediction Run

The water production in this case started late by the end of year 2037, unlike the previous cases where there was early water production. This case also shows the significant of fracture presence in the model. Without the fractures, the water production was delayed for years but as soon as the water hits the third zone as in **Fig. 7.7** where the Super-K zone is found, the water sharply produced. **Fig. 7.8** shows a 3-D view of water sweeping up to layer 3. It is clear from the figure that the water invaded the wellbore from the Super-K zone and not from the horizontal wellbore which indicates the importance of incorporating the Super-K zone in the simulation model to better understand the fluid flow mechanisms.

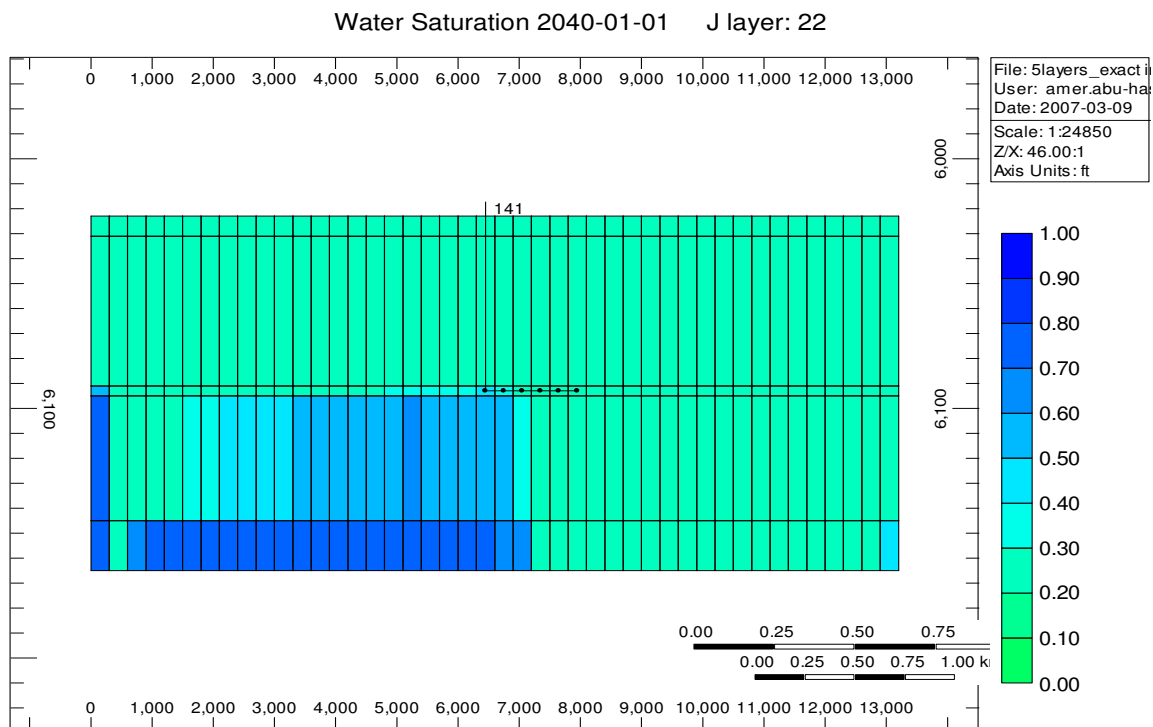


Fig. 7.7 - Water Encroachment by the End of Simulation Run

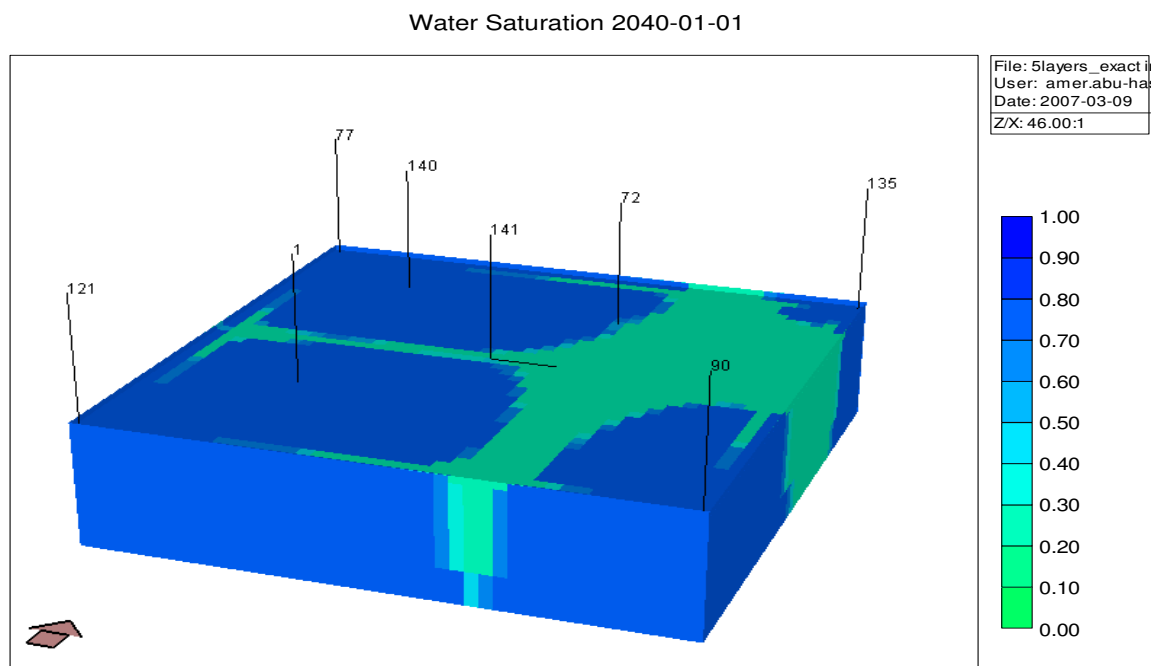


Fig. 7.8 - 3-D View of Water Flooding Up to Layer-3

7.5 Case: 5

The horizontal well is placed in layer-2 above the Super-K zone. The wellbore in this case is only in communication with the fractures but not with the Super-K layer. The result is presented in **Fig. 7.9**. As noticed, the Super-K zone did not produce any water. Water production was mainly produced from the fractures. The water cut reached 60 % in almost six years after the water invaded the fractures.

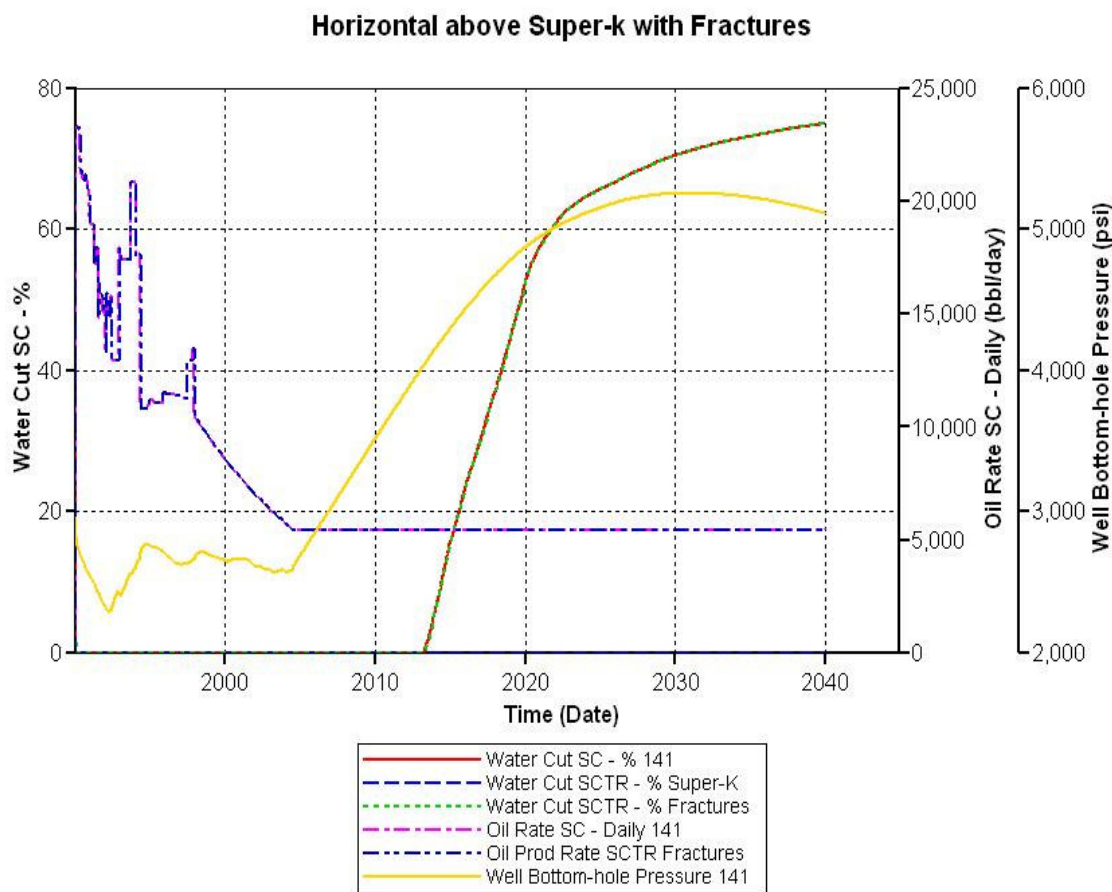


Fig. 7.9 - Case 5: Prediction Run

7.6 Case: 6

The last prediction is done for a horizontal well completed in layer 2 above the Super-K zone and there are no fractures. **Fig. 7.10** shows a late water production at

the end of the simulation run. The water cut is very low in this case even after 50 years of production. This result shows the importance of smart completion strategy for better water and oil production management. **Fig. 7.11** and **7.12** show the water encroachment in all layers and in layer-2, respectively.

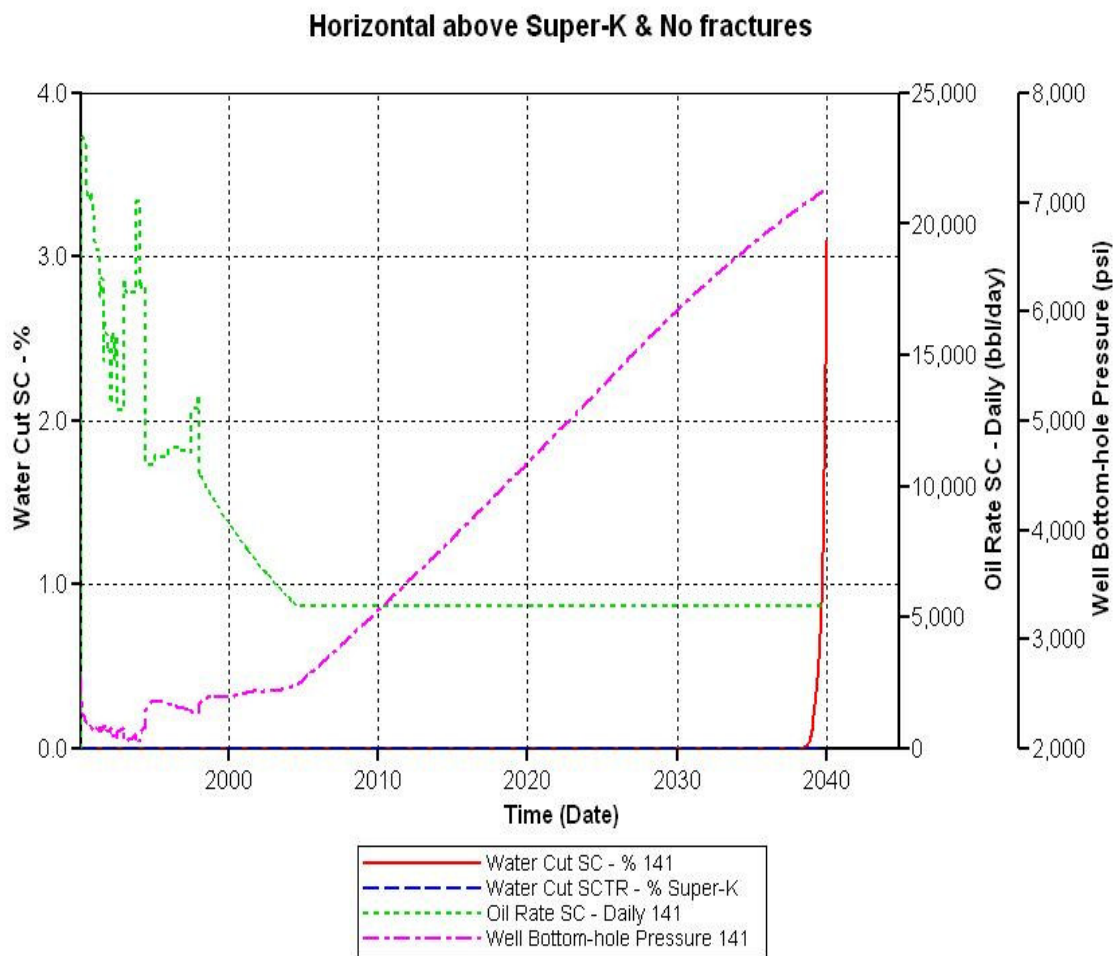


Fig. 7.10 - Case 6: Prediction Run

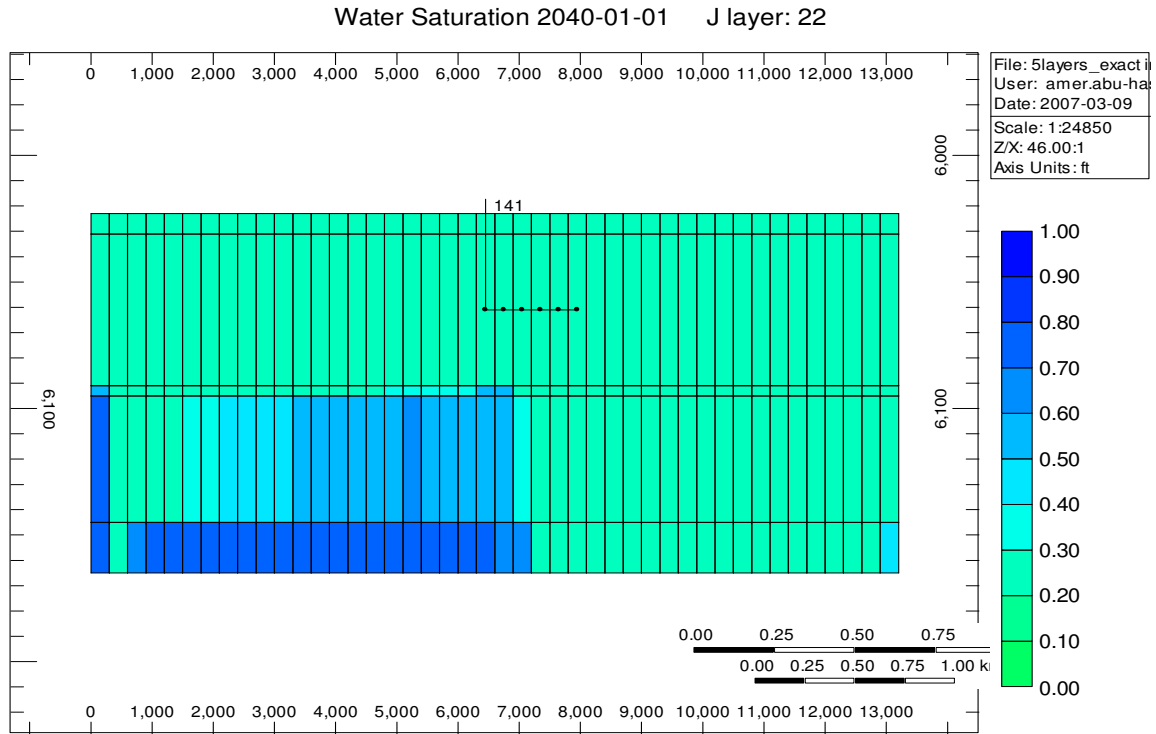


Fig. 7.11 - Water Encroachment below the Horizontal Hole

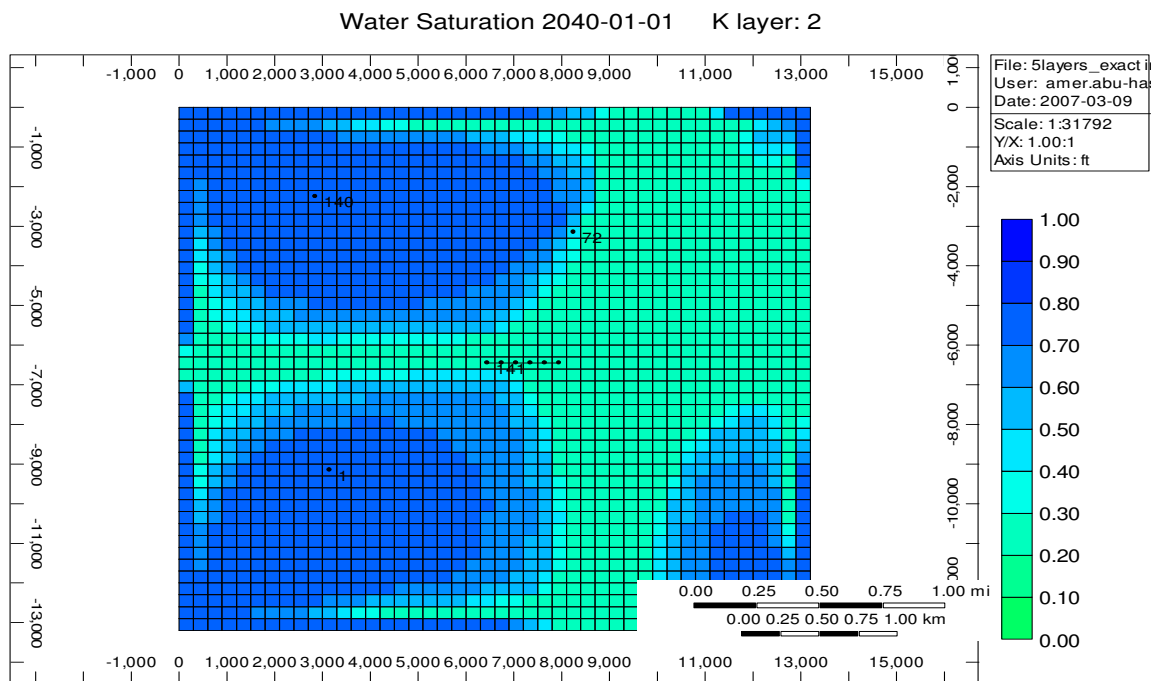


Fig. 7.12 - Water Encroachment in Layer-2

CHAPTER VIII

RECOMMENDATIONS FOR BEST COMPLETION

As seen in all the cases, it is critical to complete the wells in the right zones to avoid early water breakthrough and for better reservoir sweep efficiency. Several cases were built to see the effect of fractures and Super-K zone on production and pressure profiles. The fractures have a significant impact on early water breakthrough. In this section, best completion and recommended strategies will be highlighted for each case predicted earlier in Chapter VII.

8.1 Best Matching Case

For the first case, the vertical wellbore intersected the Super-K layer that is connected to fractures. Based on the results; refer to **Fig. 7.1**, the water cut starts increasing after year 2010 and the Super-K water production started in year 2020. **Fig. 8.1** suggested that by the end of 2013 the oil is almost swept from the fifth layer and water is being produced from the bottom of layer 4. This layer can be shut in by the end of year 2019 as the water started invading well P-141 from that layer as shown in **Fig. 8.2**. By the end of year 2021, the Super-K will be almost producing 100 % water. To reduce the water cut either a gelling polymers technique can be used or the Super-K layer should be shut in by a mechanical mean since it is only producing water. An experimental investigation was done by Alqam et al¹⁹ to modify the permeability of the Super-K layer by using gelling polymers. The only way to allow an efficient displacement of the injection and production front to proceed in a Super-K layer for better sweep efficiency is the use of gelling polymers technique rather than a mechanical mean where the Super-K

zone is completely sealed. The gel treatments can reduce the channeling of the fluid through the Super-K layer without damaging the oil producing zones.

The group found out that the presence of fractures will create problems in designing and implementing the gel treatment. They concluded that the treatment was more successful in reducing the permeability of the matrix but was less in fractured Super-K layers. The treatment can also fail on vugular or fractured carbonate, because the gel may not be able to fully fill the pore structure. Finally, the success of the gel treatment is dependent on good geologic characterizations of the Super-K texture. Al-Dhafeeri et al²⁰ findings also agree with the previous study. They also discussed the importance of the geological area of the Super-K layer, the distance of gelant penetration from the Super-K face, the residual resistance factor, and the pressure drop across the gelant bank on calculating the right volume of the disproportionate permeability reduction gelant treatment.

Another way to reduce the water production from the Super-K layer is to restrict the flow by choking the well rate. AlShehri and AlMurikhi⁶ presented a case where a choke performance test was performed on a well producing 11,500 BOPD with 30 % water cut. This well has a Super-K layer based on flowmeter run analysis. The well was choked gradually to a lower rate. At 50/64 inch choke setting, the well was almost producing no water with 8,000 BOPD.

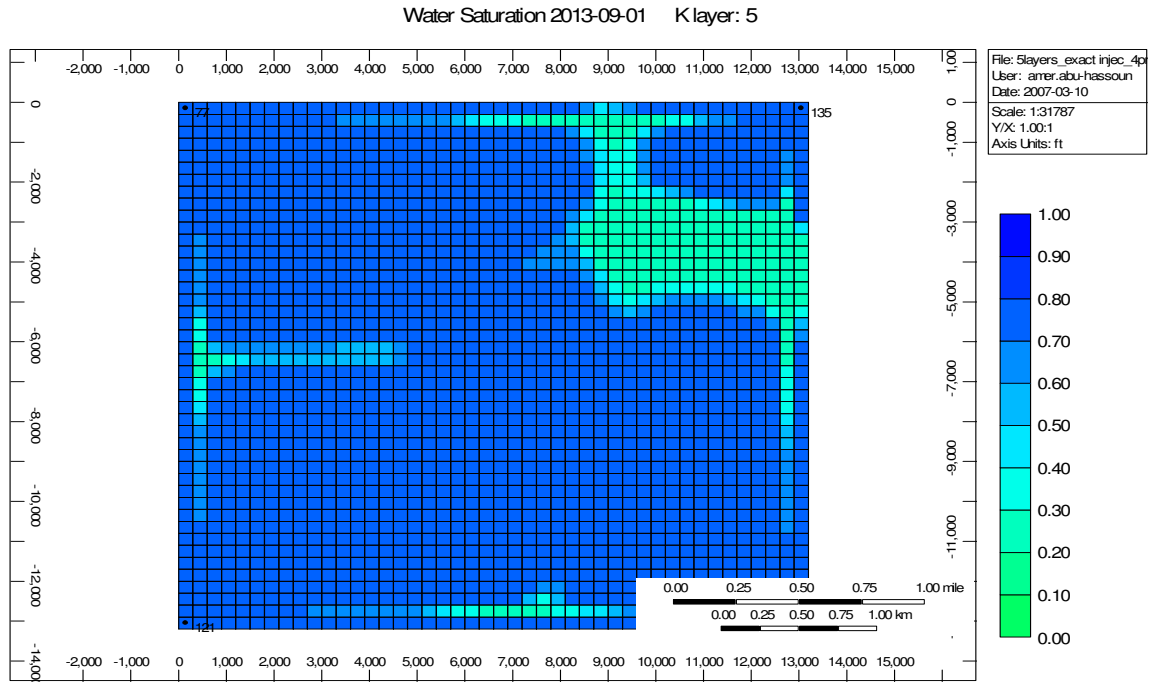


Fig. 8.1 - Layer-5 Watered Out by End of Year 2013

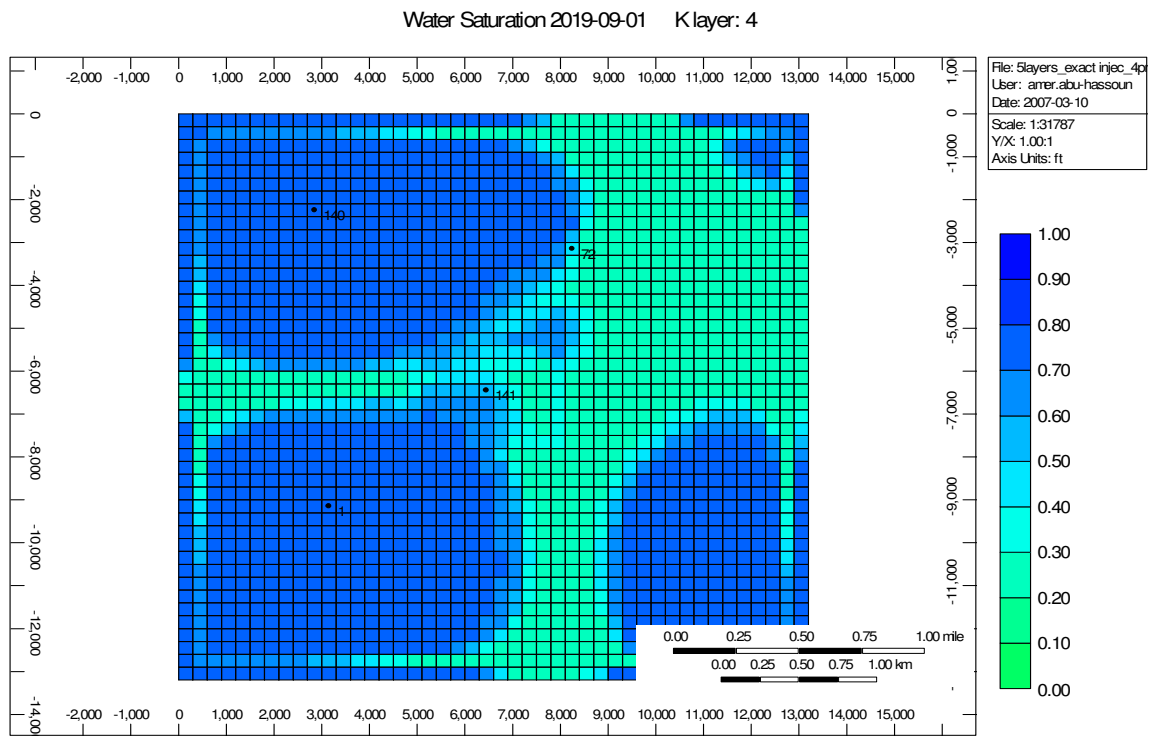


Fig. 8.2 - Water Invaded Producer P-141 in Layer-4 by End of Year 2019

Another production profile was run later and it showed that the Super-K Zone stopped producing water at the same choke setting. The Super-K layer was in communication with the lower layers through fractures. As the pressure drawdown increased, the water migrated through fractures away from the wellbore and into the high permeable zone causing the well to produce at high water cut. The well produced for four years and was able to sustain 6,000 BOPD with only 8 % water cut at 50/64 inch choke setting. Isolating the Super-K zone to produce the lower zones first, would add unnecessary operational cost; the authors concluded.

For best completion strategy in a vertical well is to be completed in a Super-K layer if it is not vertically connected to fractures. Also, completing in a Super-K layer should be avoided if the layer is vertically connected to fractures to delay any early water breakthrough from the fractures and also for better bottom-up sweep efficiency. Selectively perforating above and below the Super-K layer is recommended if the Super-K layer is in communication with the injectors through fractures.

8.2 Horizontal Completion

In the model used, it was assumed that the horizontal well is completed inside and above the Super-K layer. The Super-K layer either intersects the fractures or it may not cross any fractures/faults. The water cut is compared in all the cases. **Fig. 8.3** presents the simulation results for a horizontal wellbore completed in layer-3 and intersected the Super-K zone.

It is obvious how the fractures brought in the water to the wellbore compared to the case where there are no fractures. The well produced dry oil until it got wet late in 2039. Another comparison is made to the horizontal-hole production completed above the

Super-K layer with the horizontal hole intersecting fractures and then compared to the case where fractures are not present. **Fig. 8.4** shows how the water cut increases in both cases.

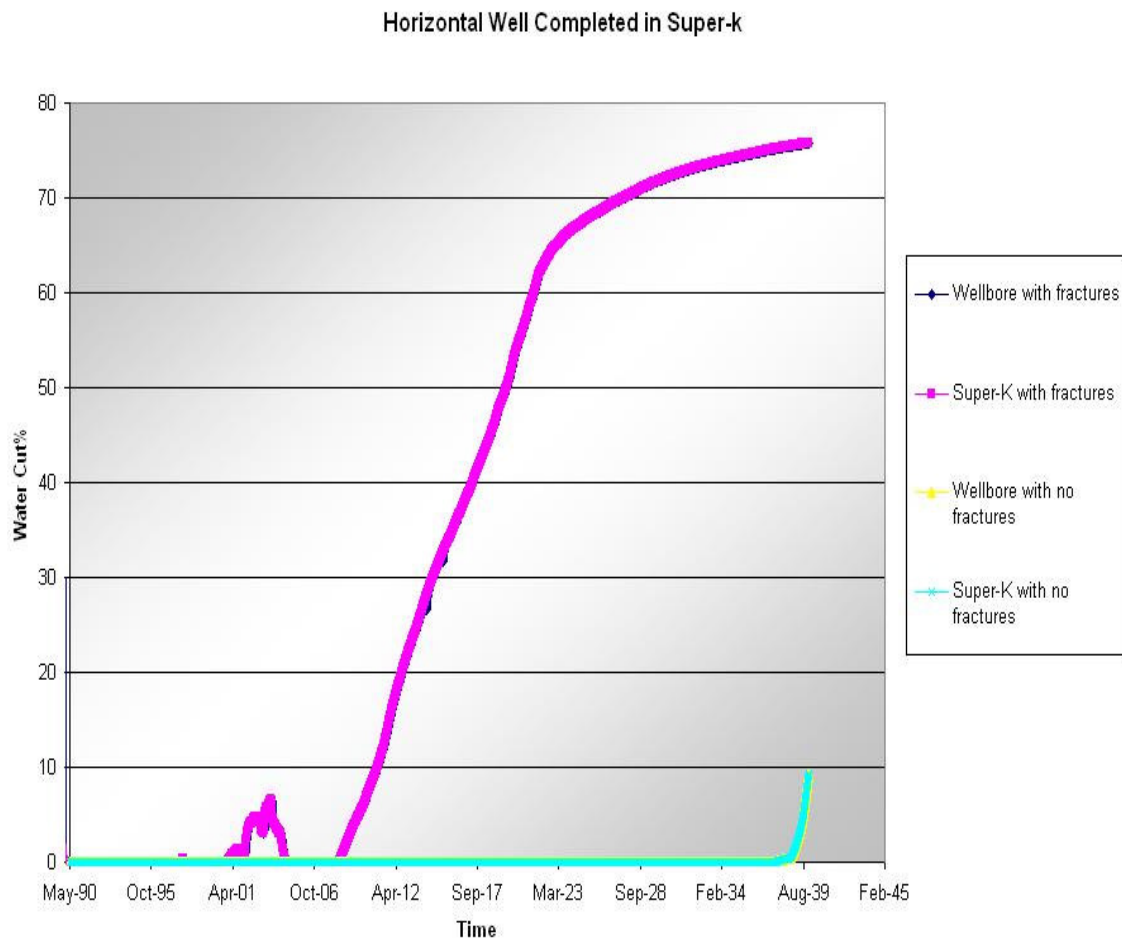


Fig. 8.3 - Comparison Plot of Production from Horizontal Wellbore

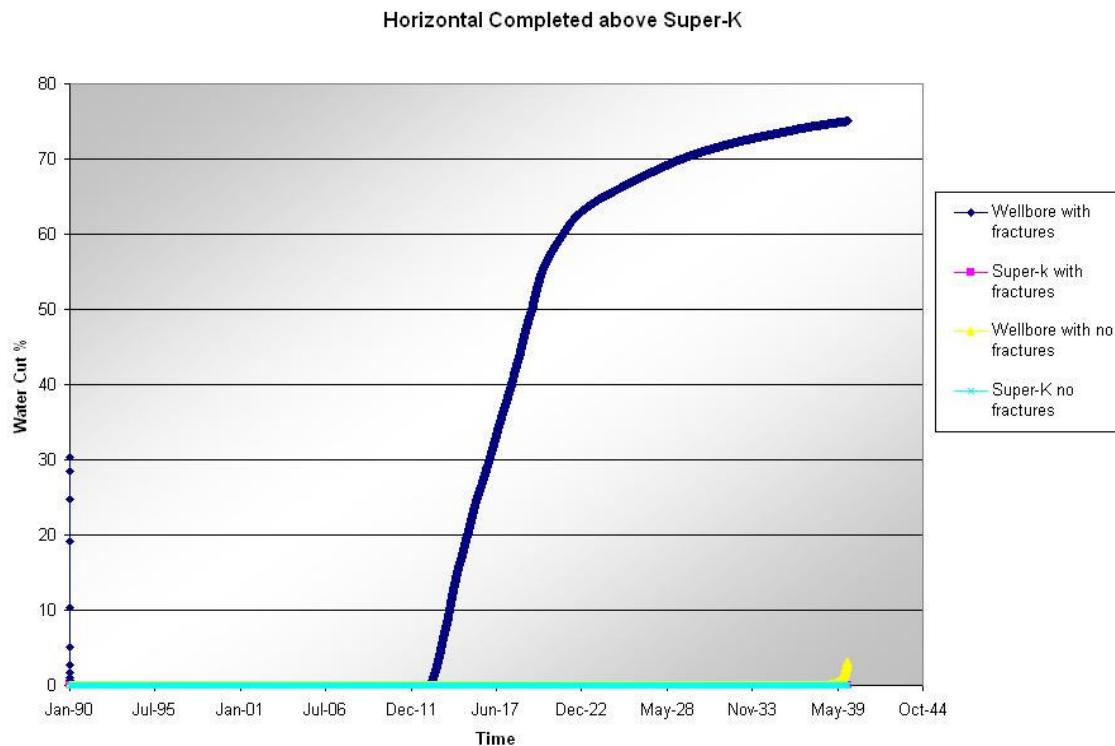


Fig. 8.4 - Water Cut Increases in Case Fractures Present

When the horizontal well is completed above the Super-K layer, the Super-K did not produce any water. As noticed in the figure, the fractures caused the wellbore to produce water earlier than the case where there are no fractures. Based on the results, the best completion is to avoid completing the horizontal wellbore in the fractures to avoid early water breakthrough. The best recommended completion is to complete the horizontal well above the Super-K zone and try avoiding any intersection with the fractures. The Super-K zone was of a secondary cause for water breakthrough in a vertical well. For quick recovery with higher oil rate, completing inside the Super-K layer is highly recommended if it is not in communication with fractures that are connected to a water source.

CHAPTER IX

CONCLUSIONS AND RECOMMENDATIONS

An extensive literature review was given to both Super-K zones and natural fractures characterization and modeling. The main outcome and conclusions from the simulation study presented in the current work to understand the fluid mechanisms of the high permeability layer called the Super-K in a naturally fractured carbonate reservoir can be summarized in the next sections.

9.1 Conclusions

- Previous studies suggested from field production performance analysis that the reservoir acts as a dual-media system recognized by early water breakthrough which is caused by high permeability thin zones called the Super-K that are connected vertically with natural fractures. However, in this study, the early water breakthrough has been shown to be contributed to the natural fractures and the Super-K produces insignificant water compared with fractures.
- The Super-K produces high water only if connected vertically with fractures. The fractures are the primary source of early water breakthrough and the Super-K layer acts as a secondary source.
- It is significant to study the open hole and production logs to find out if the Super-K layer is continuous through out the reservoir and linked to vertical fractures or occur at isolated regions.
- In naturally fractured reservoir with high thin permeable layers, the engineers and geologist generally starts the dual permeability model construction with the most complex geological selections. As the simulation history matching advances, the

fluid flow behavior and geological representation become more complex and requires more effort to simulate. Starting with the simplest parameters and assuming a homogenous reservoir is the key to a good simulation modeling.

- The dual porosity/dual permeability simulation offers several advantages in its ability to model the fluid flow complexity between different reservoir components.
- The sensitivity studies showed that fracture porosity, spacing, permeability and length play important role in bringing water prematurely to the wellbore. The simulation results show that the fractures are the main source of water prematurely breaking through the wellbore and the Super-K zone acts as a secondary source.
- Knowing the precise layer in completing the horizontal wellbore is critical to avoid any early water breakthrough if the wellbore intersects with a Super-K layer or fractures.

9.2 Recommendations

Based on the results obtained from the simulation work, the followings are some recommendations for reservoir modeling and best completion strategies in the field:

- For best simulation procedure to account for the Super-K layer in naturally fractured reservoir is to consider a dual permeability modeling. It is essential to incorporate the Super-K layer in modeling the natural fractured reservoir to get a better history match to the produced fluid
- According to Algam et al and Al-Dhafeeri et al, gelling polymers technique maybe recommended to reduce the Super-K relative permeability to water and

hence diminish water production while maintaining the relative permeability to oil.

- Along with AlShahri and AlMuraikhi findings, instead of plugging off the Super-K layer, choosing the correct choke size setting will help keep the water cut low while maintaining the oil production.
- Completing the horizontal wellbore in areas where fractures are intense should be avoided to prevent early water channeling to the wellbore.
- Completing the horizontal hole inside the Super-K layer if there are no fractures for quick recovery is advised. If there are fractures then completing above the Super-K layer is suggested.

NOMENCLATURE

B	Formation volume factor (resbbl/STB)
$bbls$	Barrels
g	Fluid gradient, psi/ft
K	Permeability
Kr	Relative Permeability
L	Fracture Spacing
n	Number of normal sets of fractures
Pf	Fracture pressure
Pm	Matrix pressure
q	Flow rate, bbls/d
S	Saturation
stb	Stock tank barrel
t	Time, days
Δt	Time step size, days
T	Fluid transmissibility, STB/D.psi
$TRAN$	Transmissibility
μ	Fluid viscosity, cp
ρ	Density, lbm/cu ft
σ	Shape factor, ft ⁻²
ϕ	Porosity, fraction
ω	Upstream weighting factor

REFERENCES

1. Voelker, J., Liu, J., Caers, J.: "A Geostatistical Method for Characterizing Superpermeability From Flow-Meter Data: Application to Ghawar Field" paper SPE 84279 presented at the SPE Annual Technical Conference and Exhibition held in Denver, Colorado, 5-8 October 2003.
2. Phelps, R.E., Strauss J.P.: "Capturing Reservoir Behavior by Simulating Vertical Fracture and Super-K Zones in the Ghawar Field" paper SPE 79048 revised for publication from paper SPE 66389 and approved on 8 June 2002.
3. Phelps, R.E. and Strauss J.P.: "Simulation of Vertical Fractures and Stratiform Permeability of the Ghawar Field" paper SPE 66389 presented at the SPE Reservoir Simulation Symposium held in Houston, 11-14 February 2001.
4. Stenger, B.A., Ameen, M.S., Al-Qahtani, S., Pham, T.R.: "Pore Pressure Control of Fracture Reactivation in the Ghawar Field, Saudi Arabia" paper SPE 77642 presented at the SPE annual Technical Conference and Exhibition held in San Antonio, Texas, 29 September - 2 October 2002.
5. Al-Dhamen, A.A., Pham, T.R., Al-Khatib, M.R.: "A Quick Method of Identifying and History Matching a Gravity Dominated Reservoir with Localized Super-Permeabilities" paper SPE 49276 presented at the SPE Annual Technical Conference and Exhibition held in New Orleans, Louisiana, 27-30 September 1998.
6. Al Shahri, A.M., Al Muraikhi, A.: "A Novel Approach to Characterize Dynamic Interaction between Super Permeability Layers with Vertical Faults and Their Affect on Flood Front Movement" paper SPE 49275 presented at the 1998 SPE

- Annual Technical Conference and Exhibition held in New Orleans, Louisiana, 27-30 September 1998.
7. Moore, D.M.: “Impact of Super Permeability on Completion and Production Strategies” paper SPE 17974 presented at the SPE Middle East Oil Technical Conference held in Manama, Bahrain, 11-14 March, 1989.
 8. Valle, A., Pham, A., Hsueh, P.T., Faulhaber, J.: “Development and Use of a Finely Gridded Window Model for a Reservoir Containing Super Permeable Channels” paper SPE 25631 presented at the SPE Middle East Oil Technical Conference and Exhibition held in Bahrain, 3-6 April 1993.
 9. Pham, T.R., Stenger, B.A., Al-Otababit, U.F.: “A Probability Approach to Development of a Large Carbonate Reservoir with Natural Fractures Stratiform Super-Permeabilites” paper SPE 81433 presented at the SPE 13th Middle East Oil Show and Conference held in Bahrain, 5-8 April 2003.
 10. Gill, H.S., Al-Zayer, R.: “Pressure Transient Derivative Signatures in Presence of Stratiform Super-K Permeability Intervals, Ghawar Arab-D Reservoir” paper SPE 88704 presented at the 11th Abu Dhabi International Petroleum Exhibition and Conference held in Abu Dhabi, U.A.E., 10-13 October 2004.
 11. Cosentino, L., Coury, Y., Daniel, J.M., Manceau, E., Ravenne, C., Lingen, P.V.: “Integrated Study of a Fractured Middle East Reservoir With Stratiform Super-K Intervals-Part 2: Upscaling and Dual-Media Simulation” paper SPE 76642 revised for publication from paper SPE 68184, first presented at the 2001 SPE Middle East Oil Show, Bahrain, 17-20 March 2001.

12. Dogru, A.H., Dreiman, W.T., Hemanthkumar, K., Fung, L.S.: “Simulation of Super-K Behavior in Ghawar by a Multi-Million Cell Parallel Simulator” paper SPE 68066 presented at the SPE Middle East Oil Show held in Bahrain, 17-20 March 2001.
13. Sarma, P., Aziz, K.: “New Transfer Functions for Simulation of Naturally Fractured Reservoirs with Dual-Porosity Models” paper SPE 90231 presented at the 2004 Annual Technical Conference and Exhibition, Houston, 26-29 September 2004.
14. Warren, J.E., Root, P.J.: “The Behavior of Naturally Fractured Reservoirs” paper SPE 426 presented at the Fall Meeting of the Society of Petroleum Engineers in Los Angeles on Oct. 7-10, 1962.
15. Kazemi, h., Merrill, L.S., Porterfield, P.R., Zeman, P.R.: “Numerical Simulation of Water-Oil Flow in Naturally Fractured Reservoirs” paper SPE 5719 presented at the SPE-AIME Fourth Symposium on Numerical Simulation of Reservoir Performance held in Los Angeles, Feb. 19-20, 1976.
16. Kazemi, H., Gilman, J.R.: “Improvements in Simulation of Naturally Fractured Reservoirs” paper SPE 10511 presented at the SPE Reservoir Simulation Symposium held in New Orleans, Jan. 31-Feb. 3 1982.
17. Mora, C.A., Wattenbarger, R.A.: “Analyst and Verification of Dual Porosity and CBM Shape Factors” paper 2006-139 presented at the Petroleum Society’s 7th Canadian International Petroleum Conference (57th Annual Technical Meeting), Calgary, Alberta, Canada, June 13-15, 2006.

18. Gilman, J.R.: “Practical Aspects of Simulation of Fractured Reservoirs” keynote speech presented at the International Forum on Reservoir Simulation held in Buhl, Baden-Baden, Germany, June 23-27, 2003.
19. Algam, M.H., Nasr-El-Din, H.A., Lynn, J.D.: “Treatment of Super-K Zones Using Gelling Polymers” paper SPE 64989 presented at the 2001 SPE International Symposium on Oilfield Chemistry held in Houston, Texas, 13-16 February 2001.
20. Al-Dhafeeri, A.M., Seright, R.S, Nasr-El-Din, H.A., Sydansk, R.D.: “High-Permeability Carbonate Zones (Super-K) in Ghawar Field (Saudi Arabia): Identified, Characterized, and Evaluated for Gel Treatments” paper SPE 97542 presented at the SPE International Improved oil Recovery Conference in Asia Pacific held in Kuala Lumpur, Malaysia, 5-6 December 2005.

APPENDIX A

MODEL PROPERTIES

Table A.1 – Reservoir and Fluid Properties

Property	Value	Description
Pbo	1,780 psi	Bubble Point Pressure
Swco	21 %	Connate Water Saturation
Kro	0.85	Relative Permeability to oil
Krwoir	0.45	Relative Permeability to Oil at Irreducible Oil
So	0.77	Oil Saturation
Pi	3,000	Initial Pressure
Vmod	20	Volume Modifier at Boundary Section
Sw	0.21	Water Saturation
Tres	195° F	Reservoir Temperature
ρ_o	52.06 lb/ft ³	Oil Density
ρ_w	63.2 lb/ft ³	Water Density
Yg	1	Gas Gravity
Bw	1.036	Water Formation Volume Factor
Cw	3.3 e ⁻⁶ 1/psi	Water Compressibility

Table A.2 – Matrix Properties

Layer	Grid Thickness(ft)	Matrix Φ %	Matrix Permeability			Fracture Spacing (ft)
			I (mD)	J (mD)	K (mD)	
1	8	20	50	50	50	300
2	60	20	90	90	90	300
3	4	20	90	90	90	300
4	50	20	50	50	50	300
5	20	15	100	100	100	300

Table A.3 – Fracture Sector Properties

Layer	Φ %	I	J	K	I	J	K
1	1	1,000	1,000	1,000	10	300	300
2	1	1,000	1,000	1,000	10	300	300
3	1	1,000	1,000	1,000	10	300	300
4	1	1,000	1,000	1,000	10	300	300

Table A.4 - Super-K Sector Properties

Layer	Φ %	Permeability (mD)		
		I	J	K
3	35	2,000	2,000	2,000

APPENDIX B

ADDITIONAL FIGURES FOR DATA USED IN SIMULATION RUNS

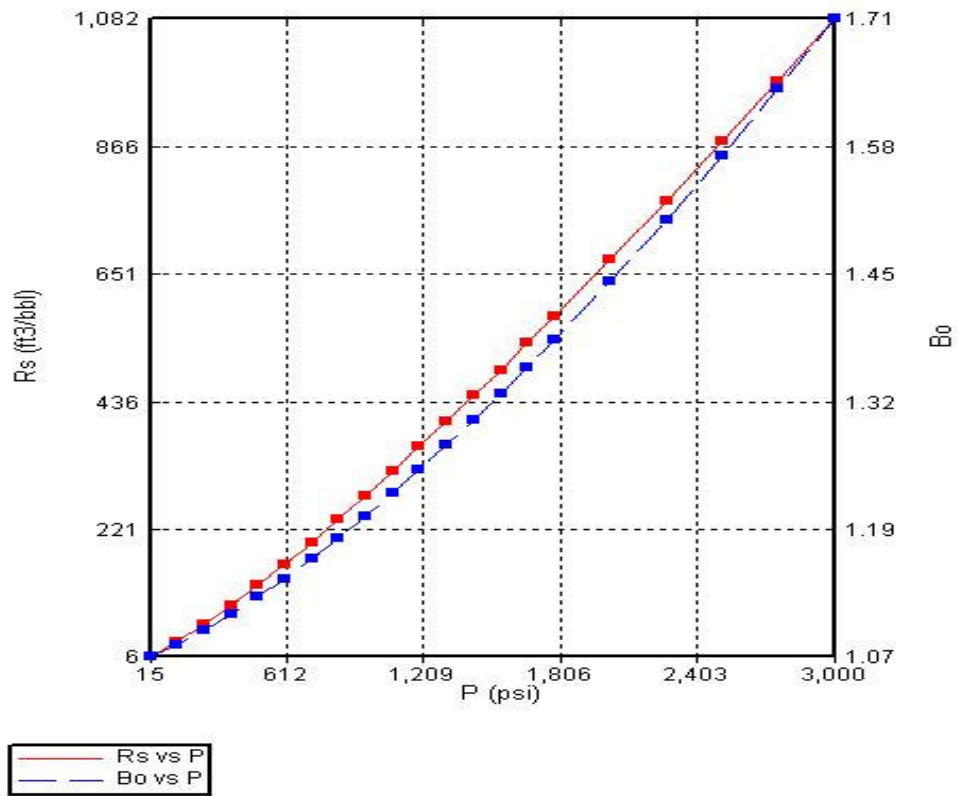


Fig. B.1 – Formation Volume Factor and Gas Solution Ratio

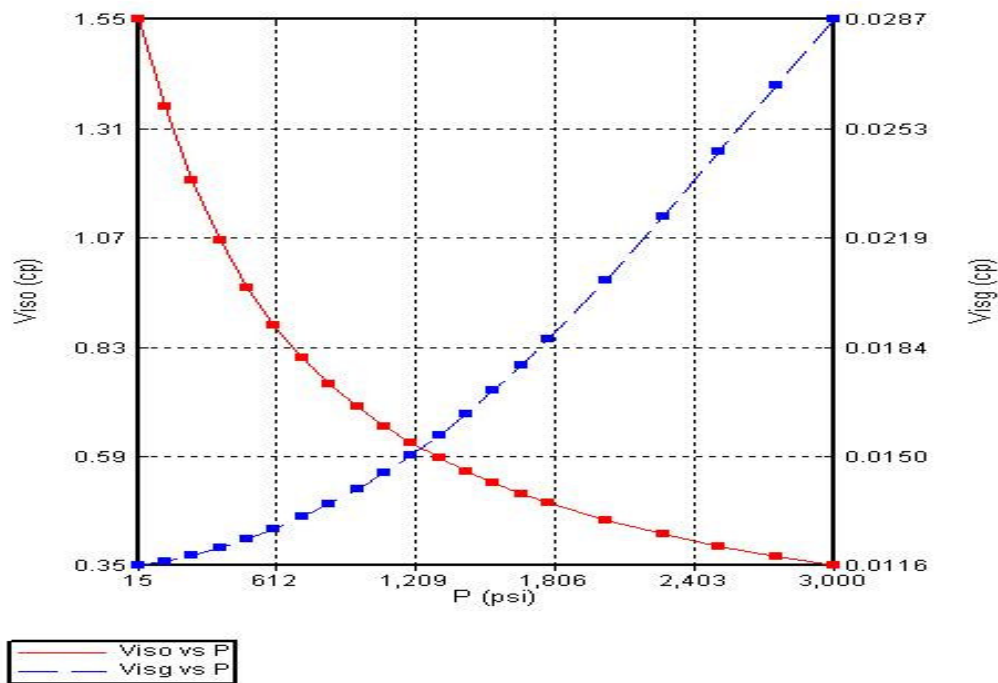


Fig. B.2 – Fluid Viscosity versus Pressure

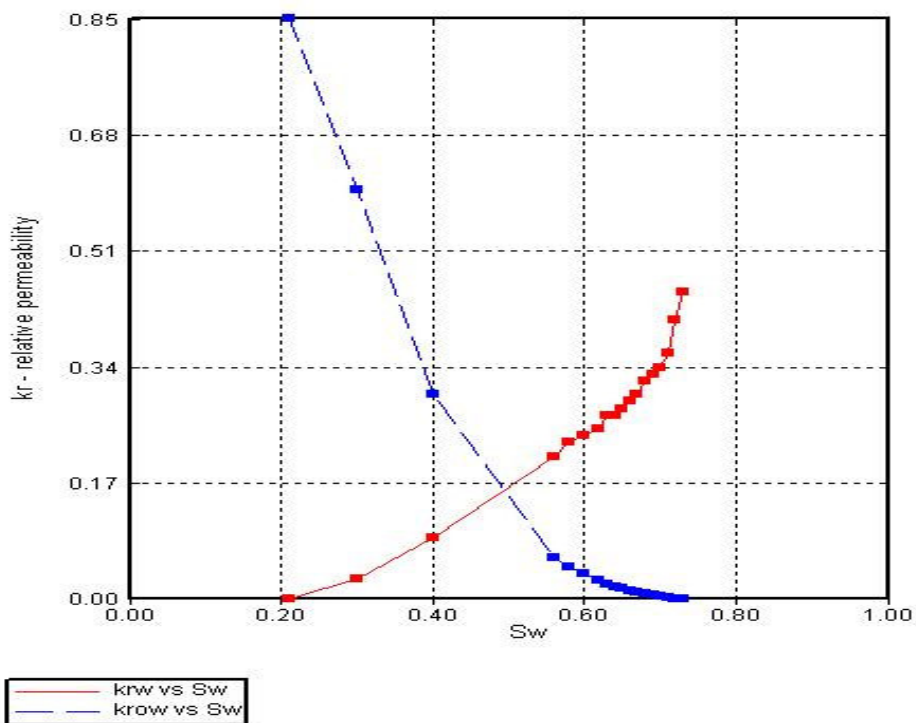


Fig. B.3 – Matrix Relative Permeability Curves

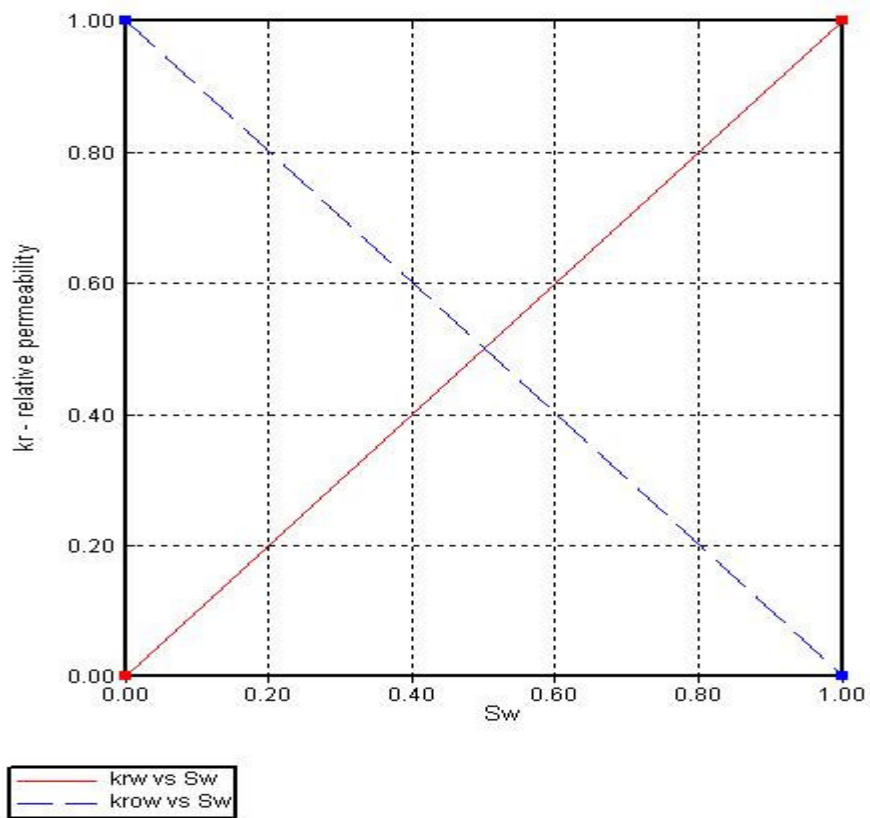


Fig. B.4 – Fractures and Super-K Relative Permeability Curves

VITA

NAME: Amer H. Abu-Hassoun

PERMANENT ADDRESS: Saudi Aramco
Dhahran, 31311
P.O. Box, 12766
Saudi Arabia

EDUCATION: B.S., Petroleum Engineering
King Fahd University of Petroleum and
Minerals,
Dhahran, Saudi Arabia
May 2001

M.S., Petroleum Engineering (Sponsored by
Saudi Aramco)
Texas A&M University, August 2007